J Stat Phys (2008) 130: 1119–1176
DOI 10.1007/s10955-007-9464-0

Exact Results for Thermodynamics of the Hydrogen Plasma: Low-Temperature Expansions Beyond Saha Theory

A. Alastuey · V. Ballenegger · F. Cornu · Ph.A. Martin

Received: 20 April 2007 / Accepted: 6 November 2007 /
Published online: 14 December 2007

Abstract We study hydrogen in the Saha regime, within the physical picture in terms of a quantum proton-electron plasma. Long ago, Saha showed that, at sufficiently low densities and low temperatures, the system behaves almost as an ideal mixture made with hydrogen atoms in their groundstate, ionized protons and ionized electrons. More recently, that result has been rigorously proved in some scaling limit where both temperature and density vanish. In that Saha regime, we derive exact low-temperature expansions for the pressure and internal energy, where density ρ is rescaled in units of a temperature-dependent density ρ^* which controls the cross-over between full ionization ($\rho \ll \rho^*$) and full atomic recombination ($\rho \gg \rho^*$). Each term reduces to a function of ρ/ρ^* times temperature-dependent functions which decay exponentially fast when temperature T vanishes. Scaled expansions are ordered with respect to the corresponding decay rates. Leading terms do reduce to ideal contributions obtained within Saha theory. We consistently compute all corrections which are exponentially smaller by a factor $\exp(\beta E_H)$ at most, where E_H is the negative groundstate energy of a hydrogen atom and $\beta = 1/(k_B T)$. They include all effects arising from both the Coulomb potential and the quantum nature of the particles: excitations of atoms H, formation of molecules H_2, ions H_2^+ and H^-, thermal and pressure ionization, plasma polarization, screening, interactions between atoms and ionized charges, etc. Scaled low-temperature

A. Alastuey (✉)
Laboratoire de Physique, Université de Lyon, ENS Lyon, CNRS, 46 allée d'Italie, 69364 Lyon Cedex 07, France
e-mail: angel.alastuey@ens-lyon.fr

V. Ballenegger
Institut UTINAM, Université de Franche-Comté, CNRS, 16 route de Gray, 25030 Besançon Cedex, France

F. Cornu
Laboratoire de Physique Théorique, Université Paris-Sud, CNRS, Bâtiment 210, 91405 Orsay Cedex, France

Ph.A. Martin
Institut de Théorie des Phénomènes Physiques, École Polytechnique Fédérale de Lausanne, 1015 Lausanne, Switzerland

expansions can be viewed as partial resummations of usual virial expansions up to arbitrary high orders in the density.

1 Introduction

Hydrogen is an important element, both at a theoretical level and for practical purposes. Here, we consider a non-relativistic quantum hydrogen plasma, made of protons and electrons with respective masses m_p and m_e, which interact *via* the familiar $1/r$-Coulomb potential (see Sect. 2.1). As far as thermodynamic properties of that system are concerned, an exact calculation at finite temperature T and finite density ρ, remains far beyond present human abilities. Nonetheless, by exploiting the exact knowledge of the spectrum of hydrogen atom and using Morita's method [51], Ebeling [23] first computed low-density expansions for pressure and free energy up to order ρ^2 at fixed non-zero temperature, in a closed analytical form (see also Ref. [39]). When ρ goes to zero, the system becomes fully ionized (see Ref. [43] for a rigorous proof). At order ρ^2, the recombination of a small fraction of charges into hydrogen atoms is exactly taken into account. Such low-density expansions have been more recently completed up to order $\rho^{5/2}$ [4–7]. Those results have been checked afterwards in Ref. [37], and their high-temperature form in the one-component case does coincide with that derived in Ref. [20]. In the opposite limit where ρ goes to infinity at zero temperature, the system behaves as a mixture of free Fermi gases, and expansions in inverse powers of ρ have been calculated (see Refs. [29] and [50] for the first calculations in the one-component case, and also Ref. [39] for similar works or extensions).

The previous exact asymptotic expansions are suitable for regimes where the system is almost fully ionized. The purpose of the present paper is to derive a similar expansion in the so-called Saha regime, where a non-vanishing fraction of charges is recombined into hydrogen atoms. That regime was introduced long ago [60] in the framework of the chemical picture. Assuming that the system is an ideal mixture of protons, electrons, and hydrogen atoms, its composition is then determined by applying the usual mass action law [26]. More recently, by starting from the physical description of the system in terms of a quantum plasma, it has been proved through successive works by Fefferman [27], Lieb et al. [18], Macris and Martin [45], that Saha approach is asymptotically exact in a scaling limit mixing the temperature and the chemical potential (see Sect. 2.2). As argued in Sect. 2.3, that limit defines quite diluted and low temperature conditions, namely the Saha regime, under which non-ideal contributions are small perturbations. In order to compute the corresponding contributions, we consider a formalism that combines the path integral representation of a quantum gas to familiar Mayer diagrammatics (see Sect. 2.4). Our key starting point in that framework is the so-called screened cluster expansion (SCE) of particle densities in terms of fugacities [8], which turns to be quite appropriate for studying recombined phases as illustrated in Refs. [10–12] (dielectric response of an atomic gas) or [9] (partial screening of van der Waals forces by free charges). The physical content of SCE is close to ideas first introduced by Rogers [54] for describing atomic or molecular recombination within the physical picture. In that approach, virial coefficients are numerically estimated within a priori modelizations, which incorporate quantum effects at short distances and classical Debye screening at large distances. The corresponding so-called ACTEX method has been developed through successive works [55, 56, 58, 59]. It has also been applied to hydrogen [57], with quite good results at low and moderate densities as described in Ref. [48]. Nevertheless, in the Saha regime, exact asymptotic expansions with analytical prescriptions for computing the successive terms, have not been derived within ACTEX method.

In Sect. 3, using the parametrization of chemical potential in terms of temperature introduced in Ref. [45], we show that every contribution in SCE of particle densities, decays exponentially fast when T goes to zero. Thanks to available inequalities for the spectrum of the considered Coulomb Hamiltonian, we extract the leading terms which do arise from free (ionized) protons and electrons, as well as from atoms H in their groundstate with energy $E_H = -me^4/(2\hbar^2)$ where m is the reduced mass $m = m_p m_e/(m_p + m_e)$. Next corrections are ordered with respect to their decay rate in the zero-temperature limit. They account for a large variety of physical effects: plasma polarization, formation of molecules H_2, ions H_2^+ and H^-, interactions between ionized charges and Hydrogen atoms. Such corrections are defined without any ambiguity or *a priori* modelizations, so they do not depend on any adjustable phenomenological parameter. In particular, SCE provides well-behaved expressions for the partition functions of a molecule H_2 or ions H_2^+ and H^- in the vacuum, which are the generalizations of quantum virial functions for the hydrogen atom [23] to more complex entities. Notice also that ionic contributions to charge neutrality or screening are consistently incorporated, as it should.

The equation of state (EOS) is derived by using thermodynamic identities in Sect. 4. This leads to our main result, namely scaled low-temperature (SLT) expansion of the pressure P around ideal Saha pressure

$$\beta P/\rho^* = \beta P_{\text{Saha}}/\rho^* + \sum_{k=1}^{\infty} \beta P_k/\rho^*, \tag{1.1}$$

considered as a function of the temperature and of the dimensionless density variable ρ/ρ^* where ρ is the electron number density (which is equal to the proton number density by neutrality). The temperature-dependent reference density ρ^* defined by

$$\rho^* = \frac{\exp(\beta E_H)}{2(2\pi\lambda_{pe}^2)^{3/2}} \quad \text{with } \lambda_{pe} = (\beta\hbar^2/m)^{1/2}, \tag{1.2}$$

determines the cross-over between full ionization for $\rho \ll \rho^*$, and full recombination for $\rho \gg \rho^*$ (see Sect. 2.2). Since E_H is negative, $E_H \simeq -13.6$ eV, ρ^* decays exponentially fast at low temperatures. In expansion (1.1), it is convenient to express the pressure in units of $k_B T\rho^*$ which turns out to be the natural reference pressure in the Saha regime. Then, each term in (1.1) is dimensionless. The first term is the usual Saha pressure expressed in terms of ρ/ρ^*

$$\beta P_{\text{Saha}}/\rho^* = \rho/\rho^* + (1 + 2\rho/\rho^*)^{1/2} - 1. \tag{1.3}$$

We see indeed that for $\rho \ll \rho^*$, the system becomes fully ionized ($\beta P_{\text{Saha}} \sim 2\rho$), whereas for $\rho \gg \rho^*$ all ionized charges recombine into neutral hydrogen atoms ($\beta P_{\text{Saha}} \sim \rho$). Each term in expansion (1.1) beyond that leading ideal contribution has the form of a non-linear function of ratio ρ/ρ^*, times a temperature-dependent function $h_k(\beta)$ (or possibly a polynomial in the $h_l(\beta)$, $l \le k$). The $h_k(\beta)$ decay exponentially fast when T vanishes and are ordered with respect to their decay rates $h_k(\beta) \sim e^{-\beta\delta_k}$, $0 < \delta_1 < \delta_2 < \cdots$. Hence the expansion (1.1) is organized as a series of exponential terms with increasingly faster exponential decay as $T \to 0$. The h_k-functions and their decay rates are governed by a balance between energy and entropy involving the ground-state energy $E^{(0)}_{N_p,N_e}$ of Coulomb Hamiltonian H_{N_p,N_e} for N_p protons and N_e electrons in mutual interaction. We determine the pressure in the Saha regime by computing exactly all terms in expansion (1.1) smaller than leading ideal

contribution $\beta P_{\rm Saha}/\rho^*$ of order 1 by exponentially decaying factors of maximum order $\exp(\beta E_H)$. We find

$$\begin{aligned} &\beta P_k/\rho^* = (\text{function of } \rho/\rho^*) \times h_k(\beta), \quad h_k(\beta) \sim e^{-\beta\delta_k},\ k = 1, 2, 3, 4, \\ &\beta P_5/\rho^* = (\text{function of } \rho/\rho^*) \times [h_1(\beta)]^2 \end{aligned} \tag{1.4}$$

with (δ_k in electronvolt units, $E^{(0)}_{2,1} = E_{H_2^+}$, $E^{(0)}_{1,2} = E_{H^-}$, $E^{(0)}_{2,2} = E_{H_2}$)

$$\begin{aligned} \delta_1 &= |E_H|/2 \simeq 6.8, \\ \delta_2 &= |3E_H - E_{H_2}| \simeq 9.1, \\ \delta_3 &= 3|E_H|/4 \simeq 10.2, \\ \delta_4 &= |2E_H - E_{H_2^+}| \simeq 11.0. \end{aligned} \tag{1.5}$$

The explicit forms of the density-dependent functions and of the $h_k(\beta)$ can be found in Sects. 4.1 and 4.2 together with a discussion of their interpretation and relative importance in different density and temperature regimes. In short, the h_k-functions incorporate various corrections to the ideal Saha term which can be described by

- $h_1(\beta)$: plasma polarization around ionized charges
- $h_2(\beta)$: formation of H_2 molecules and atom-atom interactions
- $h_3(\beta)$: atomic excitations and interactions between ionized charges
- $h_4(\beta)$: formation of H_2^+ and H^- ions, atom-charge interactions, and screening of atomic groundstate

The construction of SLT expansion (1.1), defined by taking the zero-temperature limit at fixed ratio ρ/ρ^*, is itself an important new result. It provides a non-trivial structure for the various corrections to ideal Saha pressure, which are properly ordered in that scaling limit. It turns out that keeping only the first correction $\beta P_1/\rho^*$, is equivalent to a modification of the Saha ionization rate which has been derived previously by several authors (see e.g. [41] and references quoted in [39]). To our knowledge, next terms $\beta P_k/\rho^*$ ($2 \le k \le 5$) are entirely new, and do not have counterparts in the literature. We provide their exact expressions, which involve suitably truncated few-body partition functions. Two-body truncated partition functions are merely related to quantum virial functions first introduced by Ebeling (see e.g. [39] and references quoted therein). Three- and four-body truncated partition functions are introduced and defined here for the first time. Previous terms ($2 \le k \le 5$) also account, beyond standard calculations, for interactions between recombined entities as well as screening effects. For instance, contributions of atom-atom interactions in $\beta P_2/\rho^*$ are evaluated without any a priori modelization, while screening of atomic groundstate embedded in $\beta P_4/\rho^*$ incorporates further corrections to the familiar Debye shift.

Corrections in SLT expansion (1.1) are ordered with respect to their decay rates when the temperature vanishes at fixed ratio ρ/ρ^*. The behavior of such corrections along a given low-temperature isotherm when the density is varied, displays some interesting physics. For very small densities $\rho \ll \rho^*$, all density-dependent functions in front of the $h_k's$ can be expanded in powers of ρ. Then, we retrieve the well-known virial expansion at fixed temperature up to order ρ^2 included (see Sect. 4.2). In particular, the leading correction of order $\rho^{3/2}$ is the familiar classical Debye term arising from the polarization contribution $\beta P_1/\rho^*$. When the density is increased, virial density-expansion can no longer be used, but SLT expansion still works and accounts for non-perturbative effects with respect to finite

values of ρ/ρ^*. Up to moderate densities $\rho \simeq \rho^*$, $\beta P_1/\rho^*$ remains the leading correction to ideal Saha terms. Interestingly, that polarization contribution is reduced at higher densities $\rho \gg \rho^*$ because most protons and electrons are recombined into atoms H. Then, molecular contributions embedded in $\beta P_2/\rho^*$ provide the first correction to Saha pressure, since they also overcome contributions of atom-atom interactions, at least for a sufficiently low temperature isotherm. Ultimately, they are responsible for the breakdown of expansion (1.1) at too large densities. Our results clearly provide a better analytical knowledge of the thermodynamics in an extended part of the phase diagram, as illustrated by the validity domain drawn in Fig. 12 of Sect. 4.3. The SLT expansions can be viewed as infinite resummations of low-density expansions.

We emphasize again that the EOS (1.1) incorporates the screening effects in a coherent and consistent way for the whole range of densities $\rho \ll \rho^*$ (strongly ionized gas) and $\rho \gg \rho^*$ (recombined gas). When the interaction is Coulombic, one has to face the divergence of the sum of bound state contributions to the partition function of an isolated atom arising from the infinite number of Rydberg states. That important and well-known problem is usually dealt with the Planck-Larkin prescription to cut off states of energies E_n larger than $k_B T$ (see e.g. the discussion in [24]). In our implementation of the physical picture for the recombined phase, no divergence occurs since the partition function of the hydrogen atom appears naturally in a convergent truncated form, as a consequence of collective screening effects. Only that truncated partition function embedding both bound and ionized states is free from ambiguity. More comments about that point are offered in Sect. 3.2.

Collective screening effects also give raise to well-behaved partition functions for more complex entities, like ions H^- and H_2^+, or molecules H_2. Such partition functions are naturally defined according to a truncation procedure similar to that introduced for the atomic partition function. They also involve contributions from both bound and dissociated states. The molecular partition function accounts thus not only for molecular bound states, but also for diffusion states made with two protons and two electrons. The finiteness of few-body truncated partition functions is of course crucial in the analysis of their low-temperature behaviors, which are shown to be controlled by Boltzmann factors $\exp(-\beta E_H)$, $\exp(-\beta E_{H^-})$, $\exp(-\beta E_{H_2^+})$, $\exp(-\beta E_{H_2})$, associated with the corresponding recombined entities in their groundstate (as would trivially be expected in a system with short range forces [25, 35]). Contributions from excited or diffusion states are well-defined in those truncated partition functions, and they may be neglected when the temperature is low enough.

An exact treatment of screening in the many-body problem is also required to establish the correct classification of terms in the expansion (1.1) according to decaying exponentials. For instance, in addition to obvious contributions of atomic bound states, there are correction terms proportional to the inverse screening length κ (or powers of it), which is itself proportional to the square root of the density $\kappa \sim \sqrt{\rho}$. Since the latter is also exponentially small in the Saha regime (see Sect. 2.2), contributions of collective screening effects have to be compared to pure atomic terms, and may be predominant as exemplified by the first correction $\beta P_1/\rho^*$. Such systematic classification could not have been obtained without a unified theory which deals exactly with the interplay between screening effects and the other physical phenomena at stake (primarily the formation of atomic and molecular bound states).

Though SLT expansions are asymptotic, i.e. a priori valid in the zero-temperature limit, they can be used for quantitative purposes within a rather wide range of temperatures and densities. We have performed numerical calculations, for both the EOS and the internal energy. For T of the order a few thousand kelvins, the $h_k(\beta)$'s are not accurately reproduced by their simple low-temperature asymptotic forms: further contributions, which arise

in particular from excited states of the recombined entities, must also be taken into account. Within a simple criterion on the order of magnitude of the various corrections to Saha pressure, we draw the validity domain of SLT expansion (1.1) in the plane (β, ρ) (see Fig. 12 in Sect. 4.3). That validity domain exemplifies the quantitative interest of our calculations, which can be applied to physical systems under observable conditions, like the Sun photosphere for instance. Furthermore, we have compared our findings to those of Militzer and Ceperley [48] obtained within Path Integral Monte Carlo (PIMC) simulations (PIMC methods have been implemented through successive works [15–17, 47, 49]). The agreement is satisfactory, as it should since PIMC results are computationally exact within statistical errors (see e.g. Ref. [40]). The detail of that comparison, as well as all our numerical results, will be presented in a forthcoming paper [1].

From a mathematical view point, all manifestations of screening stem from the screened potential introduced in Sect. 2.4 and studied in [13]. That potential can be viewed, in the quantum mechanical context, as the analogue of the classical Debye-Hückel potential. Because of its central role, we have devoted the long Appendix A: to a number of related properties which are used in our analysis. In Appendix B:, the low temperature behaviors of the truncated atomic, ionic and molecular partition functions mentioned above, are determined by methods using Green functions and path integral representations. In Appendix C:, we compute the contributions of interactions between atoms and ionized charges.

2 Saha Regime and Screened Cluster Expansion

2.1 Definition of the Model

The hydrogen plasma is a two-component system made of protons and electrons. In the present non-relativistic limit, the proton and the electron are viewed as quantum point particles with respective charges, masses, and spins, $e_p = e$ and $e_e = -e$, m_p and m_e, $\sigma_p = 1/2$ and $\sigma_e = 1/2$. The kinetic energy operator for each particle of species $\alpha = p, e$ with position $\mathbf{x}$ takes the Schrödinger form $-\hbar^2/(2m_\alpha)\Delta$ where Δ is the Laplacian with respect to $\mathbf{x}$. Two particles separated by a distance r interact via the instantaneous Coulomb potential $v(r) = 1/r$. The corresponding Coulomb Hamiltonian H_{N_p,N_e} for N_p protons and N_e electrons reads

$$H_{N_p,N_e} = -\sum_{i=1}^{N} \frac{\hbar^2}{2m_{\alpha_i}} \Delta_i + \frac{1}{2} \sum_{i \neq j} e_{\alpha_i} e_{\alpha_j} v(|\mathbf{x}_i - \mathbf{x}_j|) \tag{2.1}$$

where $N = N_p + N_e$ is the total number of particles. In (2.1), the subscript i is attached to protons for $i = 1, \ldots, N_p$ and to electrons for $i = N_p + 1, \ldots, N_p + N_e$, so the species index α_i reduces either to p or e while $\mathbf{x}_i$ denotes either the position $\mathbf{R}_i$ of the i-th proton or the position $\mathbf{r}_j$ of the j-th electron ($j = i - N_p$).

The system is enclosed in a box with volume Λ, in contact with a thermostat at temperature T and a reservoir of particles that fixes the chemical potentials equal to μ_p and μ_e for protons and electrons respectively. Its grand-partition function Ξ is

$$\Xi = \mathrm{Tr} \exp[-\beta(H_{N_p,N_e} - \mu_p N_p - \mu_e N_e)]. \tag{2.2}$$

In (2.2), the trace is taken over all states symmetrized according to the Fermionic nature of each species; the boundary conditions for the wave functions at the surface of the box can be

chosen of the Dirichlet type. Lieb and Lebowitz [44] have proved that the thermodynamic limit ($\Lambda \to \infty$ at fixed β and μ_α) exists, thanks to Fermi statistics and screening. Indeed, the Fermionic statistics of at least one species implies the H-stability [21, 22]

$$H_{N_p,N_e} > -B(N_p + N_e), \quad B > 0 \tag{2.3}$$

that prevents the collapse of the system. On the other hand, screening ensures that it does not explode. In a fluid phase, the infinite system maintains local neutrality, i.e. the homogeneous local particle densities ρ_p and ρ_e for protons and electrons remain equal for any choice of the chemical potentials μ_α. In other words, the common particle density $\rho = \rho_p = \rho_e$, as well as all other bulk equilibrium quantities, depend on the sole combination

$$\mu = (\mu_p + \mu_e)/2, \tag{2.4}$$

and not on the difference $\nu = (\mu_e - \mu_p)/2$. In particular, in terms of the fugacities $z_\alpha = \exp(\beta\mu_\alpha)$, this means that both the density ρ and the pressure P are functions of only β and $z = (z_p z_e)^{1/2} = \exp(\beta\mu)$. Therefore individual chemical potentials μ_e, μ_p are not uniquely determined: we can choose their difference ν at will without changing the bulk densities. Among the possible choices, it is particularly convenient to set

$$\mu_p = \mu - \frac{3}{2} k_B T \ln \frac{\lambda_e}{\lambda_p}, \qquad \mu_e = \mu + \frac{3}{2} k_B T \ln \frac{\lambda_e}{\lambda_p} \tag{2.5}$$

where $\lambda_\alpha = (\beta\hbar^2/m_\alpha)^{1/2}$ is the thermal de Broglie wavelength of species α. This choice guarantees that Maxwell-Boltzmann densities of free (no interactions) proton and electron gases, respectively

$$\begin{aligned} \rho_p^{id} &= 2z_p/(2\pi\lambda_p^2)^{3/2}, \\ \rho_e^{id} &= 2z_e/(2\pi\lambda_e^2)^{3/2}, \end{aligned} \tag{2.6}$$

are identical, i.e.

$$\rho_p^{id} = \rho_e^{id} = 2z/(2\pi\lambda^2)^{3/2} \tag{2.7}$$

with $\lambda = (\lambda_p \lambda_e)^{1/2}$. The factors 2 in (2.6) accounts for spin degeneracy.

The enforced neutrality of the ideal mixtures is equivalent to the linear relation

$$\sum_\alpha e_\alpha z_\alpha/(2\pi\lambda_\alpha^2)^{3/2} = 0 \tag{2.8}$$

between the activities z_p and z_e, sometimes called the pseudo neutrality condition. That condition can be imposed without loss of generality when dealing with fugacity expansions in the grand canonical ensemble. As shown in Sect. 3, it considerably simplifies the analysis of diagrammatic series for the interacting system. If we consider other fugacities (z_p', z_e') which do not satisfy the pseudo neutrality condition, an infinite number of graphs contributes to any term with a given order in low-density expansions. The calculations of those terms then become rather cumbersome. Nevertheless, beyond that technical complication, their final expression would be identical to that derived by starting with the above fugacities satisfying both condition (2.8) and $z_p z_e = z_p' z_e'$, in agreement with Lieb and Lebowitz proof [44].

2.2 Rigorous Results at Low Density and Low Temperature

We briefly recall the Saha theory in its simplest form. From the elementary view point of the thermodynamic of ideal substances, equilibrium ionization phases can be considered in the so-called chemical picture [26] as mixtures of noninteracting gases of electrons, protons, and hydrogen atoms, with chemical potential μ_{at} obeying the law of chemical equilibrium $\mu_{at} = \mu_e + \mu_p$. According to (2.7) the corresponding densities of electrons and protons are

$$\rho_p^{id} = \rho_e^{id} = 2\left(\frac{(m_p m_e)^{1/2}}{2\pi\beta\hbar^2}\right)^{3/2} \exp(\beta\mu), \tag{2.9}$$

whereas the atomic density is

$$\rho_{at}^{id} = 4\left(\frac{M}{2\pi\beta\hbar^2}\right)^{3/2} \exp(-\beta(E_H - 2\mu)) \tag{2.10}$$

where $M = m_p + m_e$ is the atomic mass and the factor 4 is the number of spin states. Apart from the binding energy E_H of the Hydrogen atom, all other effects of the Coulomb interaction are disregarded, so the Saha EOS is that of a mixture of perfect gases

$$\beta P_{\text{Saha}} = \rho_p^{id} + \rho_e^{id} + \rho_{at}^{id}. \tag{2.11}$$

We see in (2.9) and (2.10) that, when $\mu = E_H$, all densities are of the same exponential order at low temperatures: this corresponds to the coexistence of ionized and atomic phases. It is appropriate to characterize the set of ionization equilibrium phases by a temperature-dependent chemical potential [45]

$$\mu = \mu(\beta) = E_H + k_B T \ln w \tag{2.12}$$

where w is a fixed parameter $0 < w < \infty$. As shown from (2.9) and (2.10), that parameter determines the relative proportion of atoms to ionized charges through

$$\frac{\rho_{at}^{id}}{\rho_{p,e}^{id}} = 2w\left(\frac{M}{m}\right)^{3/4} = \frac{\gamma}{2}, \tag{2.13}$$

where we have introduced the equivalent parameter $\gamma = 4(M/m)^{3/4}w$. According to the above definitions, the fugacity $z = \exp(\beta\mu)$ can be seen as parametrized by either w or γ at fixed temperature, i.e. $z = w\exp(\beta E_H)$ or

$$z = \left(\frac{m}{M}\right)^{3/4} \gamma \exp(\beta E_H)/4. \tag{2.14}$$

For further purposes, it is convenient to consider the temperature dependent reference density ρ^* defined by (1.2) in the Introduction. Then we can rewrite ideal densities as

$$\rho_p^{id} = \rho_e^{id} = \rho^*\gamma \tag{2.15}$$

and

$$\rho_{at}^{id} = \rho^* \frac{\gamma^2}{2}. \tag{2.16}$$

In terms of γ, the proton (or electron) density $\rho = \rho_p^{id} + \rho_{at}^{id} = \rho_e^{id} + \rho_{at}^{id}$ and the Saha pressure (2.11) respectively read

$$\rho = \rho^* \left(\gamma + \frac{\gamma^2}{2} \right) \tag{2.17}$$

and

$$\beta P_{\text{Saha}} = \rho^* \left(2\gamma + \frac{\gamma^2}{2} \right). \tag{2.18}$$

Inversion of relation (2.17) provides γ, and hence the chemical potential μ, as a function of the reduced density ρ/ρ^*. Substitution of that function in (2.18) finally yields the Saha EOS (1.3) for the dimensionless pressure written as a function of ρ/ρ^* (note that our density variable is half of the total number density). As said in the Introduction, ρ^* is the cross-over density between full ionization and atomic recombination.

The Saha picture has been rigorously justified from the statistical mechanics of the full interacting electron-proton gas in the following asymptotic sense. When the temperature goes to zero at fixed negative values of μ, the system obviously becomes highly dilute because all fugacities then vanish exponentially fast. If low temperatures favor recombination of electrons and protons into bound entities with negative ground state energies, on the contrary low densities favor dissociation. The chemical composition of the system will result of those two competing energy and entropy effects. That problem has been studied in a rigorous way by Fefferman [27], who proved the two following results using a refined version of the stability of matter (2.3) (see the discussion after (2.30) and Ref. [14] for a review). First, when $\beta \to \infty$ with $\mu < E_H$ (μ fixed), the pressure tends to that of an ideal mixture of protons and electrons with respective densities ρ_p^{id} and ρ_e^{id} (2.9) i.e. the system becomes fully ionized. Second, there exists some $\delta > 0$ such that, when $\beta \to \infty$ with $E_H < \mu < E_H + \delta$ (μ fixed), the pressure tends to that of an ideal gas of hydrogen atoms in their groundstate with density (2.10). In that case, there is full atomic recombination.

The previous discussion of the Saha EOS suggests that ionized protons, ionized electrons and Hydrogen atoms should coexist at $\mu = E_H$. This has been firmly settled by Lieb et al. [18] and also Macris and Martin [45] who proved that, when one introduces the temperature dependent chemical potential (2.12) and let $\beta \to \infty$, the EOS tends to that of an ideal mixture of protons, electrons, and Hydrogen-atoms in their ground state, namely

$$\beta P = (\rho_p^{id} + \rho_e^{id} + \rho_{at}^{id})[1 + O(\exp(-\beta\epsilon))] = \beta P_{\text{Saha}}[1 + O(\exp(-\beta\epsilon))] \tag{2.19}$$

for β large enough and $\epsilon > 0$. The original work of Fefferman provides a power-law bound $1/\beta$ to the error term; that bound was improved to an exponential one in [18]. Thus we see that all ideal densities vanish exponentially fast, while corrections to ideal terms in (2.19) decay exponentially faster. The mathematical methods used in [27] and [18] are adequate to obtain a rigorous control of the dominant term (the Saha pressure), but apparently not adapted to explicitly calculate the corrections. In this work, it is our purpose to develop tools that enable to systematically compute those corrections, by expanding the pressure beyond the Saha term in an exact way (see (1.1)). In order to characterize the Saha regime in our study of the interacting system, we shall still use the parametrization (2.14) of the fugacity z associated with the zero-temperature limit, in terms of the parameter γ.

2.3 Simple Physical Considerations about the Fugacity Expansion

Saha equation of state (2.19) can be recovered, at a heuristic level, from simple considerations on low fugacities series for the pressure. Those considerations will serve as a guide to the analytic estimations of various non-ideal contributions to the full EOS at finite temperature and density performed in next sections. Low fugacity series are easily inferred, at a formal level, from the identity

$$\beta P = \frac{\ln \Xi}{\Lambda}, \tag{2.20}$$

where the thermodynamic limit $\Lambda \to \infty$ is implicitly taken, as in the whole paper. They read

$$\beta P = \sum_{(N_p,N_e)\neq(0,0)} z_p^{N_p} z_e^{N_e} B_{N_p,N_e} \tag{2.21}$$

where Mayer coefficients B_{N_p,N_e} in (2.21) can be expressed as suitable traces,

$$B_{N_p,N_e} = \frac{1}{\Lambda} \mathrm{Tr}[\exp(-\beta H_{N_p,N_e})]_{\mathrm{Mayer}}. \tag{2.22}$$

The first Mayer operators $[\exp(-\beta H_{N_p,N_e})]_{\mathrm{Mayer}}$ read

$$\begin{aligned}
&[\exp(-\beta H_{1,0})]_{\mathrm{Mayer}} = \exp(-\beta H_{1,0}),\\
&[\exp(-\beta H_{0,1})]_{\mathrm{Mayer}} = \exp(-\beta H_{0,1}),\\
&[\exp(-\beta H_{1,1})]_{\mathrm{Mayer}} = \exp(-\beta H_{1,1}) - \exp(-\beta H_{1,0})\exp(-\beta H_{0,1}),\\
&[\exp(-\beta H_{2,0})]_{\mathrm{Mayer}} = \exp(-\beta H_{2,0}) - \frac{1}{2}\exp(-\beta H_{1,0})\exp(-\beta H_{1,0}),\\
&\ldots,
\end{aligned} \tag{2.23}$$

while a similar expression holds for any $[\exp(-\beta H_{N_p,N_e})]_{\mathrm{Mayer}}$

$$[\exp(-\beta H_{N_p,N_e})]_{\mathrm{Mayer}} = \exp(-\beta H_{N_p,N_e}) - \cdots. \tag{2.24}$$

In (2.24), terms left over reduce to a linear combination of products of Gibbs operators $\exp(-\beta H_{M_p,M_e})$ ($M_p \leq N_p$, $M_e \leq N_e$) associated with all possible partitions of N_p protons and N_e electrons. Traces (2.22) must be taken over Fermionic states which are products of anti-symmetrized states for each set of degrees of freedom associated with a Gibbs operator $\exp(-\beta H_{M_p,M_e})$. For instance, in space of positions and spins, $B_{2,0}$ reads

$$\begin{aligned}
B_{2,0} = \frac{1}{\Lambda}\int \mathrm{d}\mathbf{R}_1 \int \mathrm{d}\mathbf{R}_2 [&2\langle \mathbf{R}_1\mathbf{R}_2|\exp(-\beta H_{2,0})|\mathbf{R}_1\mathbf{R}_2\rangle\\
&- 2\langle \mathbf{R}_1|\exp(-\beta H_{1,0})|\mathbf{R}_1\rangle\langle \mathbf{R}_2|\exp(-\beta H_{1,0})|\mathbf{R}_2\rangle\\
&- \langle \mathbf{R}_2\mathbf{R}_1|\exp(-\beta H_{2,0})|\mathbf{R}_1\mathbf{R}_2\rangle].
\end{aligned} \tag{2.25}$$

For the term $\exp(-\beta H_{1,0})\exp(-\beta H_{1,0})$ subtracted in $[\exp(-\beta H_{2,0})]_{\mathrm{Mayer}}$, each Gibbs operator $\exp(-\beta H_{1,0})$ refers to a single proton, so no anti-symmetrization occurs and only diagonal matrix elements of $\exp(-\beta H_{1,0})$ appear in (2.25). Truncated Mayer operators can also be expressed in terms of Ursell operators [32–34].

Despite Mayer coefficients B_{N_p,N_e} diverge, leading contributions to the equation of state can be easily picked out in formal series (2.21), as follows. For ($N_p = 1$, $N_e = 0$) and ($N_p = 0$, $N_e = 1$), we obtain the simple exact expressions

$$B_{1,0} = \frac{2}{(2\pi\lambda_p^2)^{3/2}} \tag{2.26}$$

and

$$B_{0,1} = \frac{2}{(2\pi\lambda_e^2)^{3/2}}. \tag{2.27}$$

After multiplication by fugacity factors $\exp(\beta\mu_p)$ and $\exp(\beta\mu_e)$ respectively, we obtain the related contributions to pressure (2.21) which reduce, of course, to the ideal Maxwell-Boltzmann densities of ionized protons (ρ_p^{id}) and ionized electrons (ρ_e^{id}). For ($N_p = 1$, $N_e = 1$), it is reasonable to expect that hydrogen atoms with internal ground state energy E_H provide the leading low-temperature contribution which reads

$$\frac{4}{(2\pi\lambda_H^2)^{3/2}} \exp(-\beta E_H), \tag{2.28}$$

with $\lambda_H = (\beta\hbar^2/M)^{1/2}$ while factor 4 is due to spin degeneracy. The corresponding contribution to (2.21) is nothing but the ideal Maxwell-Boltzmann density ρ_{at}^{id} of Hydrogen atoms in their ground state. In the Saha regime, ideal densities of ionized protons (ρ_p^{id}), ionized electrons (ρ_e^{id}) and hydrogen atoms (ρ_{at}^{id}) are all found to be of the same order of magnitude $\exp(\beta E_H)$ disregarding powers of β, because of (2.12).

All other contributions to the EOS are expected to be small corrections to Saha pressure, as suggested by the following simple arguments and estimations. The Saha regime defines quite diluted conditions since ρ vanishes exponentially fast. Therefore, ionized charges and hydrogen atoms are expected to be weakly coupled and weakly degenerate. Let us introduce the various length and energy scales defined in Table 1, where we assume that each atom

Table 1 Length and energy scales in a quantum hydrogen plasma

Symbol	Value	Physical signification
Length		
a_B	$\hbar^2/(me^2)$	Bohr radius
$\lambda_{p,e,at}$	$\hbar(\beta/m_{p,e,at})^{1/2}$	de Broglie lengths
l_B	βe^2	Bjerrum length
a	$(3/(4\pi\rho))^{1/3}$	Mean interparticle distance
κ^{-1}	$(4\pi\beta e^2[\rho_p^{id} + \rho_e^{id}])^{-1/2}$	Debye screening length
l_Q	$\kappa^{-1}\lvert\ln(\kappa\lambda)\rvert$	Quantum screening distance
Energy		
ϵ_{H-H}	$e^2a_B^2/a^3$	Atom-atom interaction energy
ϵ_{H-c}	e^2a_B/a^2	Atom-charge interaction energy
ϵ_{c-c}	e^2/a	Charge-charge interaction energy
ϵ_{kin}	k_BT	Classical kinetic energy
E_H	$\lvert E_H\rvert = me^4/(2\hbar^2)$	Atom ground-state energy

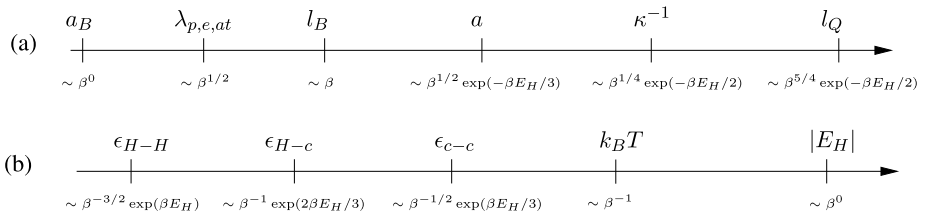

Fig. 1 Hierarchy of **a** length and **b** energy scales in the Saha regime

carries, roughly speaking, an instantaneous dipole of order ea_B, while the physical signification of l_Q is given in next Sect. 2.4. According to the hierarchies between those length and energy scales described in Fig. 1, both exchange and interaction contributions for ionized charges and hydrogen atoms should be exponentially smaller than above ideal terms. Similarly, we can estimate the contributions of complex entities which result from the quantum mechanical binding of N_e electrons and N_p protons, i.e. the existence of a bound state in the spectrum of H_{N_p,N_e} with negative ground state energy $E^{(0)}_{N_p,N_e}$. The ideal contribution of a given complex entity is easily extracted from B_{N_p,N_e}, and it is of order $\exp(-\beta E^{(0)}_{N_p,N_e})$. After multiplication by fugacity factor $\exp[\beta(\mu_p N_p + \mu_e N_e)]$, we find a contribution to pressure (2.21) which is of order

$$\exp[-\beta(E^{(0)}_{N_p,N_e} - (N_p + N_e - 1)E_H]\exp(\beta E_H), \tag{2.29}$$

where we have used parametrization (2.12) of the chemical potential. Ideal contribution (2.29) decays exponentially faster than $\exp(\beta E_H)$ for $(N_p, N_e) \neq (1,1), (1,0), (0,1)$, by virtue of inequality

$$E^{(0)}_{N_p,N_e} - (N_p + N_e - 1)E_H > 0, \quad (N_p, N_e) \neq (1,0), (0,1), (1,1) \tag{2.30}$$

which is a key ingredient in Fefferman's proof [27]. Although not yet proved, that inequality is satisfied by known complex entities [28] as illustrated below. Of course, and as for ionized charges and hydrogen atoms, exchange and interactions contributions for complex entities should be smaller than ideal ones.

Above heuristic arguments suggest that corrections to ideal Saha pressure (2.11) decay exponentially faster than leading terms when T vanishes, in agreement with the rigorous bound involved in (2.19). A precise evaluation of those corrections will be performed in Sect. 3 by using screened cluster expansion described in next Sect. 2.4. That method removes all long range Coulomb divergencies which plague Mayer coefficients B_{N_p,N_e}. It provides well-defined recipes for computing contributions from both interactions and complex entities. The simplest entities which appear are the molecule H_2 with groundstate energy $E^{(0)}_{2,2} = E_{H_2} \simeq -31.7$ eV, ion H_2^+ with $E^{(0)}_{2,1} = E_{H_2^+} \simeq -16.2$ eV, and ion H^- with $E^{(0)}_{1,2} = E_{H^-} \simeq -14.3$ eV. Notice that such groundstate energies do satisfy inequality 2.30. For complex entities made with five or more particles, we will assume inequality

$$E^{(0)}_{N_p,N_e} > (N_p + N_e - 2)E_H, \quad N_p + N_e \geq 5. \tag{2.31}$$

That inequality, more constraining than (2.30), is indeed satisfied by known stable complex entities. For instance, $E^{(0)}_{3,2} = E_{H_3^+} \simeq -36.5$ eV and $E^{(0)}_{2,3} = E_{H_2^-} \simeq -28.5$ eV are indeed larger than $3E_H \simeq -40.8$ eV. Previous groundstate energies are computed within the method

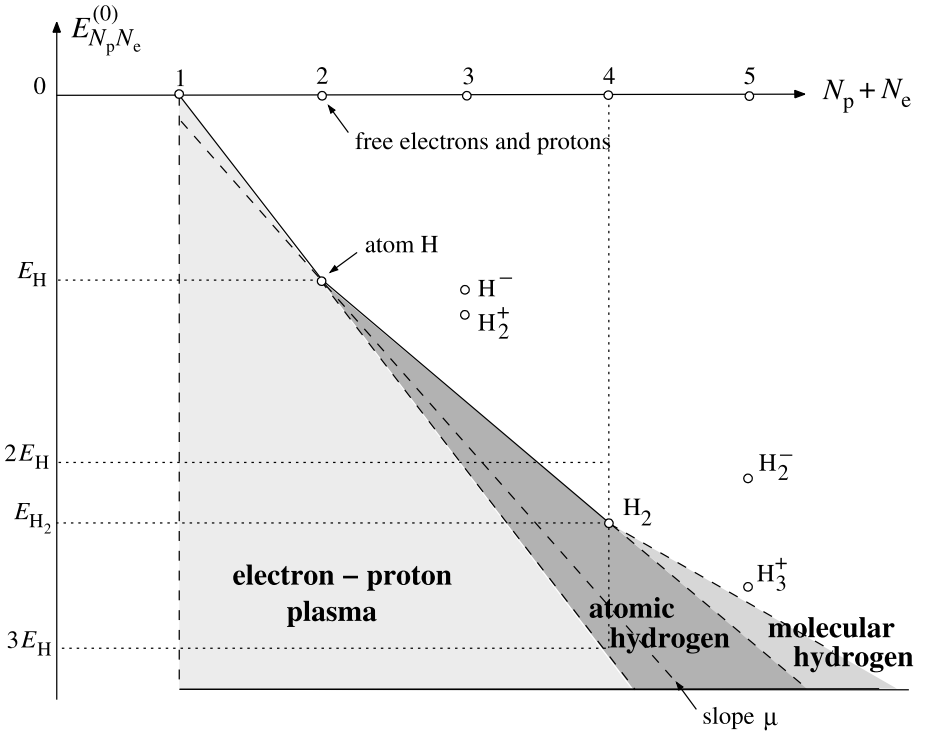

Fig. 2 Geometrical representation of inequalities (2.30). Consider a line of slope $\mu < 0$ which goes through the point associated with the hydrogen atom. If all the points $(N_p + N_e, E^{(0)}_{N_p,N_e})$ associated with other entities lie above that line, the inequalities (2.30) hold for that value of μ, and the system tends to a dilute atomic gas in the limit $\beta \to \infty$

described in [52]. The corresponding values are in excellent agreement with experiments and reported data in the literature. The resulting stability regimes of ionized, atomic and molecular phases are shown in Fig. 2.

2.4 Screened Cluster Expansion within Loop Formalism

Screened cluster expansions are devised within an auxiliary classical system of charged loops. As first shown by Ginibre [30], Ξ is identical to the grand-partition function of a classical system made with loops. That transformation starts with the expression of Ξ in space of positions and spins, and use of Feynman-Kac formula [38, 53, 61, 62],

$$\begin{aligned}
&\langle \mathbf{x}'_1 \cdots \mathbf{x}'_N | \exp(-\beta H_{N_p,N_e}) | \mathbf{x}_1 \cdots \mathbf{x}_N \rangle \\
&= \prod_{i=1}^{N} \frac{\exp[-(\mathbf{x}'_i - \mathbf{x}_i)^2/(2\lambda^2_{\alpha_i})]}{(2\pi\lambda^2_{\alpha_i})^{3/2}} \int \prod_{i=1}^{N} \mathcal{D}(\boldsymbol{\xi}_i) \exp\Big[-\frac{\beta}{2} \sum_{i \neq j} e_{\alpha_i} e_{\alpha_j} \\
&\quad \times \int_0^1 \mathrm{d}s\, v(|(1-s)(\mathbf{x}_i - \mathbf{x}_j) + s(\mathbf{x}'_i - \mathbf{x}'_j) + \lambda_{\alpha_i} \boldsymbol{\xi}_i(s) - \lambda_{\alpha_j} \boldsymbol{\xi}_j(s)|) \Big]. \quad (2.32)
\end{aligned}$$

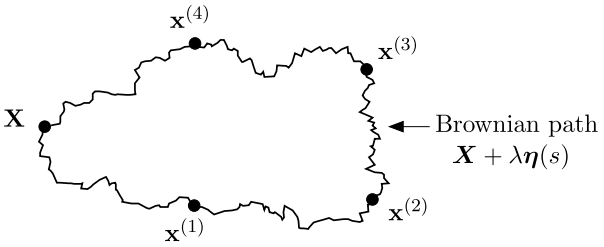

Fig. 3 A loop $\mathcal{L} = (\alpha, q, \mathbf{X}, \boldsymbol{\eta}(s))$ made up of 5 particles

In the r.h.s. of (2.32), functional integrations are performed over Brownian bridges $\boldsymbol{\xi}_i(s)$ ($\boldsymbol{\xi}_i(0) = \boldsymbol{\xi}_i(1) = 0$) with the normalized Gaussian measure $\mathcal{D}(\boldsymbol{\xi})$ defined by its covariance (see (2.34) with $q = 1$). Each Brownian bridge $\boldsymbol{\xi}_i(s)$ defines a path $(1-s)\mathbf{x}_i + s\mathbf{x}_i' + \lambda_{\alpha_i}\boldsymbol{\xi}_i(s)$ associated with a given particle. A loop $\mathcal{L}$ is then defined as the collection of open paths associated with particles exchanged in a given permutation cycle. This leads to the identity [14, 19, 46]

$$\Xi = \Xi_{loop} = \sum_{N=0}^{\infty} \frac{1}{N!} \int \prod_{i=1}^{N} \mathcal{D}(\mathcal{L}_i) z(\mathcal{L}_i) \prod_{i<j} \exp(-\beta V(\mathcal{L}_i, \mathcal{L}_j)), \tag{2.33}$$

where fugacity $z(\mathcal{L}_i)$ and two-body potential $V(\mathcal{L}_i, \mathcal{L}_j)$ are defined below.

A loop $\mathcal{L}$ is characterized by its position $\mathbf{X}$, species $\alpha = p, e$ and number q of exchanged particles, while its shape is defined by a closed Brownian path $\boldsymbol{\eta}(s)$ with $s \in [0, q]$ and $\boldsymbol{\eta}(0) = \boldsymbol{\eta}(q) = 0$. Genuine particle positions in matrix elements of $\exp(-\beta(H_{N_p,N_e})$ reduce to $\mathbf{x}^{(k)} = \mathbf{X} + \lambda_\alpha \boldsymbol{\eta}(k)$ with k integer, $k = 0, \ldots, q-1$ ($\mathbf{x}^{(0)} = \mathbf{x}^{(q)} = \mathbf{X}$) (see Fig. 3). Phase-space measure $\mathcal{D}(\mathcal{L})$ is the product of discrete summations over α and q, spatial integration over $\mathbf{X}$ and functional integration over $\boldsymbol{\eta}(s)$ with normalized Gaussian measure $\mathcal{D}(\boldsymbol{\eta})$ defined by its covariance

$$\int \mathcal{D}(\boldsymbol{\eta}) \eta_\mu(s) \eta_\nu(t) = \delta_{\mu\nu} q \inf(s/q, t/q)(1 - \sup(s/q, t/q)). \tag{2.34}$$

Fugacity $z(\mathcal{L})$ reads [14, 19]

$$z(\mathcal{L}) = (-1)^{q-1} \frac{2}{q} \frac{z_\alpha^q}{(2\pi q \lambda_\alpha^2)^{3/2}} \times \exp\left[-\frac{\beta e^2}{2} \int_0^q \mathrm{d}s \int_0^q \mathrm{d}t (1 - \delta_{[s],[t]}) \tilde{\delta}(s-t) v(|\lambda_\alpha \boldsymbol{\eta}(s) - \lambda_\alpha \boldsymbol{\eta}(t)|) \right] \tag{2.35}$$

where $\tilde{\delta}(s-t) = \sum_{n=-\infty}^{\infty} \delta(s-t-n)$ is Dirac comb, while $[s]$ ($[t]$) denotes the integer part of s (t). In (2.35), factor $(1 - \delta_{[s],[t]})$ avoids counting point particle self-energy contributions, while Dirac comb ensures that only loop elements with equal times (modulo an integer) interact, an essential feature specific to quantum mechanics. Eventually, two-body potential $V(\mathcal{L}_i, \mathcal{L}_j)$ reduces to

$$V(\mathcal{L}_i, \mathcal{L}_j) = e_{\alpha_i} e_{\alpha_j} \int_0^{q_i} \mathrm{d}s \int_0^{q_j} \mathrm{d}t \tilde{\delta}(s-t) v(|\mathbf{X}_i + \lambda_{\alpha_i} \boldsymbol{\eta}_i(s) - \mathbf{X}_j - \lambda_{\alpha_j} \boldsymbol{\eta}_j(t)|). \tag{2.36}$$

At large distances, V behaves as the Coulomb potential between point charges $q_i e_{\alpha_i}$ and $q_j e_{\alpha_j}$, i.e. $V(\mathcal{L}_i, \mathcal{L}_j) \sim q_i q_j e_{\alpha_i} e_{\alpha_j} / |\mathbf{X}_i - \mathbf{X}_j|$. Therefore, usual Mayer diagrammatics for

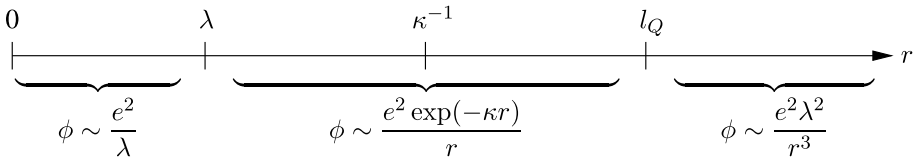

Fig. 4 Order of magnitude of effective potential ϕ at various distances. In region $\lambda < r < l_Q$, interactions are exponentially screened according to Debye potential. For $r > l_Q$, ϕ is dominated by (unscreened) multipolar interactions

loops are plagued with long-range divergences. As in the case of classical Coulomb fluids, they are removed by summing infinite chains built with V. This amounts to replace V by screened potential ϕ which can be viewed as the quantum analog of Debye potential [13]. The explicit formula for the Fourier transform of ϕ is recalled in Appendix A:. Its spatial behaviors, according to the hierarchy of scales displayed in Fig. 1, are roughly summarized in Fig. 4, where only orders of magnitude of ϕ are given (we set $r = |\mathbf{X}_i - \mathbf{X}_j|$ and omit all shape dependences which occur for $r < \lambda$ or $l_Q < r$). Notice that familiar exponential decay of ϕ breaks down at large distances $r \gg l_Q$. The asymptotic dipolar behavior of ϕ is sufficient for ensuring that every graph built with ϕ is finite [2, 3].

As detailed in [8], so-called screened cluster expansion for protonic density ρ_p follows from an exact transformation of formal Mayer diagrammatics for loop density $\rho(\mathcal{L}_a)$ which provides

$$\rho_p = \sum_G \frac{1}{S(G)} \int \mathcal{D}(C_a) Z_\phi^T(C_a) q_a \int \prod_{i=1}^{n} \mathcal{D}(C_i) Z_\phi^T(C_i) \Big[\prod \mathcal{F}_\phi \Big]_G \tag{2.37}$$

(a similar expression holds for ρ_e). In (2.37), bare potential V is replaced by screened potential ϕ. Graphs G are identical to usual Mayer graphs, where points are now particle clusters, except for some specific rules (arising from the replacement of V by ϕ) which are described below. Each cluster C_i $(i = 0, \ldots, n)$ contains $N_i^{(p)}$ protons and $N_i^{(e)}$ electrons. The internal state of a cluster $C(N_p, N_e)$ $(C \in \{C_i, i = 0, \ldots, n\})$ is determined by L_p and L_e loops $(\mathcal{L}_1^{(\alpha)}, \ldots, \mathcal{L}_{L_\alpha}^{(\alpha)})$ in which the N_p protons and N_e electrons are distributed (in root cluster $C_0 = C_a$, $\mathcal{L}_1^{(p)}$ is identified to $\mathcal{L}_a$ which contains the root proton). Integration within phase space measure $\mathcal{D}(C)$ reduces to the sum over all possible distributions of particles into loops combined with integrations over loop positions and shapes (with $\mathbf{X}_1^{(p)} = \mathbf{X}_a$ fixed at the origin for loop $\mathcal{L}_1^{(p)} = \mathcal{L}_a$). Statistical weight $Z_\phi^T(C)$ for a cluster $C(N_p, N_e)$ reads

$$Z_\phi^T(C) = \frac{\prod_{k=1}^{L_p} z_\phi(\mathcal{L}_k^{(p)}) \prod_{k=1}^{L_e} z_\phi(\mathcal{L}_k^{(e)})}{\prod_{q=1}^{N_p} n_p(q)! \prod_{q=1}^{N_e} n_e(q)!} \mathcal{B}_\phi^T(\{\mathcal{L}_k^{(\alpha)}\}), \tag{2.38}$$

where $n_\alpha(q)$ is the number of loops containing q particles of species α (for C_a, $n_p(q_a)!$ is replaced by $(n_p(q_a) - 1)!$). Weight $z_\phi(\mathcal{L})$ reduces to

$$z_\phi(\mathcal{L}) = z(\mathcal{L}) \exp[I_R(\mathcal{L})] \tag{2.39}$$

with ring sum $I_R(\mathcal{L})$ given by

$$I_R(\mathcal{L}) = \frac{1}{2} \int \mathcal{D}(\mathcal{L}_1) z(\mathcal{L}_1) \beta V(\mathcal{L}, \mathcal{L}_1) \beta \phi(\mathcal{L}_1, \mathcal{L}). \tag{2.40}$$

Truncated Mayer coefficient $\mathcal{B}^T_{\phi,N}$ is defined by a suitable truncation of usual Mayer coefficient $\mathcal{B}_{\phi,N}$ for N loops with pair interactions ϕ. This truncation ensures that $\mathcal{B}^T_{\phi,N}$ remains integrable over relative distances between loops when ϕ is replaced by V. First truncated Mayer coefficients are

$$\mathcal{B}^T_{\phi,1} = 1, \qquad \mathcal{B}^T_{\phi,2} = \exp(-\beta\phi) - 1 + \beta\phi - \frac{\beta^2\phi^2}{2!} + \frac{\beta^3\phi^3}{3!}, \qquad \ldots. \tag{2.41}$$

Bond $\mathcal{F}_\phi(C_i, C_j)$ can be either $-\beta\Phi$, $\beta^2\Phi^2/2!$, $-\beta^3\Phi^3/3!$, where total potential $\Phi(C_i, C_j)$ is the sum of pairwise interactions $\phi(\mathcal{L}, \mathcal{L}')$ over loops $\mathcal{L}$ and $\mathcal{L}'$ defining internal states of C_i and C_j respectively.

As for ordinary Mayer diagrams, two clusters are connected by at most one bond, and graph G is connected. Here, symmetry factor $S(G)$ is computed by permuting only clusters with identical numbers of protons and electrons. Moreover, for a cluster C different from C_a, the internal state of which is determined by a single loop $\mathcal{L}_1^{(\alpha)}$, when C is either, the intermediate cluster of a convolution $(-\beta\Phi) * (-\beta\Phi)$, or connected to the rest of the graph by a single bond $\beta^2\Phi^2/2!$, expression (2.38) of its statistical weight must be replaced by

$$Z^T_\phi(C) = z_\phi(\mathcal{L}_1^{(\alpha)}) - z(\mathcal{L}_1^{(\alpha)}). \tag{2.42}$$

Eventually, summation in (2.37) involves only graphs G which are no longer integrable over relative distances between clusters $\{C_i, i = 0, \ldots, n\}$ when ϕ is replaced by V. Screened cluster expansion for the pressure is inferred from use of (2.37) in thermodynamics identities, as described in Sect. 4.

3 Estimations of Ideal and Non-Ideal Contributions to Fugacity Expansions of Particle Densities

Now, we proceed to asymptotic estimations, in the Saha regime, of all contributions to $\rho = \rho_p$ in screened cluster expansion (2.37). Every contribution to ρ_p is expressed, similarly to (2.15) and (2.16), as ρ^* times a power of γ, and times a dimensionless temperature-dependent function. This provides a formal representation of ρ/ρ^* in powers of γ, where the coefficients depend only on temperature (see (4.2)). At low temperatures, every coefficient decays exponentially fast. In Sects. 3.1–3.6, we select all contributions which are smaller than leading terms (2.15) and (2.16) (divided by ρ^*) by exponentially decaying factors of maximum order $\exp(\beta E_H)$ ($\beta \to \infty$). In Sect. 3.7, we show that all other contributions decay faster by factors exponentially smaller than $\exp(\beta E_H)$. Beyond leading ideal contributions of ionized protons (2.15) and hydrogen atoms (2.16) (which are recovered in Sects. 3.1 and 3.2), we determine first corrections arising from their mutual interactions (Sects. 3.1, 3.4, 3.5 and 3.6). Such corrections are at most of order $(\rho^{id}_{p,e,at})^2$, so they are smaller than leading terms by exponential factor $\exp(\beta E_H)$. We also study ideal-like contributions of recombined entities, molecules H_2, ions H^- and H_2^+ (Sects. 3.3 and 3.6) which must be accounted for at that order. In the following, a graph with N_p protons and N_e electrons will be obviously denoted G_{N_p,N_e} (for $N_p + N_e > 1$, there are several graphs with identical particle numbers).

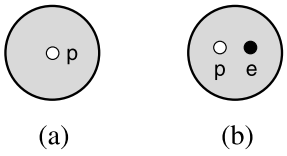

Fig. 5 Graphs representing simple entities: **a** ionized proton and **b** hydrogen atom

3.1 Ionized Proton and Plasma Polarization

An ionized proton appears in graph $G_{1,0}$ (see Fig. 5a) made with the sole root cluster C_a containing a single proton. The internal state of C_a is defined by the sole protonic loop $\mathcal{L}_a^{(p)}$ with $q_a = 1$. The contribution of $G_{1,0}$ to (2.37) then reads

$$\int \mathcal{D}(\boldsymbol{\xi}_a) z_\phi(\mathcal{L}_a^{(p)}) = \frac{2z_p}{(2\pi\lambda_p^2)^{3/2}} \int \mathcal{D}(\boldsymbol{\xi}_a) \exp(I_R(\mathcal{L}_a^{(p)})). \tag{3.1}$$

We stress that collective effects are embedded in ring sum $I_R(\mathcal{L}_a^{(p)})$. Thus, strictly speaking, $G_{1,0}$ describes an ionized proton dressed by the surrounding plasma of ionized protons and electrons. Within the present framework, that dressing mechanism accounts for the familiar plasma polarization induced by an immersed charge.

In the Saha regime, ring sum $I_R(\mathcal{L}_a^{(p)})$ can be evaluated by using the exact expression of ϕ (see Appendix A:). The corresponding asymptotic behavior can be easily recovered *via* the following simple estimation of convolution integral (2.40). At leading order, only terms $q_1 = 1$ ($\alpha_1 = p, e$) need to be retained into $\mathcal{D}(\mathcal{L}_1)$. Moreover the integration over position $\mathbf{X}_1$ is controlled by relative distances $|\mathbf{X}_1 - \mathbf{X}_a|$ of order κ^{-1}. At such distances, $\phi(\mathcal{L}_1, \mathcal{L}_a^{(p)})$ can be replaced by its Debye form, while $V(\mathcal{L}_a^{(p)}, \mathcal{L}_1)$ merely reduces to $ee_{\alpha_1}/|\mathbf{X}_1 - \mathbf{X}_a|$. This gives

$$I_R(\mathcal{L}_a^{(p)}) \sim \frac{\beta e^2 \kappa^2}{8\pi} \int \mathrm{d}\mathbf{X}_1 \int \mathcal{D}(\boldsymbol{\xi}_1) \frac{\exp(-\kappa|\mathbf{X}_1 - \mathbf{X}_a|)}{|\mathbf{X}_1 - \mathbf{X}_a|^2} \sim \frac{\beta e^2 \kappa}{2}, \tag{3.2}$$

in perfect agreement with the detailed analysis of Appendix A:.

Since $\beta e^2 \kappa$ is small (see Fig. 1), dressing effects in (3.1) can be treated perturbatively by expanding $\exp(I_R(\mathcal{L}_a^{(p)}))$ in powers of I_R. The resulting leading contribution of $G_{1,0}$ reads

$$\frac{2z_p}{(2\pi\lambda_p^2)^{3/2}} \int \mathcal{D}(\boldsymbol{\xi}_a) = \frac{2z_p}{(2\pi\lambda_p^2)^{3/2}} = \rho_p^{id} = \rho^* \gamma, \tag{3.3}$$

where functional integration over $\boldsymbol{\xi}_a$ merely reduces to 1 by normalization of Gaussian measure $\mathcal{D}(\boldsymbol{\xi}_a)$. That leading term reduces to ideal Maxwell-Boltzmann density of ionized protons (2.15) (i.e. bare contribution $z_p B_{1,0}$ as it should).

Taking into account (3.2), we find that first correction to (3.3) is rewritten as

$$\frac{2z_p}{(2\pi\lambda_p^2)^{3/2}} \int \mathcal{D}(\boldsymbol{\xi}_a) I_R(\mathcal{L}_a^{(p)}) \sim \frac{2z_p}{(2\pi\lambda_p^2)^{3/2}} \beta e^2 \kappa \int \mathcal{D}(\boldsymbol{\xi}_a) = \rho_p^{id} \frac{\beta e^2 \kappa}{2}. \tag{3.4}$$

Contribution (3.4) involves a factor $z^{3/2}$, and hence a factor $\gamma^{3/2}$ times $\exp(3\beta E_H/2)$. One factor $\exp(\beta E_H)$ may be absorbed into the prefactor ρ^*. It remains a factor $\exp(\beta E_H/2)$, which multiplies the remaining part of the contribution. Therefore, we rewrite (3.4) as

$$\rho_p^{id} \frac{\beta e^2 \kappa}{2} = \rho^* \gamma^{3/2} S_{3/2}(1, 0) \exp(\beta E_H/2), \tag{3.5}$$

where we define screening function

$$S_{3/2}(1,0) = \frac{(\beta|E_H|)^{3/4}}{\pi^{1/4}}. \tag{3.6}$$

Index 3/2 of screening function refers to the power of γ and $(1,0)$ to the single proton cluster. All subsequent contributions will be written according to the same prescription.

First correction (3.4) accounts for familiar plasma polarization induced by a single proton (i.e. cluster $(1,0)$) at lowest order. Its simple structure results from the almost classical and weakly coupled nature of the plasma mentioned in Sect. 2.3. Higher order collective corrections proportional to γ^p (with p integer or half-integer), can be rewritten similarly to (3.4) *via* the definition of screening functions $S_p(1,0)$ which depend only on β. For instance, next correction to (3.4) merely reduces to

$$\rho^* \gamma^2 S_2(1,0) \exp(\beta E_H), \tag{3.7}$$

with

$$S_2(1,0) = \frac{(\beta|E_H|)^{3/2}}{2\sqrt{\pi}} - \left(1 + \left(\frac{2m}{m_p}\right)^{1/2}\right)\frac{\beta|E_H|}{8}. \tag{3.8}$$

The first contribution in the r.h.s. of (3.8) arises from the quadratic term in the expansion of $\exp(I_R(\mathcal{L}_a^{(p)}))$, while the second one arises from the linear term where loop-shape dependence of $I_R(\mathcal{L}_a^{(p)})$ beyond classical form (3.3) is taken into account (see (A.11)). Further corrections are exponentially smaller than (3.7) as shown in Appendix A:.

The dressing mechanism associated with plasma polarization occurs for any particle in all other graphs G_{N_p,N_e}. At lowest order, every ring factor $\exp(I_R)$ can be replaced by 1, and first corrections are obtained by using (3.2).

3.2 Hydrogen Atom: Recombination and Dissociation Contributions

A hydrogen atom is expected to appear in graph $G_{1,1}$ made with single root cluster C_a (see Fig. 5b). The contribution of $G_{1,1}$ reads

$$\begin{aligned}
&\int \mathcal{D}(\boldsymbol{\xi}_a) z_\phi(\mathcal{L}_a^{(p)}) \int \mathrm{d}\mathbf{X}_1 \int \mathcal{D}(\boldsymbol{\xi}_1) z_\phi(\mathcal{L}_1^{(e)}) \mathcal{B}_\phi^T(\mathcal{L}_a^{(p)}, \mathcal{L}_1^{(e)}) \\
&= \frac{4 z_p z_e}{(2\pi\lambda^2)^3} \int \mathcal{D}(\boldsymbol{\xi}_a) \exp(I_R(a)) \int \mathrm{d}\mathbf{X}_1 \int \mathcal{D}(\boldsymbol{\xi}_1) \exp(I_R(1)) \\
&\quad \times \left[\exp(-\beta\phi(a,1)) - 1 + \beta\phi(a,1) - \frac{\beta^2\phi^2(a,1)}{2!} + \frac{\beta^3\phi^3(a,1)}{3!}\right]
\end{aligned} \tag{3.9}$$

(with obvious simplified notations for the dependence of I_R and ϕ on loops $\mathcal{L}_a^{(p)}$ and $\mathcal{L}_1^{(e)}$). In (3.9), protonic loop $\mathcal{L}_a^{(p)}$ and electronic loop $\mathcal{L}_1^{(e)}$ contain one proton ($q_a = 1$) and one electron ($q_1 = 1$) respectively. Each of those particles are dressed like the ionized proton in $G_{1,0}$. Furthermore, their mutual interaction ϕ involves screening effects, which are also due to the surrounding plasma of ionized protons and electrons. At leading order, since $\phi(a,1)$ reduces to V at finite distances $|\mathbf{X}_1 - \mathbf{X}_a|$ (see Appendix A:), $\mathcal{B}_\phi^T(a,1)$ can be replaced by $\mathcal{B}^T(a,1)$ defined by (2.41) with V in place of ϕ. The resulting bare contribution of $G_{1,1}$, as well as first corrections due to collective effects, are successively estimated as follows.

3.2.1 Bare Contribution in the Vacuum

The bare contribution of $G_{1,1}$ reads

$$\frac{4z_p z_e}{(2\pi\lambda^2)^3}\int \mathrm{d}\mathbf{X}_1 \int \mathcal{D}(\boldsymbol{\xi}_a)\mathcal{D}(\boldsymbol{\xi}_1) \times\left[\exp(-\beta V(a,1)) - 1 + \beta V(a,1) - \frac{\beta^2 V^2(a,1)}{2!} + \frac{\beta^3 V^3(a,1)}{3!}\right]. \quad (3.10)$$

In (3.10), functional integrations over shapes $\boldsymbol{\xi}_a$ and $\boldsymbol{\xi}_1$ can be exactly rewritten in terms of matrix elements of suitable operators by applying backwards Feynman-Kac formula (2.32). For the exponential factor in $\mathcal{B}^T(a,1)$, we obviously obtain

$$\frac{1}{(2\pi\lambda_p^2)^{3/2}(2\pi\lambda_e^2)^{3/2}}\int \mathcal{D}(\boldsymbol{\xi}_a)\mathcal{D}(\boldsymbol{\xi}_1)\exp(-\beta V(a,1)) = \langle \mathbf{R}_a\mathbf{r}_1|\exp(-\beta H_{1,1})|\mathbf{R}_a\mathbf{r}_1\rangle \quad (3.11)$$

with $\mathbf{R}_a = \mathbf{X}_a$ and $\mathbf{r}_1 = \mathbf{X}_1$. Functional integrations of powers of $V(a,1)$ in $\mathcal{B}^T(a,1)$, are related to the corresponding terms arising in Dyson expansion of $\langle \mathbf{R}_a\mathbf{r}_1|\exp(-\beta H_{1,1})|\mathbf{R}_a\mathbf{r}_1\rangle$ with respect to interaction part $V_{1,1}$ of $H_{1,1}$. Moreover, let us introduce position $\mathbf{R}^* = (m_p\mathbf{R}_a + m_e\mathbf{r}_1)/M$ of the atom mass center, and one-body Hamiltonian H_{pe} of relative particle with position $\mathbf{r}^* = \mathbf{r}_1 - \mathbf{R}_a$. Then, bare contribution (3.10) becomes

$$\rho^*\frac{\gamma^2}{8}Z(1,1)\exp(\beta E_H), \quad (3.12)$$

with

$$Z(1,1) = \frac{(2\pi\lambda_H^2)^{3/2}}{\Lambda}\mathrm{Tr}[\exp(-\beta H_{1,1})]^T_{\mathrm{Mayer}} = 4\int \mathrm{d}\mathbf{r}^*\langle\mathbf{r}^*|[\exp(-\beta H_{pe})]^T_{\mathrm{Mayer}}|\mathbf{r}^*\rangle, \quad (3.13)$$

where $[\exp(-\beta H_{pe})]^T_{\mathrm{Mayer}}$ stands for truncated Mayer operator

$$\begin{aligned}
&[\exp(-\beta H_{pe})]^T_{\mathrm{Mayer}}\\
&\quad = \exp(-\beta H_{pe}) - \exp(-\beta K_{pe})\\
&\qquad + \int_0^\beta \mathrm{d}\tau_1 \exp[-(\beta-\tau_1)K_{pe}]V_{pe}\exp[-\tau_1 K_{pe}]\\
&\qquad - \int_0^\beta \mathrm{d}\tau_1\int_0^{\tau_1}\mathrm{d}\tau_2 \exp[-(\beta-\tau_1)K_{pe}]V_{pe}\exp[-(\tau_1-\tau_2)K_{pe}]V_{pe}\exp[-\tau_2 K_{pe}]\\
&\qquad + \int_0^\beta \mathrm{d}\tau_1\int_0^{\tau_1}\mathrm{d}\tau_2\int_0^{\tau_2}\mathrm{d}\tau_3 \exp[-(\beta-\tau_1)K_{pe}]V_{pe}\exp[-(\tau_1-\tau_2)K_{pe}]\\
&\qquad \times V_{pe}\exp[-(\tau_2-\tau_3)K_{pe}]V_{pe}\exp[-\tau_3 K_{pe}] \quad (3.14)
\end{aligned}$$

($K_{pe} = -\hbar^2\Delta/(2m)$ and $V_{pe} = -e^2/r$).

Partition function (3.13) is similar to the so-called direct quantum virial function first introduced by Ebeling [23] (see Sect. 4.1). It incorporates contributions from both bound states (recombination of proton and electron into an hydrogen atom) and diffusion states (dissociation of an hydrogen atom into ionized proton and electron). Contrary to the trace of $[\exp(-\beta H_{pe})]_{\rm Mayer}$, $Z(1,1)$ is finite because $\langle \mathbf{r}^*|[\exp(-\beta H_{pe})]^T_{\rm Mayer}|\mathbf{r}^*\rangle$ decays as $1/(r^*)^4$ at large distances. Though truncation in $[\exp(-\beta H_{pe})]^T_{\rm Mayer}$ can be traced back to collective screening effects, $Z(1,1)$ depends only on temperature, and no longer on density.

In order to estimate (3.13) at low temperatures, we can heuristically extend the very simple argument used in Section 2.3 for estimating $B_{1,1}$. For $r^* \sim a_B$, contribution of ground state $\psi_0(r^*)$ of H_{pe} to $\langle \mathbf{r}^*|\exp(-\beta H_{pe})|\mathbf{r}^*\rangle$ exponentially dominates all other contributions because of the finite gap between E_H and the rest of the spectrum. Moreover, truncated terms in $[\exp(-\beta H_{pe})]^T_{\rm Mayer}$, which are crucial for ensuring the finiteness of the trace, do not generate exponentially growing terms at low temperatures, because they only involve Gibbs operators associated with kinetic Hamiltonian K_{pe}. Therefore, the leading behavior of (3.13) when $\beta \to \infty$, obtained by replacing $\langle \mathbf{r}^*|[\exp(-\beta H_{pe})]^T|\mathbf{r}^*\rangle$ by $|\psi_0(\mathbf{r}^*)|^2 \exp(-\beta E_H)$, merely is

$$Z(1,1) \sim 4\exp(-\beta E_H). \tag{3.15}$$

Beyond the previous heuristic argument, we present in Appendix B: a non-perturbative derivation of (3.15), which is quite useful for further purposes (see Sects. 3.3 and 3.7) since it provides convincing low-temperature estimations of quantities similar to (3.13) involving three or more particles.

Eventually, according to formula (3.12), the leading bare contribution of $G_{1,1}$ reads

$$\rho^* \frac{\gamma^2}{2}, \tag{3.16}$$

which is nothing but ideal contribution (2.16) of hydrogen atoms in their groundstate. Beyond leading term (3.16), the rest of the bare contribution of $G_{1,1}$ can be rewritten as

$$\rho^* \frac{\gamma^2}{8} Z_{exc}(1,1)\exp(\beta E_H), \tag{3.17}$$

with $Z_{exc}(1,1) = Z(1,1) - 4\exp(-\beta E_H)$. At low temperatures, leading contribution to (3.17) arises from the first excited level ($E_H^{(1)} = E_H/4$) of the hydrogen atom and reads

$$2\rho^*\gamma^2 \exp\left(\frac{3\beta E_H}{4}\right). \tag{3.18}$$

It can be viewed as the ideal density of hydrogen atoms in their first excited state. As expected, that level is less populated than the ground state by exponentially decaying Boltzmann factor $\exp(3\beta E_H/4)$ associated with energy difference $E_H^{(1)} - E_H = -3E_H/4$ (apart from the trivial factor 4 arising from orbital degeneracy of the first excited state).

If the identification of atomic states contributions (like (3.16) or (3.18)) makes sense in the zero-temperature limit defining Saha regime, at finite temperatures the definition of an atomic part Z_H in $Z(1,1)$ is arbitrary, as it has been noticed for a long time (see Ref. [39] and references quoted therein). That ambiguity is related to the fact that contributions of bound states with $|E_H^{(p)}| \leq k_B T$ cannot be disentangled from that of diffusion states since they have the same order of magnitude. A possible definition of Z_H is a finite sum of terms

analogous to (3.18) up to p_{max} such that $|E_H^{(p_{max})}| \simeq k_B T$: that procedure accounts for expected thermal ionization which prevents the existence of highly excited hydrogen atoms in so-called Rydberg states. As emphasized in Ref. [39], only the full contribution embedded in $Z(1,1)$, obviously independent of above arbitrariness, is relevant for thermodynamics. Notice that diffusion state contributions describe (unscreened) short-distance interactions between ionized proton and electron. Such contributions are similar to that involved in $G_{2,0}$ (see Sect. 3.3), and they are smaller than ideal contribution (3.16) by exponential factor $\exp(\beta E_H)$ apart from powers of β.

3.2.2 Collective Corrections

The first contributions of $G_{1,1}$ due to collective effects are obtained by expanding, in (3.9), ring factors $\exp(I_R(a))$ and $\exp(I_R(1))$ in powers of $I_R(a)$ and $I_R(1)$, and Mayer coefficient $\mathcal{B}_\phi^T(a,1)$ in powers of $(\phi - V)(a,1)$. At lowest order, $I_R(a)$ and $I_R(1)$ behave as $\beta e^2\kappa/2$, while $(\phi - V)(a,1)$ behaves as $e^2\kappa$ at distances $r < \beta e^2$. Therefore, first polarization corrections, which are smaller than leading bare contribution (3.16) by an extra factor $\beta e^2\kappa$, cancel out: an Hydrogen atom, which is a neutral entity, does not polarize its surrounding plasma at lowest order.

Collective corrections to (3.16) are then determined by the behavior of I_R and $(\phi - V)$ beyond the previous simple constants. In other words, the bare proton-electron Coulomb potential is modified, beyond the familiar Debye shift, by a coupling between quantum fluctuations of both particles and the surrounding plasma. That effect cannot be incorporated into an effective potential. The corresponding calculation, performed in Appendix A:, gives at lowest order,

$$\rho^* \gamma^3 S_3(1,1) \exp(2\beta E_H), \tag{3.19}$$

where screening function $S_3(1,1)$ for cluster $(1,1)$ is given by (A.16). Contribution (3.19) is exponentially smaller than (3.16) by factor $\exp(\beta E_H)$ and must be retained at that order, because $S_3(1,1)$ behaves as a power of β times $\exp(-\beta E_H)$ (see (A.17)). As shown in Appendix A:, higher order collective corrections decay exponentially faster than (3.19).

3.3 Other Complex Entities

3.3.1 Two-Proton Cluster

A two-proton cluster is described by graph $G_{2,0}$ made with single root cluster C_a (see Fig. 6a). There are two possible loop configurations for the internal state of root cluster C_a: either the two protons belong to two different loops $\mathcal{L}_a^{(p)}$ and $\mathcal{L}_1^{(p)}$, or they belong to a single loop $\mathcal{L}_a^{(p)}$. The corresponding contribution reads

$$\begin{aligned}
&\int \mathcal{D}(\boldsymbol{\xi}_a) z_\phi(\mathcal{L}_a^{(p)}) \int \mathrm{d}\mathbf{X}_1 \int \mathcal{D}(\boldsymbol{\xi}_1) z_\phi(\mathcal{L}_1^{(p)}) \mathcal{B}_\phi^T(\mathcal{L}_a^{(p)}, \mathcal{L}_1^{(p)}) + \int \mathcal{D}(\boldsymbol{\eta}_a) 2 z_\phi(\mathcal{L}_a^{(p)}) \\
&= \frac{4 z_p^2}{(2\pi\lambda_p^2)^3} \int \mathrm{d}\mathbf{X}_1 \int \mathcal{D}(\boldsymbol{\xi}_a)\mathcal{D}(\boldsymbol{\xi}_1) \exp(I_R(a)) \exp(I_R(1)) \\
&\quad \times \left[\exp(-\beta\phi(a,1)) - 1 + \beta\phi(a,1) - \frac{\beta^2\phi^2(a,1)}{2!} + \frac{\beta^3\phi^3(a,1)}{3!} \right] \\
&\quad - \frac{2 z_p^2}{(4\pi\lambda_p^2)^{3/2}} \int \mathcal{D}(\boldsymbol{\eta}_a) \exp(I_R(a)) \exp(-\beta U(a)).
\end{aligned} \tag{3.20}$$

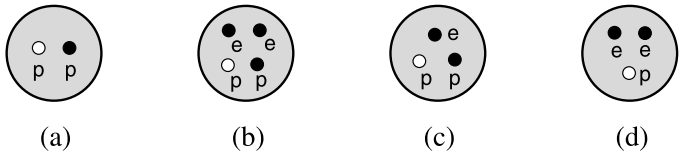

Fig. 6 Graphs representing various complex entities: **a** two-proton cluster; **b** molecule H_2; **c** ion H_2^+; **d** ion H^-

Like (3.9), (3.20) incorporates collective effects, i.e. dressing of each proton and screening of their mutual interactions.

At leading order, after applying backwards Feynman-Kac formula (2.32), we find that the bare contribution of Fig. 6a reduces to

$$\rho^* \frac{\gamma^2}{\sqrt{2}} \left(\frac{m}{m_p} \right)^{3/2} Z(2,0) \exp(\beta E_H), \tag{3.21}$$

with

$$\begin{aligned} Z(2,0) &= \frac{(\pi \lambda_p^2)^{3/2}}{\Lambda} \mathrm{Tr}[\exp(-\beta H_{2,0})]^T_{\mathrm{Mayer}} \\ &= \int \mathrm{d}\mathbf{r}^* \{ 2\langle \mathbf{r}^* | [\exp(-\beta H_{pp})]^T_{\mathrm{Mayer}} | \mathbf{r}^* \rangle - \langle -\mathbf{r}^* | \exp(-\beta H_{pp}) | \mathbf{r}^* \rangle \}. \end{aligned} \tag{3.22}$$

In (3.22), H_{pp} is the one-body Hamiltonian of relative particle with position $\mathbf{r}^* = \mathbf{R}_1 - \mathbf{R}_a$ and mass $m_{pp} = m_p/2$, $H_{pp} = K_{pp} + V_{pp}$ with $K_{pp} = -\hbar^2 \Delta/(2m_{pp})$ and $V_{pp} = e^2/r$. Moreover, $[\exp(-\beta H_{pp})]^T_{\mathrm{Mayer}}$ is defined as (3.14) with K_{pp} and V_{pp} in place of K_{pe} and V_{pe} respectively. Like $Z(1,1)$, $Z(2,0)$ is also merely related to Ebeling quantum virial functions (see Sect. 4.1). Thanks to truncation in $[\exp(-\beta H_{pp})]^T_{\mathrm{Mayer}}$, the integral over $\mathbf{r}^*$ does converge contrary to the integral in (2.25) that formally defines $B_{2,0}$. Because of the continuous nature of the spectrum of H_{pp} which starts at zero, $Z(2,0)$ behaves as a power law at low temperatures. Contribution (3.21) then decays faster than ρ^* by exponential factor $\exp(\beta E_H)$ (discarding powers of β).

Collective corrections to (3.21) arise from expansions of ring factors and of Mayer coefficient in (3.20). At lowest order, we can use $I_R(a) \sim I_R(1) \sim \beta e^2 \kappa/2$ and $(\phi - V)(a,1) \sim -e^2\kappa$ $(r < \beta e^2)$ for $q_a = q_1 = 1$, while $I_R(a) \sim 2\beta e^2 \kappa$ for $q_a = 2$. Therefore, the first polarization correction to (3.21), which can be treated at a purely classical level, is smaller than ρ^* by factor $\exp(3\beta E_H/2)$.

3.3.2 Molecule H_2

Contribution of a molecule H_2 is embedded in graph $G_{2,2}$ made with the single root cluster C_a containing two protons and two electrons (Fig. 6b). Again, dressing of particles as well as screening of their mutual interactions can be treated perturbatively in the Saha regime. At leading order, the resulting bare contribution of $G_{2,2}$ is then transformed into

$$\rho^* \gamma^4 \frac{\sqrt{2}}{32} \left(\frac{m}{M} \right)^{3/2} Z(2,2) \exp(3\beta E_H), \tag{3.23}$$

with

$$
\begin{aligned}
Z(2,2) &= \frac{(2\pi\lambda_{H_2}^2)^{3/2}}{\Lambda}\,\mathrm{Tr}[\exp(-\beta H_{2,2})]^T_{\mathrm{Mayer}} \\
&= (2\pi\lambda_{H_2}^2)^{3/2}\int \mathrm{d}\mathbf{R}_1\mathrm{d}\mathbf{r}_1\mathrm{d}\mathbf{r}_2\{4\langle\mathbf{R}_a\mathbf{R}_1\mathbf{r}_1\mathbf{r}_2|\exp(-\beta H_{2,2})|\mathbf{R}_a\mathbf{R}_1\mathbf{r}_1\mathbf{r}_2\rangle \\
&\quad - 2\langle\mathbf{R}_1\mathbf{R}_a\mathbf{r}_1\mathbf{r}_2|\exp(-\beta H_{2,2})|\mathbf{R}_a\mathbf{R}_1\mathbf{r}_1\mathbf{r}_2\rangle \\
&\quad - 2\langle\mathbf{R}_a\mathbf{R}_1\mathbf{r}_2\mathbf{r}_1|\exp(-\beta H_{2,2})|\mathbf{R}_a\mathbf{R}_1\mathbf{r}_1\mathbf{r}_2\rangle \\
&\quad + \langle\mathbf{R}_1\mathbf{R}_a\mathbf{r}_2\mathbf{r}_1|\exp(-\beta H_{2,2})|\mathbf{R}_a\mathbf{R}_1\mathbf{r}_1\mathbf{r}_2\rangle + \cdots\}
\end{aligned}
\tag{3.24}
$$

($\lambda_{H_2} = (\beta\hbar^2/(2M))^{1/2}$). Like (3.14), truncated Mayer operator $[\exp(-\beta H_{2,2})]^T_{\mathrm{Mayer}}$ is defined as a suitable truncation of $[\exp(-\beta H_{2,2})]_{\mathrm{Mayer}}$ inherited from the structure of coefficients $\mathcal{B}^T_{\phi,N}$ ($N = 1, 2, 3, 4$). In addition to the terms already present in $[\exp(-\beta H_{2,2})]_{\mathrm{Mayer}}$, that truncation involves products of imaginary-time evolutions of interaction potentials between subsets of two protons and two electrons (for our purpose, it is not necessary to detail here all the numerous terms involved in that truncation). This ensures that $[\exp(-\beta H_{2,2})]^T_{\mathrm{Mayer}}$ has a finite trace contrary to $[\exp(-\beta H_{2,2})]_{\mathrm{Mayer}}$.

Similarly to (3.13), partition function (3.24) incorporates contributions from both recombination into molecules H_2, and dissociation (interactions at short distances between atoms H, ions H_2^+, ions H^-, ionized protons and ionized electrons). At low temperatures, the leading behavior of $Z(2,2)$ is determined by applying the method described in Appendix B:. A key ingredient is the discrete nature of the spectrum of $H_{2,2}$ (discarding the trivial contribution of the center of mass) near its infimum. Moreover, we assume quite weak bounds for three- and four-body Coulomb Green functions, inspired in part from their known exact two-body counterparts [36]. Then, we show that leading contribution to $Z(2,2)$ arises from the first four terms in the r.h.s of (3.24) evaluated for the ground state of molecule H_2 with energy $E_{H_2} = E^{(0)}_{2,2}$. Thus, despite truncated terms beyond matrix elements of $\exp(-\beta H_{2,2})$ not written explicitly in the r.h.s. of (3.24), are crucial for ensuring finiteness of $Z(2,2)$, they do not affect its leading low-temperature behavior which merely reads

$$
Z(2,2) \sim \exp(-\beta E_{H_2}) \tag{3.25}
$$

when $\beta \to \infty$. Since H_2 contains two protons, the resulting contribution (3.23) is twice ideal density $\rho^{id}_{H_2}$ of molecules H_2 in their para-groundstate where the two protons, as well as the two electrons, have opposite spin orientations, while the total angular momentum is zero.

First thermal corrections to (3.25) arise from molecular excited states. Contrarily to the atomic case, such states are not exactly known. However, according to the usual phenomenology, they are expected to be well described by para-states and ortho-states (the two protons have the same spin orientation) with non-zero angular momenta describing global rotations of the molecule [42]. Moreover, excited states with still higher energies can be associated with proton vibrations and ultimately electronic excitations [42].

Beyond above purely molecular terms, $Z(2,2)$ also incorporates short-range contributions which account for interactions between products of molecular dissociation, as well as the corresponding exchange effects. Similarly to the case of $Z(1,1)$ where atomic contributions are mixed to those of interactions between ionized-charges, the extraction of either a molecular part Z_{H_2} or an atom-atom contribution in $Z(2,2)$, remains arbitrary. Again, that arbitrariness does not cause any trouble for thermodynamics which depend only on the full contribution $Z(2,2)$.

Collective corrections to (3.23) embedded in $G_{2,2}$ can be studied as above (see Sect. 3.2). Like atom H, molecule H_2 is neutral so it does not polarize (at lowest order) the surrounding plasma. First collective corrections are then smaller than (3.25) by an extra factor $(\beta e^2\kappa)^2$ of order $\exp(\beta E_H)$. Therefore, they are smaller than ρ^* by a factor $\exp[\beta(4E_H - E_{H_2})]$, which is itself exponentially smaller than $\exp(\beta E_H)$ by virtue of inequality $3E_H < E_{H_2}$.

3.3.3 Ions H^- and H_2^+

Ions H_2^+ and H^- appear in graphs $G_{2,1}$ (Fig. 6c) and $G_{1,2}$ (Fig. 6d) respectively. The corresponding bare contributions are rewritten as

$$\rho^* \frac{\gamma^3}{16} \left(\frac{m_e(M+m_p)}{M^2} \right)^{3/2} Z(2,1) \exp(2\beta E_H) \tag{3.26}$$

and

$$\rho^* \frac{\gamma^3}{32} \left(\frac{m_p(M+m_e)}{M^2} \right)^{3/2} Z(1,2) \exp(2\beta E_H), \tag{3.27}$$

with

$$Z(2,1) = \frac{(2\pi\lambda_{H_2^+}^2)^{3/2}}{\Lambda} \mathrm{Tr}[\exp(-\beta H_{2,1})]^T_{\mathrm{Mayer}} \tag{3.28}$$

and

$$Z(1,2) = \frac{(2\pi\lambda_{H^-}^2)^{3/2}}{\Lambda} \mathrm{Tr}[\exp(-\beta H_{1,2})]^T_{\mathrm{Mayer}} \tag{3.29}$$

($\lambda_{H_2^+} = (\beta\hbar^2/(M+m_p))^{1/2}$ and $\lambda_{H^-} = (\beta\hbar^2/(M+m_e))^{1/2}$). Truncated Mayer operators $[\exp(-\beta H_{2,1})]^T_{\mathrm{Mayer}}$ and $[\exp(-\beta H_{1,2})]^T_{\mathrm{Mayer}}$ are defined similarly to $[\exp(-\beta H_{2,2})]^T_{\mathrm{Mayer}}$ and $[\exp(-\beta H_{1,1})]^T_{\mathrm{Mayer}}$. The low-temperature behaviors of (3.26) and (3.27) are determined by applying the method described in Appendix B:. As for (3.13) and (3.24), truncated terms beyond $\exp(-\beta H_{2,1})$ or $\exp(-\beta H_{1,2})$ do not contribute at leading order. Therefore, we find that (3.26) behaves as

$$\rho^* \frac{\gamma^3}{8} \left(\frac{m_e(M+m_p)}{M^2} \right)^{3/2} \exp[\beta(2E_H - E_{H_2^+})] = 2\rho_{H_2^+}^{id}, \tag{3.30}$$

where $\rho_{H_2^+}^{id}$ is the ideal density of ions H_2^+ in their groundstate with energy $E_{H_2^+} = E_{2,1}^{(0)}$, which is doubly degenerated because of electron spin. Similarly, we obtain leading behavior of (3.27), i.e.

$$\rho^* \frac{\gamma^3}{16} \left(\frac{m_p(M+m_e)}{M^2} \right)^{3/2} \exp[\beta(2E_H - E_{H^-})] = \rho_{H^-}^{id}, \tag{3.31}$$

where $\rho_{H^-}^{id}$ is the ideal density of ions H^- in their groundstate with energy $E_{H^-} = E_{1,2}^{(0)}$, which is doubly degenerated because of proton spin. Like (3.23), those ideal contributions decay exponentially faster than ρ^* in the Saha regime. Density effects embedded in $G_{2,1}$ and $G_{1,2}$ are similar to those encountered above for an ionized proton. They provide contributions which are smaller than ρ^* by factors $\exp(\beta(5E_H/2 - E_{H_2^+}))$ and $\exp(\beta(5E_H/2 - E_{H^-}))$, while such factors are themselves exponentially small compared

to $\exp(\beta E_H)$ by virtue of inequalities $3E_H/2 < E_{H_2^+}$ and $3E_H/2 < E_{H^-}$ (see numerical values given in Sect. 2.3).

3.4 Interactions between Ionized Charges beyond Polarization Effects

Since the Saha regime is quite diluted and weakly coupled (see Sect. 2.3), leading contributions of screened interactions are embedded in the polarization mechanism described in Sect. 3.1 for a graph with a single particle. This provides well-known Debye correction (3.4). Beyond that mean-field contribution, next contributions of interactions between ionized charges arise from graphs involving two particles, namely $G_{1,1}$ and $G_{2,0}$ shown in Figs. 5b, 6a and 7a–c. As quoted above, graphs made with one cluster (Figs. 5b and 6a) involve contributions of unscreened interactions at short distances. Graphs made with two clusters, C_a (one proton) and C_1 (one proton or one electron), connected by a single bond $\mathcal{F}_\phi(C_a, C_1)$ which can be either $-\beta\Phi$ (Fig. 7a), $\beta^2\Phi^2/2!$ (Fig. 7b), or $-\beta^3\Phi^3/3!$ (Fig. 7c), account for large-distance screened contributions which are estimated as follows.

Graphs shown in Fig. 7a (with $\alpha = p, e$) provide contribution

$$
\begin{aligned}
&-\beta \int \mathrm{d}\mathbf{X}_1 \int \mathcal{D}(\boldsymbol{\xi}_a)\mathcal{D}(\boldsymbol{\xi}_1) z_\phi(\mathcal{L}_a^{(p)})[z_\phi(\mathcal{L}_1^{(p)})\phi(\mathcal{L}_a^{(p)}, \mathcal{L}_1^{(p)}) + z_\phi(\mathcal{L}_1^{(e)})\phi(\mathcal{L}_a^{(p)}, \mathcal{L}_1^{(e)})] \\
&\quad = -\frac{4\beta z_p}{(2\pi\lambda_p^2)^{3/2}} \int \mathrm{d}\mathbf{X}_1 \int \mathcal{D}(\boldsymbol{\xi}_a)\mathcal{D}(\boldsymbol{\xi}_1) \exp(I_R(\mathcal{L}_a^{(p)})) \\
&\qquad \times \left[\frac{z_p}{(2\pi\lambda_p^2)^{3/2}} \exp(I_R(\mathcal{L}_1^{(p)}))\phi(\mathcal{L}_a^{(p)}, \mathcal{L}_1^{(p)}) \right. \\
&\qquad \left. + \frac{z_e}{(2\pi\lambda_e^2)^{3/2}} \exp(I_R(\mathcal{L}_1^{(e)}))\phi(\mathcal{L}_a^{(p)}, \mathcal{L}_1^{(e)}) \right].
\end{aligned}
\tag{3.32}
$$

The expansion of ring factors $\exp(I_R(\mathcal{L}_a^{(p)}))$ and $\exp(I_R(\mathcal{L}_1^{(p)}))$ provides a first contribution which vanishes by virtue of identity (A.3) derived in Appendix A:. The first non-vanishing contribution arises from linear terms $I_R(\mathcal{L}_1^{(p)})$ and $I_R(\mathcal{L}_1^{(e)})$ where loop-shape dependences beyond classical behavior (3.2) are included. At lowest order, ϕ can then be replaced by its classical Debye form, and the resulting leading contribution of Fig. 7a is

$$
-\rho^* \frac{\gamma^2}{2} [S_2(1,0) - S_2(0,1)] \exp(\beta E_H) \tag{3.33}
$$

with

$$
S_2(0,1) = \frac{(\beta|E_H|)^{3/2}}{2\sqrt{\pi}} - \left(1 + \left(\frac{2m}{m_e}\right)^{1/2}\right) \frac{\beta|E_H|}{8}, \tag{3.34}
$$

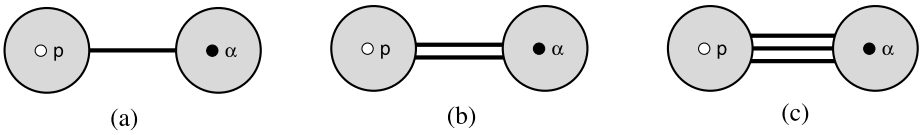

Fig. 7 Graphs describing screened interactions between one proton and one electron ($\alpha = e$), or between two ionized protons ($\alpha = p$)

which follows from (A.11). Further contributions decay exponentially faster than $\rho^* \exp(\beta E_H)$.

Because weight of cluster C_1 has specific form (2.42), contribution of Fig. 7b reads

$$\begin{aligned}
&\frac{\beta^2}{2}\int \mathrm{d}\mathbf{X}_1 \int \mathcal{D}(\boldsymbol{\xi}_a)\mathcal{D}(\boldsymbol{\xi}_1) z_\phi(\mathcal{L}_a^{(p)})[(z_\phi(\mathcal{L}_1^{(p)}) - z(\mathcal{L}_1^{(p)}))\phi^2(\mathcal{L}_a^{(p)}, \mathcal{L}_1^{(p)}) \\
&\quad + (z_\phi(\mathcal{L}_1^{(e)}) - z(\mathcal{L}_1^{(e)}))\phi^2(\mathcal{L}_a^{(p)}, \mathcal{L}_1^{(e)})] \\
&= \frac{2\beta^2 z_p}{(2\pi\lambda_p^2)^{3/2}} \int \mathrm{d}\mathbf{X}_1 \int \mathcal{D}(\boldsymbol{\xi}_a)\mathcal{D}(\boldsymbol{\xi}_1) \exp(I_R(\mathcal{L}_a^{(p)})) \\
&\quad \times \left[\frac{z_p}{(2\pi\lambda_p^2)^{3/2}} (\exp(I_R(\mathcal{L}_1^{(p)})) - 1)\phi^2(\mathcal{L}_a^{(p)}, \mathcal{L}_1^{(p)}) \right. \\
&\quad \left. + \frac{z_e}{(2\pi\lambda_e^2)^{3/2}} (\exp(I_R(\mathcal{L}_1^{(e)})) - 1)\phi^2(\mathcal{L}_a^{(p)}, \mathcal{L}_1^{(e)}) \right].
\end{aligned} \tag{3.35}$$

At lowest order, we can replace factors $(\exp(I_R(\mathcal{L}_1^{(p)})) - 1)$ and $(\exp(I_R(\mathcal{L}_1^{(e)})) - 1)$ by $\beta e^2\kappa/2$ on one hand, and ϕ by its classical Debye form on another hand. This provides the leading contribution of (3.35)

$$\begin{aligned}
&(\rho_p^{id})^2 \frac{\beta^3 e^6}{2}\kappa \int \mathrm{d}\mathbf{X}_1 \frac{\exp(-2\kappa|\mathbf{X}_1 - \mathbf{X}_a|)}{|\mathbf{X}_1 - \mathbf{X}_a|^2} \\
&\quad = \pi(\rho_p^{id})^2\beta^3 e^6 = \rho^*\gamma^2[W(1,0|1,0) + W(1,0|0,1)]\exp(\beta E_H)
\end{aligned} \tag{3.36}$$

with

$$W(1,0|1,0) = W(1,0|0,1) = \frac{(\beta|E_H|)^{3/2}}{4\sqrt{\pi}}, \tag{3.37}$$

in agreement with asymptotic formula (A.6) derived in Appendix A:. Functions W can be interpreted as resulting from effective interactions between ionized charges generated by quadratic fluctuations of ϕ. Next corrections to (3.36) decay exponentially faster than $\rho^* \exp(\beta E_H)$, as inferred from (A.6) and (A.11).

Eventually, contribution of Fig. 7c is

$$\begin{aligned}
&\frac{-\beta^3}{3!}\int \mathrm{d}\mathbf{X}_1 \int \mathcal{D}(\boldsymbol{\xi}_a)\mathcal{D}(\boldsymbol{\xi}_1) z_\phi(\mathcal{L}_a^{(p)}) \left[z_\phi(\mathcal{L}_1^{(p)})\phi^3(\mathcal{L}_a^{(p)}, \mathcal{L}_1^{(p)}) + z_\phi(\mathcal{L}_1^{(e)})\phi^3(\mathcal{L}_a^{(p)}, \mathcal{L}_1^{(e)}) \right] \\
&\quad = -\frac{2\beta^3 z_p}{3(2\pi\lambda_p^2)^{3/2}} \int \mathrm{d}\mathbf{X}_1 \int \mathcal{D}(\boldsymbol{\xi}_a)\mathcal{D}(\boldsymbol{\xi}_1) \exp(I_R(\mathcal{L}_a^{(p)})) \\
&\quad \times \left[\frac{z_p}{(2\pi\lambda_p^2)^{3/2}} \exp(I_R(\mathcal{L}_1^{(p)}))\phi^3(\mathcal{L}_a^{(p)}, \mathcal{L}_1^{(p)}) \right. \\
&\quad \left. + \frac{z_e}{(2\pi\lambda_e^2)^{3/2}} \exp(I_R(\mathcal{L}_1^{(e)}))\phi^3(\mathcal{L}_a^{(p)}, \mathcal{L}_1^{(e)}) \right],
\end{aligned} \tag{3.38}$$

with $q_a = q_1 = 1$, $\boldsymbol{\eta}_a^{(p)} = \boldsymbol{\xi}_a$ and $\boldsymbol{\eta}_1^{(p,e)} = \boldsymbol{\xi}_1$. All collective effects can be omitted in (3.38) at lowest order, so leading contribution reads

$$-\rho^* \gamma^2 \frac{c_p (\beta |E_H|)^{3/2}}{12\pi^{3/2}} \exp(\beta E_H) \tag{3.39}$$

with numerical constant c_p given by (A.8). Next corrections to (3.39) decay exponentially faster than $\rho^* \exp(\beta E_H)$.

3.5 Interactions between an Atom and an Atom or an Ionized Charge

As argued in Sect. 2.3, atoms H are expected to be weakly coupled under Saha conditions, like ionized charges (see Sects. 3.1 and 3.4). Leading contributions of interactions between atoms and ionized charges should then involve either two atoms or a single one. As quoted in Sect. 3.3, short-range parts of those contributions are embedded in Figs. 6b–d made with a single cluster. Here, we consider other graphs made with two clusters which account for complementary parts including long-range effects.

3.5.1 Atom-Atom Interactions

Figures 8a–c describe interactions between two atoms. Contrary to the case of ionized charges, screening effects can now be omitted at leading order, because each atom is neutral. In other words, potential $\Phi(C_a, C_1)$ between clusters C_a and C_1 can be replaced by its bare counterpart $V(C_a, C_1)$, which decays as a dipolar interaction (the corresponding $1/R^3$-decay is sufficient for ensuring integrability in Fig. 8a for symmetry reasons). Of course, in statistical weights defining internal states of C_a and C_1, collective effects can be also ignored at leading order. Then contribution of Fig. 8a vanishes by symmetry, while the resulting bare contributions of Figs. 8b and 8c can be rewritten in terms of matrix elements of Gibbs operators by applying backwards Feynman-Kac formula (2.32). Leading contribution of Fig. 8b reads

$$\begin{aligned} z_p^2 z_e^2 \int \mathrm{d}\mathbf{R}_1 \mathrm{d}\mathbf{r}_1 \mathrm{d}\mathbf{r}_2 \Big\{ & 16 \langle \mathbf{R}_a \mathbf{R}_1 \mathbf{r}_1 \mathbf{r}_2 | \\ & \times \int_0^\beta \mathrm{d}\tau_1 \int_0^{\tau_1} \mathrm{d}\tau_2 \exp[-(\beta - \tau_1)(H_{at} + H_{at})] V_{at,at} \\ & \times \exp[-(\tau_1 - \tau_2)(H_{at} + H_{at})] V_{at,at} \\ & \times \exp[-\tau_2 (H_{at} + H_{at})] | \mathbf{R}_a \mathbf{R}_1 \mathbf{r}_1 \mathbf{r}_2 \rangle + \cdots \Big\}, \end{aligned} \tag{3.40}$$

where $H_{at} = H_{1,1}$ is the Hamiltonian of a single atom, while $V_{at,at}$ is the interaction potential between two atoms. Terms $\cdots$ in (3.40) have a structure analogous to those subtracted

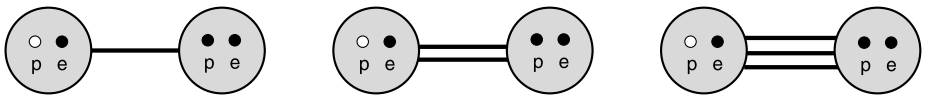

Fig. 8 Graphs accounting for interactions between two hydrogen atoms

from $\exp(-\beta H_{pe})$ in (3.14). The corresponding truncation, inherited from that in the $\mathcal{B}^T$'s, is analogous to that defining individual atomic partition functions: it ensures that spatial integration over $\mathbf{R}_1, \mathbf{r}_1, \mathbf{r}_2$ does converge. An expression similar to (3.40) can be obtained for Fig. 8c.

Full bare contribution of Figs. 8b and 8c takes the form (see Appendix C:)

$$\rho^* \gamma^4 W(1,1|1,1) \exp(3\beta E_H), \tag{3.41}$$

discarding terms which decay exponentially faster than $\rho^* \exp(\beta E_H)$. When $\beta \to \infty$, $W(1,1|1,1)$ behaves as

$$W(1,1|1,1) \sim \frac{c_{at,at}}{32\pi^{3/2}(\beta|E_H|)^{1/2}} \exp(-2\beta E_H) \tag{3.42}$$

where $c_{at,at}$ is the pure numerical coefficient (C.1). Function $W(1,1|1,1)$ accounts for unscreened interactions between two hydrogen atoms in their groundstate. Contributions from both short and large separations R are involved. In particular, contributions from familiar van der Waals interactions $U_{H-H}(R) = -A_{H-H}/R^6$ (with positive constant A_{H-H} computed from quantum perturbation theory at zero temperature [42]), do emerge through the large-distance ($R = |\mathbf{R}_2^* - \mathbf{R}_1^*| \gg \lambda_H$) behavior

$$\begin{aligned} &\langle \mathbf{R}_a \mathbf{R}_1 \mathbf{r}_1 \mathbf{r}_2 | \int_0^\beta \mathrm{d}\tau_1 \int_0^{\tau_1} \mathrm{d}\tau_2 \exp[-(\beta-\tau_1)(H_{at}+H_{at})] V_{at,at} \\ &\quad \times \exp[-(\tau_1-\tau_2)(H_{at}+H_{at})] V_{at,at} \exp[-\tau_2(H_{at}+H_{at})] | \mathbf{R}_a \mathbf{R}_1 \mathbf{r}_1 \mathbf{r}_2 \rangle \\ &\sim -\frac{\exp(-2\beta E_H)}{(2\pi\lambda_H^2)^3} |\psi_0(r_1^*)|^2 |\psi_0(r_2^*)|^2 \beta U_{H-H}(|\mathbf{R}_1^* - \mathbf{R}_2^*|), \end{aligned} \tag{3.43}$$

for spatial configurations $r_1^* \sim r_2^* \sim a_B$ and sufficiently low temperatures.

Collective corrections to (3.41) are exponentially smaller than its leading behavior. Notice that they arise from various effects: plasma polarization associated with ring factors $\exp(I_R)$, Debye exponential screening of interactions at scales κ^{-1}, and also modification of $1/R^6$-tails at distances larger than l_Q as detailed elsewhere [9].

3.5.2 Atom-Proton and Atom-Electron Interactions

Figs. 9a–f account for interactions between one atom H and a single ionized charge. Leading contribution of Fig. 9a (obtained by replacing ring factors by 1) vanishes by virtue of

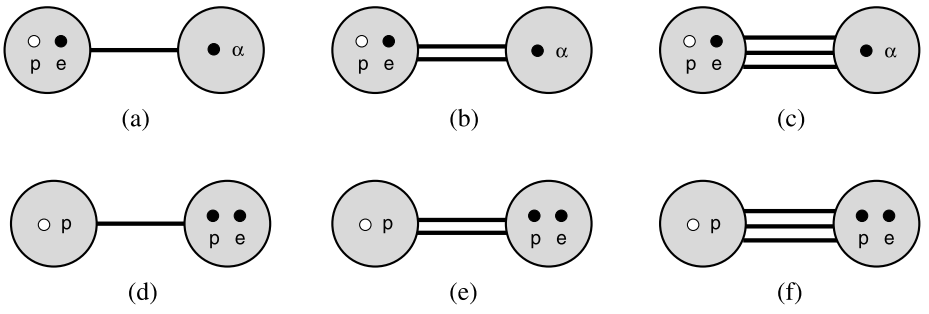

Fig. 9 Graphs accounting for interactions between a hydrogen atom and an ionized charge ($\alpha = p$ or e)

identity (A.3). Like Fig. 8a, bare contribution of Fig. 9d also vanishes for symmetry reasons. Therefore contributions of Figs. 9a and 9d decay faster than $\rho^* \exp(\beta E_H)$. Figs. 9e and 9f provide contributions obviously identical to that of Figs. 9b and 9c with $\alpha = p$. In Figs. 9b and 9c, all collective effects can be neglected at leading order, in particular $\phi(C_a, C_1)$ can be replaced by bare potential $V(C_a, C_1)$. Within that substitution, integrability at large distances R between C_a and C_1, is obviously ensured thanks to dipole-charge $1/R^2$ decay of $V(C_a, C_1)$. The resulting bare contributions of above graphs are rewritten in terms of matrix elements of Gibbs operators similarly to (3.40). For instance, bare contribution of Fig. 9b with $\alpha = p$ reads

$$z_p^2 z_e \int \mathrm{d}\mathbf{R}_1 \mathrm{d}\mathbf{r}_1 \{8\langle \mathbf{R}_a \mathbf{R}_1 \mathbf{r}_1| \int_0^\beta \mathrm{d}\tau_1 \int_0^{\tau_1} \mathrm{d}\tau_2 \exp[-(\beta-\tau_1)(H_{at}+H_p)] V_{at,p} \\ \times \exp[-(\tau_1-\tau_2)(H_{at}+H_p)] V_{at,p} \exp[-\tau_2(H_{at}+H_p)] |\mathbf{R}_a \mathbf{R}_1 \mathbf{r}_1\rangle + \cdots\} \quad (3.44)$$

where $H_p = H_{1,0}$ is the Hamiltonian of a single proton, while $V_{at,p}$ is the total interaction potential between an atom and a proton. Like in (3.40), terms $\cdots$ in (3.44) have a structure analogous to those subtracted from $\exp(-\beta H_{pe})$ in (3.14), which ensures spatial integrability over $\mathbf{R}_1$ and $\mathbf{r}_1$. Bare contributions of the other considered graphs can be expressed similarly to (3.44).

As shown in Appendix C:, the full bare contribution of Figs. 9a–f behaves as

$$\rho^* \gamma^3 [2W(1,1|1,0) + W(1,1|0,1)] \exp(2\beta E_H), \quad (3.45)$$

plus terms which decay exponentially faster than $\rho^* \exp(\beta E_H)$ when $\beta \to \infty$. Functions $W(1,1|1,0)$ and $W(1,1|0,1)$ account for unscreened interactions between an atom in its groundstate and an ionized charge. Their low-temperature behaviors are

$$W(1,1|1,0) \sim \frac{c_{at,p}}{16\pi^{3/2}(\beta|E_H|)^{1/2}} \exp(-\beta E_H), \\ W(1,1|0,1) \sim \frac{c_{at,e}}{16\pi^{3/2}(\beta|E_H|)^{1/2}} \exp(-\beta E_H) \quad (3.46)$$

where $c_{at,\alpha}$ are pure numerical constants (C.3). Long-range contributions to $W(1,1|1,0)$ and $W(1,1|0,1)$ do reduce to that of the attractive interactions $U_{H-\alpha}(R) = -A_{H-\alpha}/R^4$ between an atom H and an ionized charge, with positive constant $A_{H-p} = A_{H-e}$ computed within quantum perturbation theory at zero temperature.

First collective corrections result from plasma polarization by the considered ionized charges, and they reduce to (3.45) multiplied by simple factor $\beta e^2 \kappa/2$ of order $\exp(\beta E_H/2)$. As for atom-atom interactions, part of further density corrections result from screening of atom-proton or atom-electron interactions at large distances.

3.6 Interactions between an Ionized Proton and Charged Clusters

Screened interactions between an ionized proton and charged clusters are embedded in any graph made with a root cluster C_a containing a single proton connected to a charged cluster C_1 *via* a bond $-\beta\Phi$. As shown below, such a graph provides a contribution which behaves, at leading order, as that of the part connected to C_a through C_1. Moreover, that mechanism enforces charge neutrality ($\rho_p = \rho_e$) by symmetrizing protonic and electronic contributions to SCE of ρ_p.

3.6.1 Two-Proton and Two-Electron Clusters

In Figs. 10a and 10b, C_1 contains either two protons or two electrons. Leading contribution of Fig. 10a arises from relative distances between clusters C_a and C_1 of order κ^{-1}, while relative distances between particles inside cluster C_1 are of order βe^2. For such configurations, $\Phi(C_a, C_1)$ can be replaced by its Debye classical form $-2\beta e^2 \exp(-\kappa X)/X$, where $\mathbf{X}$ is the relative distance between C_a and C_1 (cluster C_1 carries a total charge $2e$). At the same time, statistical weights Z_ϕ^T can be replaced by their bare forms. Then, integration over internal degrees of freedom of C_1 merely provides half contribution (3.21) of Fig. 6a made with a single root cluster identical to C_1: that factor $1/2$ arises from the combinatorics specific to root cluster of any graph (see comment after formula (2.38) and factor q_a in the corresponding contribution). Integration over internal degrees of freedom of C_a obviously provides ρ_p^{id}, while the remaining spatial integration over $\mathbf{X}$ reduces to

$$\int \mathrm{d}\mathbf{X}\left[-2\beta e^2 \frac{\exp(-\kappa X)}{X}\right] = -\frac{8\pi\beta e^2}{\kappa^2} = -\frac{1}{\rho_p^{id}}. \tag{3.47}$$

Eventually, leading contribution of Fig. 10a is

$$-\rho^* \frac{\gamma^2}{2\sqrt{2}} \left(\frac{m}{m_p}\right)^{3/2} Z(2,0) \exp(\beta E_H), \tag{3.48}$$

i.e. minus half bare contribution (3.21) of Fig. 6a. Next corrections to (3.47) decay exponentially faster than $\rho^* \exp(\beta E_H)$. A similar calculation provides leading contribution of Fig. 10b

$$\rho^* \frac{\gamma^2}{2\sqrt{2}} \left(\frac{m}{m_e}\right)^{3/2} Z(0,2) \exp(\beta E_H), \tag{3.49}$$

where we have used that C_1 carries a charge $-2e$. Next corrections to (3.49) also decay exponentially faster than $\rho^* \exp(\beta E_H)$.

3.6.2 Ions

Leading contributions of Figs. 10c and 10d can be treated as above. Taking into account that ion H_2^+ carries a charge e, we find for Fig. 10c

$$-\rho^* \frac{\gamma^3}{64} \left(\frac{m_e(M+m_p)}{M^2}\right)^{3/2} Z(2,1) \exp(2\beta E_H), \tag{3.50}$$

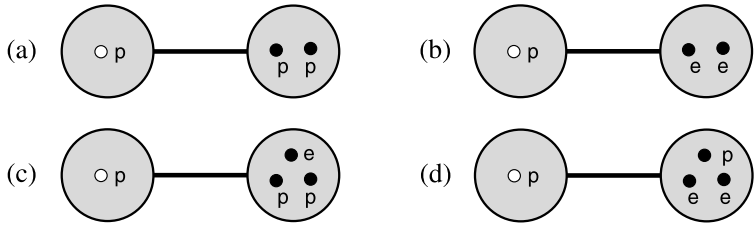

Fig. 10 Graphs accounting for interactions between an ionized proton and a charged cluster

i.e. minus one fourth bare contribution (3.26) of Fig. 6c. For Fig. 10d, no combinatorics factor $1/2$ appears when integrating over internal degrees of freedom of C_1 because C_1 contains a single proton. Since C_1 carries a charge $-e$, leading contribution of Fig. 10d becomes

$$\rho^* \frac{\gamma^3}{64} \left(\frac{m_p(M+m_e)}{M^2} \right)^{3/2} Z(1,2) \exp(2\beta E_H), \tag{3.51}$$

i.e. half bare contribution (3.27) of Fig. 6d. Contributions (3.50) and (3.51) can be interpreted as the modification of density of ionized protons due to their coupling with ions H_2^+ and H^- respectively. As mentioned above, those contributions added to that of Figs. 6c and 6d provide a full contribution to ρ_p which is indeed identical to that relative to ρ_e. Thus, charge neutrality is indeed enforced by the structure of SCE (2.37).

Next corrections to (3.50) and (3.51) decay exponentially faster than $\rho^* \exp(\beta E_H)$, as well as all other non-ideal contributions of ions H_2^+ and H^-. Part of such contributions may be related to modifications of screening length, which are taken into account by summing suitable chain graphs (we have checked that this does provide the screening Debye length for a mixture of ionized charges and ions).

3.6.3 Other Charged Clusters

Eventually, Figs. 11a–d made with three clusters C_a, C_1 and C_2, also provide leading contributions of order $\rho^* \exp(\beta E_H)$ via the same mechanism as above. At leading order, $\Phi(C_a, C_1)$ can be replaced by its Debye classical form. Then, integrations over internal degrees of freedom of clusters C_1 and C_2, and over relative distance $\mathbf{X}_2 - \mathbf{X}_1$ between those clusters, are identical (apart from obvious substitutions $p \to e$) to those relative to Figs. 7b (for 11a), 7c (for 11b), 9e (for 11c) and 9f (for 11d). Using again identity (3.47) for integration over $\mathbf{X} = \mathbf{X}_1 - \mathbf{X}_a$, and (A.7) for the integral of ϕ^3, we obtain for Fig. 11b (C_1 is made with a single particle and carries a charge $\pm e$)

$$\rho^* \gamma^2 \frac{(c_p - c_e)(\beta|E_H|)^{3/2}}{24\pi^{3/2}} \exp(\beta E_H), \tag{3.52}$$

and for Figs. 11c and 11d

$$\rho^* \frac{\gamma^3}{2} [W(1,1|0,1) - W(1,1|1,0)] \exp(2\beta E_H). \tag{3.53}$$

Total leading contribution of Fig. 11a vanishes by charge neutrality constraint (2.8). Next corrections to (3.52) and (3.53) decay exponentially faster than $\rho^* \exp(\beta E_H)$.

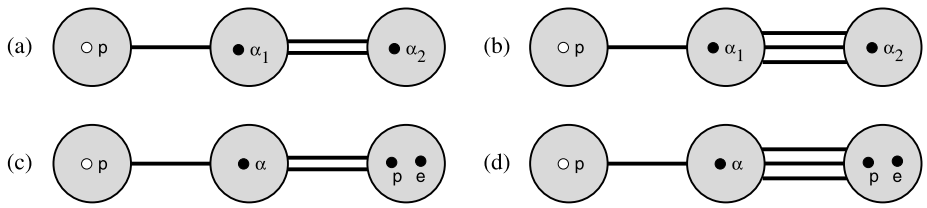

Fig. 11 Graphs of order $\rho^* \exp(\beta E_H)$ accounting for interactions between three clusters

3.7 Contributions with Arbitrary Particle Numbers

The evaluation of any contribution arising from a graph G_{N_p,N_e} made with at least three particles ($N_p + N_e \geq 3$), can be carried out by extending the methods described above for graphs with few particles. The outlines of the analysis are briefly sketched below. We first proceed to an estimation of the leading contribution. The behaviors of further collective corrections are discussed afterwards.

3.7.1 Leading Contributions

$*$ At leading order, we make the substitutions $\exp(I_R) \to 1$ and $\mathcal{B}_\phi^T \to \mathcal{B}^T$ in any weight $Z_\phi^T(C_i)$, and $(\exp(I_R) - 1) \to I_R$ in specific weight (2.42). Moreover, we explicit each $\mathcal{D}(C_i)$ in terms of spatial integrations over particle positions and of functional integrations over Brownian bridges.

$*$ Let consider two clusters C_i and C_j connected by a bond $\mathcal{F}_\phi(C_i, C_j)$. If one of them is electrically neutral, i.e. it contains the same number of protons and electrons, ϕ can be replaced by V in $\mathcal{F}_\phi(C_i, C_j)$. If both carry a net charge, ϕ must be replaced by its Debye classical form ϕ_D.

$*$ By virtue of Feynman-Kac formula, functional integrations over Brownian bridges reduce to matrix elements of either $\exp(-\beta H_{M_p,M_e})$, or interactions V evolved according to $\exp(-\tau H_{M_p,M_e})$ $(0 \leq \tau \leq \beta)$.

$*$ In graphs only made with bare bonds, integrations over positions of particles provide a function W accounting for bare interactions between clusters. If G_{N_p,N_e} contains a single cluster, such integrations give raise to partition function $Z(N_p, N_e)$.

$*$ When one or more bonds involve ϕ_D, positions of particles which belong to charged clusters connected by such bonds, are rewritten in terms of relative positions inside a given cluster and cluster position (arbitrarily defined as the position of a given particle). Let consider a charged cluster $C(M_p, M_e)$ $(M_p + M_e \neq 0)$, not connected to any neutral cluster. Integration over its position $\mathbf{X}$ can be disentangled from integrations over internal relative positions, since its internal weight $\mathcal{B}^T$ decays on a scale βe^2 much smaller than κ^{-1} which controls the decay of ϕ_D. Integration over its internal relative positions provide partition function $Z(M_p, M_e)$. Integration over $\mathbf{X}$ is performed by rescaling $\mathbf{X}$ in units of κ^{-1}. This provides multiplicative inverse powers of κ, with possible logarithmic terms $\ln(\kappa\lambda)$ arising from integrands built with ϕ_D^3.

$*$ According to above analysis and prescriptions, the leading contribution of G_{N_p,N_e} can be rewritten as (apart from a pure numerical coefficient which depends on ratio m_e/m_p)

$$\rho^* \gamma^{N_p+N_e-P/2} \exp[\beta(N_p + N_e - 1 - P/2)E_H] \prod Z \prod W \tag{3.54}$$

where each Z and each W depends only on temperature, while P is a positive integer. Term $\gamma^{-P/2} \exp(-P\beta E_H/2)$ arises from contribution $1/\kappa^P$, which is generated by both integrations over positions of charged clusters and specific weights I_R proportional to κ ($P = 0$ when G_{N_p,N_e} contains only neutral clusters).

$*$ The low-temperature behaviors of functions Z and W can be inferred from the methods exposed in Appendix B:. If there exists a bound state made with M_p protons and M_e electrons, partition function $Z(M_p, M_e)$ then behaves as

$$\exp(-\beta E^{(0)}_{M_p,M_e}), \tag{3.55}$$

apart from a multiplicative integer which accounts for groundstate degeneracy. In the other case, asymptotic behavior (3.55) has to be multiplied by some power of β. A given interaction function W behaves as the product of Boltzmann factors (3.55) associated with each interacting cluster times a power of β.

$*$ According to the above low-temperature behaviors of Z and W, leading contribution (3.54) of G_{N_p,N_e} reduces to $\rho^* \gamma^{N_p+N_e-P/2}$ times a power of β times

$$\exp[\beta(N_p + N_e - 1 - P/2)E_H] \prod \exp(-\beta E^{(0)}_{M_p,M_e}) \tag{3.56}$$

when $\beta \to \infty$. The precise form of factor (3.56) has been studied above for several graphs G_{N_p,N_e}. For all other graphs, we have checked that (3.56) is exponentially smaller than $\exp(\beta E_H)$. In particular, ideal contributions of complex entities made with more than four particles can be omitted at considered order. The analysis is achieved by using the known values of $E_{H_2^+}$, E_{H^-} and E_{H_2} given in Sect. 2.2, as well as inequality (2.31) for $M_p + M_e \geq 5$. Neutrality constraint (2.8) ensures the cancellation of the leading contributions of graphs which differ only by ending clusters made with either a single proton or a single electron: above statement then applies, strictly speaking, to the leading contribution of the sum of those graphs (for instance, see graphs $G_{1,1}$ and $G_{2,0}$ shown in Fig. 7a).

3.7.2 Collective Corrections

$*$ Collective corrections are obtained by expanding ring factors $\exp(I_R)$ in powers of I_R, and truncated Mayer coefficients $\mathcal{B}^T_\phi$ in powers of $(\phi - V)$. At the same time, both I_R and $(\phi - V)$ are expanded in positive integer powers of $\kappa\lambda$ as described in Appendix A:. Then, integration over cluster degrees of freedom involved in previous expansions, provide screening functions S. For a given graph G_{N_p,N_e}, the resulting corrections take the general form

$$\rho^* \gamma^{N_p+N_e-P/2+L/2} \exp[\beta(N_p + N_e - 1 - P/2 + L/2)E_H] \prod Z \prod W \prod S \tag{3.57}$$

with L a positive integer.

$*$ The low-temperature behavior of S is analogous to those of Z and W, and it reduces to the product of a power of β times groundstate Boltzmann factors (3.55) associated with each cluster involved in S (for instance, see the calculation of $S_3(1, 1)$ detailed in Appendix A:). Thus, and as expected from the weakly-coupled conditions enforced in the Saha regime, any correction (3.57) arising from G_{N_p,N_e} becomes exponentially smaller than its leading contribution (3.54) when $\beta \to \infty$. Collective corrections arising from graphs considered in Sects. 3.1–3.6 have been explicitly computed up to order $\rho^* \exp(\beta E_H)$ included. All other corrections, in particular those arising from other graphs, decay exponentially faster than $\rho^* \exp(\beta E_H)$.

4 Scaled Low-Temperature Expansions

According to the analysis of Sect. 3, we derive the structure of the asymptotic expansion of ρ/ρ^* (Sect. 4.1). Then, we proceed to the calculation of the pressure as a function of ρ (EOS), by using thermodynamical identities (Sect. 4.2). We derive the corresponding expansion around ideal Saha pressure (1.3), and the first four corrections are explicitly computed.

4.1 Structure of the Asymptotic Expansion of Particle Density

According to Sect. 3.7, every contribution arising from any graph G_{N_p,N_e} can be rewritten as ρ^* times γ^n times a temperature-dependent function. Power n is integer or half-integer, $n \geq 1$, while γ^n may be multiplied by integer powers of $\ln\gamma$ (it is not necessary to write explicitly such logarithmic terms since they do not play any role in the following). For a given n, there is a finite number of contributions proportional to γ^n, i.e. such that $N_p + N_e - P/2 + L/2 = n$. Their sum can be recast as

$$\rho^*\gamma^n g_n(\beta)\exp(\beta(n-1)E_H). \tag{4.1}$$

Functions $g_n(\beta)$ are expressed in terms of bare partition functions $Z(M_p, M_e)$ of clusters (M_p, M_e), bare interactions W between clusters, and screening functions S which may involve either a single or various clusters. Roughly speaking, the number of involved graphs, as well as the maximum total particle number $N_p + N_e$, increase with n.

Taking into account the results derived in Sect. 3, screened cluster expansion of common particle density $\rho = \rho_p = \rho_e$ can be formally rewritten as

$$\begin{aligned}\rho/\rho^* = \gamma + \frac{\gamma^2}{2} + \gamma^{3/2} g_{3/2}(\beta)\exp(\beta E_H/2) + \gamma^2 g_{2,exc}(\beta)\exp(\beta E_H)\\ + \sum_{n=5/2}^{\infty} \gamma^n g_n(\beta)\exp(\beta(n-1)E_H)\end{aligned} \tag{4.2}$$

where the sum runs over integer and half-integer values of n. In (4.2), we have extracted in $\gamma^2 g_2(\beta)\exp(\beta E_H)$ contribution (3.16) of atoms H in their groundstate, while the remaining part defines $g_{2,exc}(\beta)$. First two functions $g_{3/2}$ and $g_{2,exc}$ are

$$g_{3/2}(\beta) = S_{3/2}(1,0) \tag{4.3}$$

according to (3.4), and

$$\begin{aligned}g_{2,exc}(\beta) = \frac{1}{2}[S_2(1,0) + S_2(0,1)] + W(1,0|1,0) + W(1,0|0,1)\\ - \frac{(c_p + c_e)(\beta|E_H|)^{3/2}}{24\pi^{3/2}}\\ + \frac{1}{8}\left[Z_{exc}(1,1) + \left(\frac{2m}{m_p}\right)^{3/2} Z(2,0) + \left(\frac{2m}{m_e}\right)^{3/2} Z(0,2)\right]\end{aligned} \tag{4.4}$$

by summing (3.7), (3.17), (3.21), (3.33), (3.36), (3.39), (3.48), (3.49) and (3.52). Notice that (4.4) is symmetric with respect to permutations of species indexes p and e in agreement with $\rho_p = \rho_e$.

We stress that, in the Saha regime, γ is a fixed parameter not necessarily small, while $\beta \to \infty$. Then, functions $g_{2,exc}(\beta)\exp(\beta E_H)$ and $g_n(\beta)\exp(\beta(n-1)E_H)$ with $n \geq 3/2$ and $n \neq 2$, decay exponentially fast. Thus, the whole sum over n in (4.2) can be reordered according to the corresponding decay rates. Each term $\gamma^n g_n(\beta)\exp(\beta(n-1)E_H)$ is then rewritten as $\gamma^n h_k(\beta)$ where $k = k(n)$ is some integer. Functions h_k decay exponentially fast, i.e. $h_k(\beta) \sim \exp(-\beta\delta_k)$ (apart from powers of β), with decay rates δ_k ranked as $0 < \delta_1 < \delta_2 < \cdots$: h_{k+1} decays exponentially faster than h_k when $\beta \to \infty$. According to the

analytic results derived in Sects. 3.1–3.7 on the one hand, and to the numerical values of E_H, E_{H^-}, $E_{H_2^+}$, E_{H_2} (see Sect. 2.3) on the other hand, we find

$$\begin{aligned} h_1(\beta) &= g_{3/2}(\beta)\exp(\beta E_H/2), \quad & n_1 &= 3/2, \\ h_2(\beta) &= g_4(\beta)\exp(3\beta E_H), & n_2 &= 4, \\ h_3(\beta) &= g_{2,exc}(\beta)\exp(\beta E_H), & n_3 &= 2, \\ h_4(\beta) &= g_3(\beta)\exp(2\beta E_H), & n_4 &= 3. \end{aligned} \tag{4.5}$$

Their corresponding decay rates δ_k can be found in the table (1.5) given in the Introduction, while all higher-order functions $h_k(\beta)$ with $k \geq 5$ decay exponentially faster than $\exp(\beta E_H)$, i.e. their decay rates δ_k are larger than $|E_H| \simeq 13.6$. Notice that both $\gamma^{5/2} g_{5/2}(\beta)\exp(3\beta E_H/2)$ and $\gamma^{7/2} g_{7/2}(\beta)\exp(5\beta E_H/2)$ decay faster than $\exp(\beta E_H)$, so both $k(5/2)$ and $k(7/2)$ are strictly larger than 4. Within previous reordering, (4.2) becomes

$$\rho/\rho^* = \gamma + \frac{\gamma^2}{2} + \sum_{k=1}^{\infty} \gamma^{n_k} h_k(\beta). \tag{4.6}$$

At order $\exp(\beta E_H)$ included, all terms with $k \geq 5$ can be omitted in (4.6). Moreover, for the sake of consistency, it is sufficient to compute functions h_k with $1 \leq k \leq 4$ at the same order (beyond its leading behavior $\exp(-\beta\delta_k)$, h_k involves other exponentially small contributions). This gives

$$h_1(\beta) = \frac{(\beta|E_H|)^{3/4}}{\pi^{1/4}} \exp(\beta E_H/2), \tag{4.7}$$

$$h_2(\beta) = \frac{1}{64}\left(\frac{2m}{M}\right)^{3/2} Z(2,2)\exp(3\beta E_H) + W(1,1|1,1)\exp(3\beta E_H), \tag{4.8}$$

$$\begin{aligned} h_3(\beta) = -\frac{1}{2} &+ \left[1 + \frac{1}{12}\ln\left(\frac{4m}{M}\right)\right]\frac{(\beta|E_H|)^{3/2}}{\pi^{1/2}}\exp(\beta E_H) \\ &+ \frac{1}{8\pi^{1/2}}\left\{2Q(x_{pe}) + \left(\frac{2m}{m_p}\right)^{3/2}\left[Q(-x_{pp}) - \frac{1}{2}E(-x_{pp})\right]\right. \\ &\left. + \left(\frac{2m}{m_e}\right)^{3/2}\left[Q(-x_{ee}) - \frac{1}{2}E(-x_{ee})\right]\right\}\exp(\beta E_H), \end{aligned} \tag{4.9}$$

and

$$\begin{aligned} h_4(\beta) = \frac{3}{64}&\left[\left(\frac{m_e(M+m_p)}{M^2}\right)^{3/2} Z(2,1) + \left(\frac{m_p(M+m_e)}{M^2}\right)^{3/2} Z(1,2)\right]\exp(2\beta E_H) \\ &+ S_3(1,1)\exp(2\beta E_H) + \frac{3}{2}[W(1,1|1,0) + W(1,1|0,1)]\exp(2\beta E_H). \end{aligned} \tag{4.10}$$

In (4.7) and (4.9), full contributions of respectively g_1 and $g_{2,exc}$, are kept, while analytic expressions (3.3), (3.8), (3.34), (3.37) and (3.39) have been used. Moreover, and according to formula (A.12) derived in Appendix A:, $Z_{exc}(1,1)$, $Z(2,0)$ and $Z(0,2)$ have been expressed in terms of Ebeling quantum virial functions Q (direct part) and E (exchange

part) defined in Ref. [39], with arguments $x_{pe} = 2(\beta|E_H|)^{1/2}$, $x_{pp} = (2m_p/m)^{1/2}(\beta|E_H|)^{1/2}$ and $x_{ee} = (2m_e/m)^{1/2}(\beta|E_H|)^{1/2}$. Term $-1/2$ in $h_3(\beta)$ subtracts the ground-state contribution included in function $Q(x_{pe})$. In (4.8) and (4.10), contributions of g_4 and g_3 which decay exponentially faster than $\exp(\beta E_H)$ have been omitted. The resulting expression for h_2 is obtained by summing (3.23) and (3.41). Similarly, expression (4.10) for h_4 follows by summing (3.26), (3.27), (3.50), (3.51), (3.19), (3.45) and (3.53).

As a conclusion, it is useful to summarize the main features and ingredients of expansion (4.6). The h_k-functions are ordered, at sufficiently low temperatures, according to $|h_1(\beta)| > |h_2(\beta)| > |h_3(\beta)| > |h_4(\beta)| > \cdots$. They incorporate corrections to ideal Saha equation which arise from different physical phenomena, as listed in the Introduction. Explicit expressions for $h_1(\beta)$ and $h_3(\beta)$ are known, see (4.7) and Ref. [39], while $h_2(\beta)$ and $h_4(\beta)$ involve integrals associated with 3-body and 4-body problems which cannot be expressed in closed analytical forms. In $h_2(\beta)$, the internal partition function $Z(2,2)$ of a hydrogen molecule is defined in (3.24), and its low-temperature form is determined in Appendix B:. The function $W(1,1|1,1)$, which accounts for atom-atom interactions, is defined in (3.41), and its low-temperature form is computed in Appendix C:. In $h_4(\beta)$, the internal partition functions $Z(2,1)$ and $Z(1,2)$ of ions H_2^+ and H^- are defined in (3.28) and (3.29) respectively, while their asymptotic expressions at low temperatures are derived in Appendix B:. The interactions $W(1,1|1,0)$ and $W(1,1|0,1)$ between an atom and an ionized proton or electron, are defined in (3.45) and their low-temperature expressions are given in Appendix C:. Eventually, the screening function $S_3(1,1)$ of a hydrogen atom accounts for collective corrections to the bare proton-electron Coulomb potential beyond the familiar Debye shift, and it is given by formula (A.16) at low temperatures.

4.2 Equation of State

In order to compute the pressure, we consider identities

$$\begin{aligned} \rho_p &= z_p \frac{\partial \beta P}{\partial z_p}, \\ \rho_e &= z_e \frac{\partial \beta P}{\partial z_e}. \end{aligned} \tag{4.11}$$

Taking into account that P depends only on z and β, and using parametrization of z in terms of β and γ, $z = (m/M)^{3/4}\gamma \exp(\beta E_H)/4$, we rewrite such identities as

$$\frac{\partial \beta P}{\partial \gamma} = \frac{2\rho}{\gamma}, \tag{4.12}$$

where partial derivative of βP with respect to γ is taken at fixed β. After inserting expansion (4.6) of ρ into the r.h.s. of (4.12), a straightforward term by term integration with respect to γ provides

$$\beta P/\rho^* = 2\gamma + \frac{\gamma^2}{2} + \sum_{k=1}^{\infty} \frac{2\gamma^{n_k}}{n_k} h_k(\beta). \tag{4.13}$$

The required equation of state follows by inserting into (4.13) the expression of γ in terms of ρ obtained from the inversion of (4.6). That inversion can be performed perturbatively

around the simple expression

$$\gamma_{\text{Saha}} = (1 + 2\rho/\rho^*)^{1/2} - 1 \tag{4.14}$$

obtained by retaining only the first two terms of (4.6). The resulting SLT expansion of the pressure takes the form (1.1) presented in the Introduction where $\beta P_{\text{Saha}}/\rho^*$ is given by (1.3). The general structure of $\beta P_k/\rho^*$ reduces to a function of ρ/ρ^* times a polynomial in the $h_l(\beta)$'s with $l \leq k$. Therefore, for a fixed ratio ρ/ρ^*, corrections $\beta P_k/\rho^*$ decay exponentially fast when $\beta \to \infty$. Moreover, each $\beta P_{k+1}/\rho^*$ decays faster than $\beta P_k/\rho^*$ for $k \geq 0$ (with $P_0 = P_{\text{Saha}}$). First corrections in (1.1) read

$$\beta P_1/\rho^* = \frac{[(1 + 2\rho/\rho^*)^{1/2} - 3][(1 + 2\rho/\rho^*)^{1/2} - 1]^{3/2}}{3(1 + 2\rho/\rho^*)^{1/2}} h_1(\beta), \tag{4.15}$$

$$\beta P_2/\rho^* = \frac{-[(1 + 2\rho/\rho^*)^{1/2} + 2][(1 + 2\rho/\rho^*)^{1/2} - 1]^4}{2(1 + 2\rho/\rho^*)^{1/2}} h_2(\beta), \tag{4.16}$$

$$\beta P_3/\rho^* = \frac{-[(1 + 2\rho/\rho^*)^{1/2} - 1]^2}{(1 + 2\rho/\rho^*)^{1/2}} h_3(\beta), \tag{4.17}$$

$$\beta P_4/\rho^* = \frac{-[(1 + 2\rho/\rho^*)^{1/2} + 3][(1 + 2\rho/\rho^*)^{1/2} - 1]^3}{3(1 + 2\rho/\rho^*)^{1/2}} h_4(\beta), \tag{4.18}$$

and

$$\beta P_5/\rho^* = \frac{[(1 + 2\rho/\rho^*)^{1/2} - \rho/\rho^*][(1 + 2\rho/\rho^*)^{1/2} - 1]^2}{(1 + 2\rho/\rho^*)^{3/2}} [h_1(\beta)]^2. \tag{4.19}$$

Next correction $\beta P_6/\rho^*$ decays faster than $\exp(\beta E_H)$.

In previous corrections $\beta P_k/\rho^*$, functions $h_1(\beta)$ and $h_3(\beta)$ can be expressed in closed analytical forms according to (4.7) and (4.9) respectively. Similar analytical expressions for $h_2(\beta)$ and $h_4(\beta)$ are not available. Nevertheless, the low-temperature behaviors of those functions are exactly known, i.e.

$$h_2(\beta) \sim \frac{1}{64} \left(\frac{2m}{M} \right)^{3/2} \exp(\beta(3E_H - E_{H_2})) \tag{4.20}$$

and

$$h_4(\beta) \sim \frac{3}{64} \left(\frac{m_e(M + m_p)}{M^2} \right)^{3/2} \exp(\beta(2E_H - E_{H_2^+})) \tag{4.21}$$

when $\beta \to \infty$.

Eventually, the various terms in (1.1) display interesting behaviors with respect to ratio ρ/ρ^*, at fixed β sufficiently large:

- For ρ much smaller than ρ^*, each $\beta P_k/\rho^*$, as well as $\beta P_{\text{Saha}}/\rho^*$, can be expanded in powers of ρ/ρ^*. This leads to the virial expansion of βP in powers of ρ. Since all $\beta P_k/\rho^*$'s for $k \geq 6$ are at least of order $\rho^{5/2}$, the full contribution of terms with $k \leq 5$ in (1.1) provides the expansion of βP up to order ρ^2, i.e.

$$\beta P = 2\rho - \frac{2^{3/2}(2\pi)^{3/4}}{3} (\lambda_{pe})^{3/2} \exp(-\beta E_H/2) h_1(\beta) \rho^{3/2}$$

$$- (2\pi)^{3/2}(\lambda_{pe})^3 \exp(-\beta E_H)[2h_3(\beta) + 1 - 2(h_1(\beta))^2]\rho^2 + O(\rho^{5/2})$$
$$= 2\rho - \frac{(8\pi\beta e^2\rho)^{3/2}}{24\pi} - \frac{\pi}{\sqrt{2}}\left\{2\lambda_{pe}^3 Q(x_{pe}) + \lambda_{pp}^3\left[Q(-x_{pp}) - \frac{1}{2}E(-x_{pp})\right]\right.$$
$$\left. + \lambda_{ee}^3\left[Q(-x_{ee}) - \frac{1}{2}E(-x_{ee})\right]\right\}\rho^2 - \frac{\pi}{6}\ln\left(\frac{4m}{M}\right)\beta^3 e^6\rho^2 + O(\rho^{5/2}) \quad (4.22)$$

which does coincide with the well known expression derived previously by other methods [4, 23, 39] ($\lambda_{pe} = (\beta\hbar^2/m)^{1/2}$, $\lambda_{pp} = (\beta\hbar^2/m_{pp})^{1/2}$ and $\lambda_{ee} = (\beta\hbar^2/m_{ee})^{1/2}$). Notice that contribution of βP_4 is of order ρ^3, while that of βP_2 is of order ρ^4.

- For ρ of order ρ^*, leading term $\beta P_{\rm Saha}/\rho^*$, as well as each correction $\beta P_k/\rho^*$, can be viewed as infinite resummations of terms with arbitrary high orders in the above low-density expansion. Such resummations account, in a non-perturbative way with respect to density, of recombination processes for any value of the ionization rate. The relative orders of magnitude of the various corrections to Saha pressure are mainly controlled by their decay rates δ_k. Therefore the larger correction indeed is βP_1, which results from plasma polarization around a given ionized charge, evaluated within Debye classical mean-field theory. That result is equivalent to the modified Saha condition which determines the ionization rate [39, 41].
- For ρ much larger than ρ^*, $\beta P_{\rm Saha}$ behaves as

$$\beta P_{\rm Saha} \sim \rho, \quad (4.23)$$

which illustrates the almost full atomic recombination of the plasma. The larger correction to Saha pressure is now βP_2 which behaves as

$$\beta P_2 \sim -2h_2(\beta)\rho^*\left(\frac{\rho}{\rho^*}\right)^2, \quad (4.24)$$

so it overcomes βP_1 which grows only as $(\rho/\rho^*)^{3/4}$, as well as further corrections $\beta P_3 \sim (\rho/\rho^*)^{1/2}$, $\beta P_4 \sim (\rho/\rho^*)^{3/2}$ and $\beta P_5 \sim (\rho/\rho^*)^{1/2}$. Therefore molecular recombination prevails over plasma polarization. Of course, expansion (1.1) is no longer appropriate for too large values of ratio (ρ/ρ^*), since some corrections $\beta P_k/\rho^*$ become much larger than Saha pressure.

4.3 Numerical Estimations and Validity Domain of SLT Expansions

Quantitative estimations of corrections $\beta P_1/\rho^*$, $\beta P_3/\rho^*$ and $\beta P_5/\rho^*$ are easy, because functions $h_1(\beta)$ and $h_3(\beta)$ can be represented by simple analytical expressions at finite temperature. For functions $h_2(\beta)$ and $h_4(\beta)$ which involve 3 and 4-body contributions, no *explicit* finite-T representations are available beyond their low-temperature asymptotic forms determined in Appendices B and C. In order to obtain reliable values for those functions at moderate temperatures, we have used a simple approach in which important finite temperature effects (such as atomic vibrations and rotations) are phenomenologically taken into account. As mentioned in the Introduction, the corresponding numerical evaluations of the various corrections to Saha pressure (and internal energy), together with a comparison of our predicted isotherms with the results of PIMC simulations, will be presented in a forthcoming paper [1].

Here, we exhibit the validity domain of SLT expansion (1.1). A rigorous analysis of the convergence of that expansion is a tremendous mathematical task, much beyond the scope

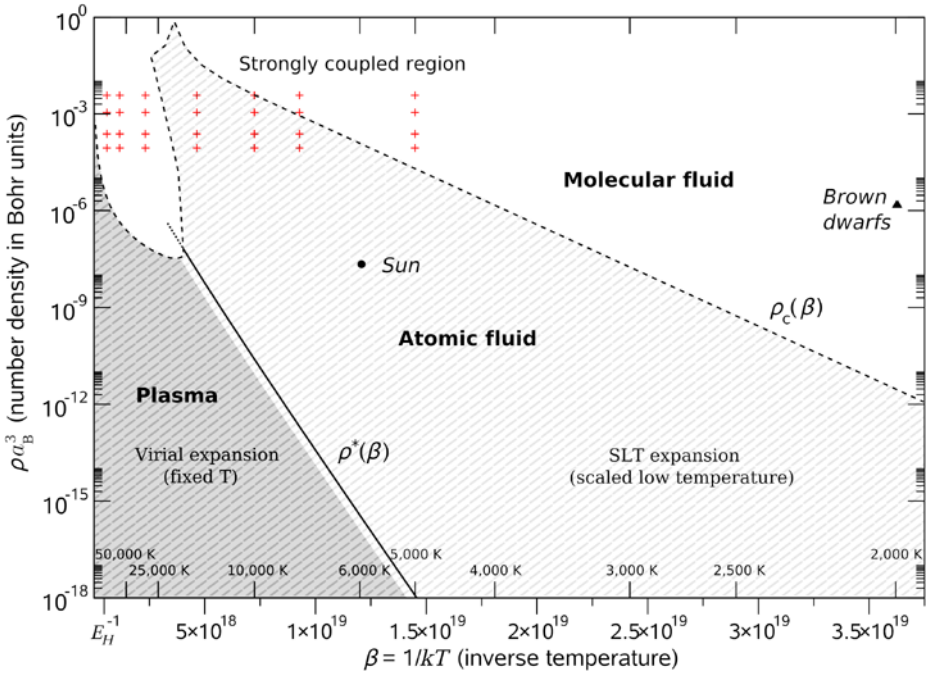

Fig. 12 Phase diagram showing the validity domains of SLT expansion (1.1) (*hatched region*) and of the virial expansion (*shaded region*). Atomic recombination density $\rho^*(\beta)$ (1.2) is a straight line at low temperatures in the $(\beta, \log\rho)$-plane. The validity domain is delimited at high densities, and for temperatures below 10000 K, by critical density $\rho_c(\beta)$ at which molecular recombination occurs. Crosses indicate state points where simulation results are available [48]. State points of astrophysical systems (Sun photosphere and Brown dwarfs) are also shown in the diagram

of the present work. We estimated a quite plausible validity domain, by employing the semi-empirical criterion $|P_k| < P_{\text{Saha}}/10$ for all five corrections ($1 \le k \le 5$): it covers the region hatched in the temperature-density plane shown in Fig. 12. The shaded region at low densities and high temperatures corresponds to the validity domain of the virial expansion (i.e. low-density expansion at fixed temperature) determined from a similar criterion. Obviously, SLT expansion improves widely upon virial expansion, by providing reliable results in the atomic phase, including the temperature and density ranges around $\rho^\star(\beta)$ which correspond to partially ionized hydrogen gases. In Fig. 12, we have also shown state points, symbolized by crosses, for which PIMC simulation results have been obtained [48]. It turns out that some of them lie within the validity domain of the SLT expansion. We have checked that our calculations, both for pressure and internal energy, are in agreement with PIMC results within statistical errors [1]. This confirms the reliability of SLT expansions in the domain inferred from the above semi-empirical criterion. Notice that such domain extends to rather high densities, up to $a/a_B = 6$ at 15000 K, which corresponds to a mean inter-particle distance of the order of twice the size of a hydrogen atom.

For temperatures below 10000 K, the validity domain is limited at high densities by molecular recombination which occurs around densities $\rho_c(\beta)$ shown as a dashed line in the phase diagram. That limitation is not intrinsic to the theory, and an SLT expansion applicable in the molecular regime can be derived as well. Such a generalization requires replacing the scaling (2.12) of the chemical potential by a similar scaling corresponding to a molec-

ular regime (see Fig. 2), and performing the inversion $\mu = \mu(\rho)$ in the appropriate density range. Notice that if ρ is not too high above ρ_c, expansion (4.6) of particle density in terms of chemical potential should remain valid. Performing a non-perturbative inversion of the chemical potential in favor of the density, should then provide accurate thermodynamical functions which account not only for atomic recombination at $\rho \sim \rho^*$, but also for molecular recombination above ρ_c.

For temperatures above 10000 K, the borderline of the validity domain has a complicated shape determined by correction term P_3 which accounts for atomic excitations and for interactions between ionized electrons and protons. At high temperatures, typically above 30000 K, thermal ionization prevents recombination of protons and electrons into atoms, and our validity criterion is then equivalent to a weak coupling condition for ionized charges, i.e. coupling parameter $\Gamma = \beta e^2/a$ smaller than some value, which also determines the validity of the virial expansion.

Eventually, state points of two astrophysical systems of interest, Sun photosphere and a typical brown dwarf atmosphere, are also shown in Fig. 12. Our equation of state (1.1) clearly holds at the temperature and density of Sun photosphere. In order to be applicable to brown dwarf atmospheres, the SLT expansion would need to be generalized to the molecular regime, as discussed above.

Acknowledgements We are very indebted to Vincent ROBERT (Laboratoire de Chimie, ENS Lyon, CNRS) for his efficient and kind support. We thank him in particular for his spectroscopic calculations (ground state energies and excitations energies of a few compounds) which we used in Sect. 2.3 [52].

Appendix A: Screened Potential and Related Integrals

A.1 Expression and Behavior of ϕ

The Fourier transform of $\phi(\mathcal{L}_i, \mathcal{L}_j)$ with respect to $\mathbf{X}_i - \mathbf{X}_j$ reads

$$\tilde{\phi}(\mathbf{k}, \chi_i, \chi_j) = e_{\alpha_i} e_{\alpha_j} \int_0^{q_i} \mathrm{d}s \int_0^{q_j} \mathrm{d}t \exp[i\mathbf{k} \cdot (\lambda_{\alpha_i} \boldsymbol{\eta}_i(s) - \lambda_{\alpha_j} \boldsymbol{\eta}_j(t))] \times \sum_{n=-\infty}^{\infty} \frac{4\pi}{k^2 + \kappa^2(k,n)} \exp[-2n\pi i(s-t)], \tag{A.1}$$

where $\chi = (\alpha, q, \boldsymbol{\eta}(\cdot))$ denotes the loop internal degrees of freedom, while function $\kappa^2(k,n)$ is defined in Ref. [13]. Functions $\kappa^2(k,n)$ are analytical in k^2 near $k = 0$, while $\kappa^2(0,n) = 0$ for $n \neq 0$ and $\kappa^2(0,0) \neq 0$ is of order κ^2 . For large values of k, $\kappa^2(k,n)$ remains bounded by a constant independent of n (of order κ^2). For $k \sim \kappa$, $\kappa^2(k,n)$ for $n \neq 0$ is smaller than $\kappa^2(k,0)$ by a factor of order $\kappa^2\lambda^2$, while $\kappa^2(k,0)$ can be replaced by κ^2.

The behaviors of ϕ with respect to relative distance $r = |\mathbf{X}_i - \mathbf{X}_j|$ (roughly described in Fig. 4), can be readily derived from those of $\tilde{\phi}$ with respect to $\mathbf{k}$, as detailed in Ref. [13]. Here, we briefly summarize that analysis. For $k \gg \kappa$, each fraction $4\pi/(k^2 + \kappa^2(k,n))$ can be replaced by $4\pi/k^2$ in (A.1), so $\phi(\mathcal{L}_i, \mathcal{L}_j)$ behaves as $V(\mathcal{L}_i, \mathcal{L}_j)$ at short distances $r \ll \kappa^{-1}$. At distances $r \sim \kappa^{-1}$, we recover the Debye classical form $\phi_D(\mathcal{L}_i, \mathcal{L}_j) = q_i e_{\alpha_i} q_j e_{\alpha_j} \exp(-\kappa r)/r$, by noting that terms $n \neq 0$ in (A.1) provide contributions smaller than the one of $n = 0$ by a factor of order $\kappa^2\lambda^2$. Eventually, terms $n \neq 0$ in (A.1) provide a singularity in the small-$\mathbf{k}$ expansion of $\tilde{\phi}(\mathbf{k}, \chi_i, \chi_j)$, which in turn induces a dipolar-like decay of $\phi(\mathcal{L}_i, \mathcal{L}_j)$ at large distances $r \gg l_Q$.

A.2 Integrals of Powers of ϕ

We consider $\phi(\mathcal{L}_a^{(p)}, \mathcal{L}_1^{(p,e)})$ where loops $\mathcal{L}_a^{(p)}$ and loop $\mathcal{L}_1^{(p,e)}$ contain, respectively, one proton ($q_a = 1$) and either one proton or one electron ($q_1 = 1$). According to the definition of $\tilde{\phi}(\mathbf{k}, \chi_a, \chi_1)$, the integral of $\phi(\mathcal{L}_a^{(p)}, \mathcal{L}_1^{(p,e)})$ over $\mathbf{X}_1$ and $\boldsymbol{\xi}_1 = \boldsymbol{\eta}_1$ is nothing but

$$\int \mathrm{d}\mathbf{X}_1 \int \mathcal{D}(\boldsymbol{\xi}_1)\phi(\mathcal{L}_a^{(p)}, \mathcal{L}_1^{(p,e)}) = \int \mathcal{D}(\boldsymbol{\xi}_1)\tilde{\phi}(\mathbf{0}, \chi_a, \chi_1). \tag{A.2}$$

The r.h.s. of (A.2) is computed by taking the limit $\mathbf{k} \to \mathbf{0}$ of expression (A.1). The corresponding contribution of a term $n \neq 0$ is obtained by expanding phase factor $\exp[i\mathbf{k} \cdot (\lambda_p \boldsymbol{\xi}_a(s) - \lambda_{p,e}\boldsymbol{\xi}_1(t))]$ in powers of $\mathbf{k}$. Since all odd moments of measure $\mathcal{D}(\boldsymbol{\xi}_1)$ vanish, as well as $\int_0^1 \mathrm{d}t \exp(2n\pi i t)$, the first non-vanishing term in that expansion is at least of order k^3. It has to be multiplied by a factor of order $1/k^2$ which arises from fraction $4\pi/(k^2 + \kappa^2(k, n))$, so the resulting contribution to the r.h.s. of (A.2) vanishes. Therefore, the sole contribution arises from term $n = 0$, i.e.

$$\int \mathrm{d}\mathbf{X}_1 \int \mathcal{D}(\boldsymbol{\xi}_1)\phi(\mathcal{L}_a^{(p)}, \mathcal{L}_1^{(p,e)}) = \pm\frac{4\pi e^2}{\kappa^2(0,0)}, \tag{A.3}$$

with a positive sign for $\mathcal{L}_1^{(p)}$ and a negative one for $\mathcal{L}_1^{(e)}$.

According to Fourier-Plancherel formula, the integral of $[\phi(\mathcal{L}_a^{(p)}, \mathcal{L}_1^{(p,e)})]^2$ over $\mathbf{X}_1$, $\boldsymbol{\xi}_a = \boldsymbol{\eta}_a$ and $\boldsymbol{\xi}_1 = \boldsymbol{\eta}_1$, is rewritten as

$$\begin{aligned}
&\int \mathrm{d}\mathbf{X}_1 \int \mathcal{D}(\boldsymbol{\xi}_a)\mathcal{D}(\boldsymbol{\xi}_1)[\phi(\mathcal{L}_a^{(p)}, \mathcal{L}_1^{(p,e)})]^2 \\
&\quad = \frac{1}{(2\pi)^3}\int \mathrm{d}\mathbf{k} \int \mathcal{D}(\boldsymbol{\xi}_a)\mathcal{D}(\boldsymbol{\xi}_1)|\tilde{\phi}(\mathbf{k}, \chi_a, \chi_1)|^2 \\
&\quad = \frac{2e^4}{\pi}\int \mathrm{d}\mathbf{k} \int_0^1 \mathrm{d}s_1 \int_0^1 \mathrm{d}t_1 \int_0^1 \mathrm{d}s_2 \int_0^1 \mathrm{d}t_2 \\
&\qquad \times \sum_{n_1, n_2 = -\infty}^{\infty} \frac{\exp[-2n_1\pi i(s_1 - t_1)]}{k^2 + \kappa^2(k, n_1)} \frac{\exp[-2n_2\pi i(s_2 - t_2)]}{k^2 + \kappa^2(k, n_2)} \\
&\qquad \times \int \mathcal{D}(\boldsymbol{\xi}_a)\exp[i\lambda_p \mathbf{k} \cdot \boldsymbol{\xi}_a(s_1 - s_2)] \int \mathcal{D}(\boldsymbol{\xi}_1)\exp[-i\lambda_{p,e}\mathbf{k} \cdot \boldsymbol{\xi}_1(t_1 - t_2)].
\end{aligned} \tag{A.4}$$

In the last equality of (A.4), we have used that the average over shape $\boldsymbol{\xi}$ of any function $f(\boldsymbol{\xi}_a(s_1) - \boldsymbol{\xi}_a(s_2))$ is identical to the average of $f(\boldsymbol{\xi}_a(s_1 - s_2))$, provided that $\boldsymbol{\xi}(s)$ for s outside $[0, 1]$ is defined as equal to $\boldsymbol{\xi}(s - [s])$ [13]. Within variable change $\mathbf{k} = \kappa\mathbf{q}$, we can replace $\kappa^2(\kappa q, n_i)$ by either κ^2 for $n_i = 0$, or 0 for $n_i \neq 0$, discarding terms which provide contributions smaller by a factor $(\kappa\lambda)^2$ at least. Summations over $n_i \neq 0$ are then performed according to identity $\sum_{n\neq 0}\exp[-2n\pi i(s - t)] = \delta(s - t) - 1$. Since measure $\mathcal{D}(\boldsymbol{\xi})$ is Gaussian with covariance (2.34) (for $q = 1$), we transform (A.4) into

$$\begin{aligned}
&\frac{8e^4}{\kappa}\int_0^1 \mathrm{d}s \int_0^1 \mathrm{d}t \int_0^\infty \mathrm{d}q \frac{q^2}{(q^2+1)^2}\exp[-\kappa^2\lambda_p^2 q^2 s(1-s)/2 - \kappa^2\lambda_{p,e}^2 q^2 t(1-t)/2] \\
&\quad + \frac{8e^4}{\kappa}\int_0^1 \mathrm{d}s \int_0^\infty \mathrm{d}q \frac{1}{q^2}\{\exp[-\kappa^2(\lambda_p^2 + \lambda_{p,e}^2)q^2 s(1-s)/2] - 1\}
\end{aligned}$$

$$-\frac{8e^4}{\kappa}\int_0^1 \mathrm{d}s\int_0^1 \mathrm{d}t\int_0^\infty \mathrm{d}q\,\frac{1}{q^2}$$
$$\times\{\exp[-\kappa^2\lambda_p^2 q^2 s(1-s)/2-\kappa^2\lambda_{p,e}^2 q^2 t(1-t)/2]-1\} \tag{A.5}$$

discarding terms of order $\kappa^{-1}O((\kappa\lambda)^2)$. The integrals over q in (A.5) are computed in terms of elementary functions of arguments $[\kappa^2\lambda_p^2 s(1-s)/2+\kappa^2\lambda_{p,e}^2 t(1-t)/2]^{1/2}$ and $[\kappa^2(\lambda_p^2+\lambda_{p,e}^2)s(1-s)/2]^{1/2}$, which can be expanded in Taylor series since $\kappa\lambda$ is small. For the leading (order κ^{-1}) and first subleading (order $\kappa^{-1}O(\kappa\lambda)$) contributions, the remaining integrals over s and t are readily calculated (some complicated double integrals over s and t arising from respectively first and third terms in (A.5) cancel out). Eventually, we obtain

$$\int \mathrm{d}\mathbf{X}_1\int \mathcal{D}(\boldsymbol{\xi}_a)\mathcal{D}(\boldsymbol{\xi}_1)[\phi(\mathcal{L}_a^{(p)},\mathcal{L}_1^{(\alpha)})]^2=\frac{2\pi e^4}{\kappa}\left[1-\frac{\sqrt{\pi}}{2\sqrt{2}}\kappa\lambda_{p\alpha}+O((\kappa\lambda)^2)\right]. \tag{A.6}$$

The integral of $[\phi(\mathcal{L}_a^{(p)},\mathcal{L}_1^{(\alpha)})]^3$ over $\mathbf{X}_1$, $\boldsymbol{\xi}_a$ and $\boldsymbol{\xi}_1$, can be evaluated within similar techniques and tricks. Discarding terms of order $O(\kappa\lambda)$, its leading behavior reduces to a constant times $\ln(\kappa\lambda_{p\alpha})$ plus another constant. When the two integrals corresponding respectively to $\alpha=p$ and $\alpha=e$ are summed together, logarithmic terms in κ cancel out. Therefore, we obtain

$$\int \mathrm{d}\mathbf{X}_1\int \mathcal{D}(\boldsymbol{\xi}_a)\int \mathcal{D}(\boldsymbol{\xi}_1)[(\phi(\mathcal{L}_a^{(p)},\mathcal{L}_1^{(p)}))^3+(\phi(\mathcal{L}_a^{(p)},\mathcal{L}_1^{(e)}))^3]=c_p e^6+O(\kappa\lambda) \tag{A.7}$$

where c_p is the constant

$$c_p=\frac{2}{\pi^3}\int_0^1 \mathrm{d}s\int_0^s \mathrm{d}t\int \mathrm{d}\mathbf{q}_1\int \mathrm{d}\mathbf{q}_2\,\frac{1}{q_1^2 q_2^2|\mathbf{q}_1+\mathbf{q}_2|^2}$$
$$\times\{\exp[-(q_1^2 s(1-s)+q_2^2 t(1-t)+2\mathbf{q}_1\cdot\mathbf{q}_2 t(1-s))]$$
$$-\exp[-(q_1^2 s(1-s)+q_2^2 t(1-t)+2\mathbf{q}_1\cdot\mathbf{q}_2 t(1-s))m_p/(2m)]\} \tag{A.8}$$

entirely determined by ratio m_p/m. As it should, leading contribution $c_p e^6$ in (A.7) is nothing but the value of the considered integral with bare potential V in place of ϕ (that bare integral does converge thanks to the $1/|\mathbf{X}_1|^4$-decay of $[V(\mathcal{L}_a^{(p)},\mathcal{L}_1^{(p)})]^3+[V(\mathcal{L}_a^{(p)},\mathcal{L}_1^{(e)})]^3$). When the root proton is replaced by a root electron ($\mathcal{L}_a^{(p)}\to\mathcal{L}_a^{(e)}$), the resulting integral behaves similarly to (A.7) where constant c_e is given by (A.8) with m_e in place of m_p.

A.3 Behavior of I_R

We consider a loop $\mathcal{L}$ containing a single particle of species α. Convolution formula (2.40) for $I_R(\mathcal{L})$ is first transformed according to Fourier-Plancherel identity, in which $\tilde{\phi}(\mathbf{k},\chi_a,\chi_1)$ is replaced by (A.1). Discarding terms smaller by a factor $O((\kappa\lambda)^2)$, only the contributions of loops $\mathcal{L}_1^{(p,e)}$ associated with a single proton or a single electron, are retained. Moreover, at the same order, after making variable change $\mathbf{k}=\kappa\mathbf{q}$, we can replace $\kappa^2(\kappa q,n)$ by either κ^2 for $n=0$, or 0 for $n\neq 0$. Using again identity $\sum_{n\neq 0}\exp[-2n\pi i(s-t)]=\delta(s-t)-1$, we then obtain

$$I_R(\mathcal{L})=\frac{\beta e^2\kappa}{2}+\frac{\beta e^2\kappa}{4\pi^2}\sum_\gamma\int_0^1 \mathrm{d}s\int_0^1 \mathrm{d}s_1\int_0^1 \mathrm{d}t_1\int \mathcal{D}(\boldsymbol{\xi}_1)\int \mathrm{d}\mathbf{q}\,\frac{1}{q^2(q^2+1)}$$

$$\times [\exp(i\kappa\mathbf{q}\cdot(\lambda_\alpha\boldsymbol{\xi}(s)-\lambda_\gamma\boldsymbol{\xi}_1(s)+\lambda_\gamma\boldsymbol{\xi}_1(s_1)-\lambda_\alpha\boldsymbol{\xi}(t_1)))-1]$$
$$+\frac{\beta e^2\kappa}{4\pi^2}\sum_\gamma\int_0^1 ds\int_0^1 ds_1\int_0^1 dt_1\int\mathcal{D}(\boldsymbol{\xi}_1)\int d\mathbf{q}\frac{1}{q^4}$$
$$\times\exp(i\kappa\mathbf{q}\cdot(\lambda_\alpha\boldsymbol{\xi}(s)-\lambda_\gamma\boldsymbol{\xi}_1(s)+\lambda_\gamma\boldsymbol{\xi}_1(s_1)))$$
$$\times[\exp(-i\kappa\mathbf{q}\cdot\lambda_\alpha\boldsymbol{\xi}(s_1))-\exp(-i\kappa\mathbf{q}\cdot\lambda_\alpha\boldsymbol{\xi}(t_1))]+\beta e^2\kappa O((\kappa\lambda)^2). \quad (A.9)$$

The leading behavior of $I_R(\mathcal{L})$ reduces to the first term in the r.h.s. of (A.9). In the second term of (A.9), we can first perform the integration over $\mathbf{q}$ thanks to Cauchy's theorem. The resulting elementary functions of the argument $\kappa|\lambda_\alpha\boldsymbol{\xi}(s)-\lambda_\gamma\boldsymbol{\xi}_1(s)+\lambda_\gamma\boldsymbol{\xi}_1(s_1)-\lambda_\alpha\boldsymbol{\xi}(t_1)|$ are then expanded in Taylor series since $\kappa\lambda$ is small. The remaining integrations over times and shape $\boldsymbol{\xi}_1$ provide a contribution of order $\beta e^2\kappa O(\kappa\lambda)$ which depends on $\boldsymbol{\xi}$. The third term in the r.h.s. of (A.9) has the same order and a similar shape-dependence, as shown by variable changes $\mathbf{q}=\kappa|\lambda_\alpha\boldsymbol{\xi}(s)-\lambda_\gamma\boldsymbol{\xi}_1(s)+\lambda_\gamma\boldsymbol{\xi}_1(s_1)-\lambda_\alpha\boldsymbol{\xi}(t)|\mathbf{u}$ with $t=s_1$ or $t=t_1$ (the integral over $\mathbf{q}$ is splitted as the sum of two integrals by adding and subtracting 1 to $[\exp(-i\kappa\mathbf{q}\cdot\lambda_\alpha\boldsymbol{\xi}(s_1))-\exp(-i\kappa\mathbf{q}\cdot\lambda_\alpha\boldsymbol{\xi}(t_1))]$).

The integration of $I_R(\mathcal{L})$ over shape $\boldsymbol{\xi}$ readily follows from (A.9). Now in the second and third terms of (A.9), it is convenient to first perform integration over shapes $\boldsymbol{\xi}$ and $\boldsymbol{\xi}_1$, using the previous trick relative to differences $\boldsymbol{\xi}(s)-\boldsymbol{\xi}(t_1)$ and $\boldsymbol{\xi}_1(s)-\boldsymbol{\xi}_1(s_1)$, as well as the Gaussian nature of measures $\mathcal{D}(\boldsymbol{\xi})$ and $\mathcal{D}(\boldsymbol{\xi}_1)$. This leads to

$$\int\mathcal{D}(\boldsymbol{\xi})I_R(\mathcal{L})=\frac{\beta e^2\kappa}{2}+\frac{\beta e^2\kappa}{\pi}\sum_\gamma\int_0^1 ds_1\int_0^1 dt_1\int_0^\infty dq\frac{1}{(q^2+1)}$$
$$\times\{\exp[-\kappa^2\lambda_\gamma^2q^2s_1(1-s_1)/2-\kappa^2\lambda_\alpha^2q^2t_1(1-t_1)/2]-1\}$$
$$+\frac{\beta e^2\kappa}{\pi}\sum_\gamma\int_0^1 ds_1\int_0^\infty dq\frac{1}{q^2}\{\exp[-\kappa^2(\lambda_\alpha^2+\lambda_\gamma^2)q^2s_1(1-s_1)/2]-1\}$$
$$-\frac{\beta e^2\kappa}{\pi}\sum_\gamma\int_0^1 ds_1\int_0^1 dt_1\int_0^\infty dq\frac{1}{q^2}$$
$$\times\{\exp[-\kappa^2\lambda_\gamma^2q^2s_1(1-s_1)/2-\kappa^2\lambda_\alpha^2q^2t_1(1-t_1)/2]-1\}$$
$$+\beta e^2\kappa O((\kappa\lambda)^2). \quad (A.10)$$

The integrals over q in the second, third and fourth terms of (A.10) are computed, similarly to that arising in (A.5), in terms of elementary functions which are afterwards expanded in powers of $\kappa\lambda$. Contributions of second and fourth terms with order $\beta e^2\kappa O(\kappa\lambda)$ cancel out, so it remains

$$\int\mathcal{D}(\boldsymbol{\xi})I_R(\mathcal{L})=\frac{\beta e^2\kappa}{2}\left[1-\frac{\sqrt{\pi}}{8\sqrt{2}}\sum_\gamma\kappa\lambda_{\alpha\gamma}+O((\kappa\lambda)^2)\right]. \quad (A.11)$$

A.4 Truncated Integrals of Powers of V

Quantum virial functions $Q(\pm x_{\alpha\gamma})$ are defined [39] through a truncation similar to that arising in $\langle\mathbf{r}|[\exp(-\beta H_{\alpha\gamma})]^T_{\text{Mayer}}|\mathbf{r}\rangle$, where matrix elements of time-evolved operators $V_{\alpha\gamma}$ and $[V_{\alpha\gamma}]^2$ are replaced by $\beta e_\alpha e_\gamma/r$ and β^2e^4/r^2 respectively, while $[V_{\alpha\gamma}]^3$-term is omitted.

Within such truncation, convergence at large distances is ensured by taking the limit $R \to \infty$ of the corresponding spatial integral inside a sphere with radius R plus logarithmic counter terms [39]. When partition functions $Z_{exc}(1,1)$, $Z(2,0)$ and $Z(0,2)$ are expressed in terms of the Q's and E's, the integrals arising from $V_{\alpha\gamma} - e_\alpha e_\gamma / r$, $V_{\alpha\gamma}^2 - e^4/r^2$ and $[V_{\alpha\gamma}]^3$ are computed within previous methods applied to similar integrals of powers of ϕ. The sum of contributions due to $V_{\alpha\gamma} - e_\alpha e_\gamma / r$ vanishes by virtue of identity $\lambda_{pp}^2 + \lambda_{ee}^2 - 2\lambda_{pe}^2 = 0$. We then find

$$\begin{aligned}
&\frac{1}{8}\left[Z_{exc}(1,1) + \left(\frac{2m}{m_p}\right)^{3/2} Z(2,0) + \left(\frac{2m}{m_e}\right)^{3/2} Z(0,2) \right] \\
&\quad = \frac{1}{8\pi^{1/2}} \left\{ 2Q(x_{pe}) + \left(\frac{2m}{m_p}\right)^{3/2} \left[Q(-x_{pp}) - \frac{1}{2} E(-x_{pp}) \right] \right. \\
&\qquad \left. + \left(\frac{2m}{m_e}\right)^{3/2} \left[Q(-x_{ee}) - \frac{1}{2} E(-x_{ee}) \right] \right\} \\
&\qquad - \frac{1}{2} \exp(-\beta E_H) + \frac{\beta^2 e^4}{32\lambda_{pe}^3} (2\lambda_{pe} + \lambda_{pp} + \lambda_{ee}) + \frac{\beta^3 e^6}{24(2\pi\lambda_{pe}^2)^{3/2}} (c_p + c_e) \\
&\qquad + \frac{\beta^3 e^6}{12(2\pi)^{1/2}\lambda_{pe}^3} \ln(\lambda_{pp}\lambda_{ee}/\lambda_{pe}^2).
\end{aligned} \tag{A.12}$$

In the r.h.s of (A.12), the first additional term to the linear combination of the Q's and E's merely arises from the substraction of groundstate contribution in $Z_{exc}(1,1)$, while the last one is due to the logarithmic counter terms introduced in the definitions of the Q's.

A.5 Integral Mixing ϕ, I_R and V

At lowest order, effects of atom polarization are entirely embedded in the integral

$$\begin{aligned}
&\frac{4z^2}{(2\pi\lambda^2)^3 \Lambda} \int \mathrm{d}\mathbf{R}\mathrm{d}\mathbf{r} \int \mathcal{D}(\boldsymbol{\xi}_a)\mathcal{D}(\boldsymbol{\xi}_1)\mathcal{B}^T(a,1) \\
&\qquad \times [I_R(\mathcal{L}_a^p) + I_R(\mathcal{L}_1^e) - \beta(\phi(\mathcal{L}_a^p, \mathcal{L}_1^e) - V(\mathcal{L}_a^p, \mathcal{L}_1^e))]
\end{aligned} \tag{A.13}$$

where we set $\mathbf{R} = \mathbf{R}_a$ and $\mathbf{r} = \mathbf{r}_1$. Similarly to the case of bare integral (3.10), the presence of Boltzmann factor $\exp(-\beta V(\mathcal{L}_a^p, \mathcal{L}_1^e))$ in $\mathcal{B}^T(a,1)$ implies that leading contributions in (A.13) arise from configurations where loop sizes are at most of order λ, while relative proton-electron distance $|\mathbf{r} - \mathbf{R}|$ is of order the extension a_B of the atom groundstate. The I_R's are then expanded with respect to small parameter $\kappa\lambda$ as above, while a similar expansion is derived for $(\phi - V)$ by starting from a convolution relation analogous to (2.40) and by noting that κa_B is also a small parameter. This provides

$$\begin{aligned}
&I_R(\mathcal{L}_a^p) + I_R(\mathcal{L}_1^e) - \beta(\phi(\mathcal{L}_a^p, \mathcal{L}_1^e) - V(\mathcal{L}_a^p, \mathcal{L}_1^e)) \\
&\quad = \frac{\beta e^2 \kappa^2}{4} \int_0^1 \mathrm{d}s \int_0^1 \mathrm{d}t [2|\mathbf{r} + \lambda_e \boldsymbol{\xi}_1(t) - \mathbf{R} - \lambda_p \boldsymbol{\xi}_a(s)| - \lambda_e |\boldsymbol{\xi}_1(t) - \boldsymbol{\xi}_1(s)| \\
&\qquad - \lambda_p |\boldsymbol{\xi}_a(t) - \boldsymbol{\xi}_a(s)|] + \beta e^2 \kappa\, O((\kappa\lambda)^2).
\end{aligned} \tag{A.14}$$

In (A.14), terms proportional to $\beta e^2 \kappa$ cancel out, as well as terms proportional to $\beta e^2 \kappa^2 |\mathbf{r} - \mathbf{R}|$ which do not depend on loop shapes.

Using (A.14) in (A.13), the functional integrations over loop shapes can be rewritten in terms of matrix elements of Gibbs operators. For instance, the integral associated with the first term $\exp(-\beta V(\mathcal{L}_a^p, \mathcal{L}_1^e))$ in truncated Mayer coefficient $\mathcal{B}^T(a,1)$ can be rewritten as

$$\begin{aligned}
&\frac{2z^2e^2\kappa^2}{\beta\Lambda}\int \mathrm{d}\mathbf{R}\mathrm{d}\mathbf{r}\mathrm{d}\mathbf{R}_1\mathrm{d}\mathbf{R}_2\mathrm{d}\mathbf{r}_1\mathrm{d}\mathbf{r}_2\\
&\quad\times\int_0^\beta \mathrm{d}\tau_1\int_0^{\tau_1}\mathrm{d}\tau_2\langle\mathbf{R}\mathbf{r}|\exp[-(\beta-\tau_1)H_{1,1}]|\mathbf{R}_1\mathbf{r}_1\rangle\\
&\quad\times\langle\mathbf{R}_1\mathbf{r}_1|\exp[-(\tau_1-\tau_2)H_{1,1}]|\mathbf{R}_2\mathbf{r}_2\rangle\langle\mathbf{R}_2\mathbf{r}_2|\exp[-\tau_2H_{1,1}]|\mathbf{R}\mathbf{r}\rangle\\
&\quad\times[2|\mathbf{r}_2-\mathbf{R}_1|-|\mathbf{r}_2-\mathbf{r}_1|-|\mathbf{R}_2-\mathbf{R}_1|] \qquad (A.15)
\end{aligned}$$

discarding terms of order $\beta e^2\kappa O((\kappa\lambda)^2)$. Next subtracted terms in $\mathcal{B}^T(a,1)$ are rewritten similarly to (A.15) where imaginary-time evolution operators are associated with purely kinetic Hamiltonian $H_{1,0}+H_{0,1}$. At low temperatures, such terms become exponentially smaller than (A.15), the behavior of which is controlled by atomic groundstate contributions. That behavior is determined by starting with decomposition $H_{1,1}=-\hbar^2\Delta_{\mathbf{R}^*}/(2M)+H_{pe}$. An eigenstate of $H_{1,1}$ reduces then to the product of a plane wave $\exp(i\mathbf{K}\cdot\mathbf{R}^*)/\Lambda^{1/2}$ for position $\mathbf{R}^*=(m_p\mathbf{R}+m_e\mathbf{r})/M$ of the atom mass center, times an internal wave function $\psi_p(\mathbf{r}^*)$ for relative position $\mathbf{r}^*=\mathbf{r}-\mathbf{R}$, while its energy reads $\hbar^2\mathbf{K}^2/(2M)+E_H^{(p)}$. For bound states, $p\to(n,l,m)$ where n is the usual quantum principal number ($E_H^{(p)}=E_H/n^2$, $1\le n$), l is the orbital number ($0\le l\le n-1$) and m is the azimuthal number $-l\le m\le l$ ($0\to(1,0,0)$ denotes the ground state); for diffusive states, $p\to(k,l,m)$ where k parametrizes the positive energy $E_H^{(p)}=\hbar^2k^2/(2m)$ while l and m are again the orbital and azimuthal numbers with $0\le l$ (the precise forms of the corresponding ψ_p's are given in Ref. [42] for instance). After changing proton and electron positions in favor of their mass center and relative particle counterparts in (A.15), the matrix elements are evaluated by suitable insertions of closure relation for the basis made with previous eigenstates. The resulting integrals over τ_1 and τ_2 are readily performed for each set of involved eigenstates. According to the scaling prescriptions defined in Sect. 3, integral (A.13) is then rewritten as (3.19) plus terms which decay exponentially faster than $\rho^*\exp(\beta E_H)$, while screening function $S_3(1,1)$ reads

$$\begin{aligned}
S_3(1,1)=\frac{\sqrt{2}(\beta|E_H|)^{1/2}}{64\pi^5}\exp(-\beta E_H)\Bigg\{&4\int\mathrm{d}\mathbf{K}\mathrm{d}\mathbf{Q}\frac{\sinh(\mathbf{K}\cdot\mathbf{Q})}{\mathbf{K}\cdot\mathbf{Q}}\exp(-(K^2+Q^2)/2)\\
&\times\int\mathrm{d}\mathbf{X}\mathrm{d}\mathbf{r}_1^*\mathrm{d}\mathbf{r}_2^*\exp(-2i\mathbf{K}\cdot\mathbf{X})|\psi_0(\mathbf{r}_1^*)|^2|\psi_0(\mathbf{r}_2^*)|^2\\
&\times\Bigg[2\left|\left(\frac{2\beta|E_H|m}{M}\right)^{1/2}\mathbf{X}+\frac{m_e}{M}\mathbf{r}_1^*+\frac{m_p}{M}\mathbf{r}_2^*\right|\\
&-\left|\left(\frac{2\beta|E_H|m}{M}\right)^{1/2}\mathbf{X}-\frac{m_p}{M}\mathbf{r}_1^*+\frac{m_p}{M}\mathbf{r}_2^*\right|\\
&-\left|\left(\frac{2\beta|E_H|m}{M}\right)^{1/2}\mathbf{X}+\frac{m_e}{M}\mathbf{r}_1^*-\frac{m_e}{M}\mathbf{r}_2^*\right|\Bigg]
\end{aligned}$$

$$+\sum_{p\neq 0}\int \mathrm{d}\mathbf{K}\mathrm{d}\mathbf{Q}\frac{\exp(-K^2/2)}{\beta(E_H^{(p)}-E_H)+Q^2/2-K^2/2}$$

$$\times\int \mathrm{d}\mathbf{X}\mathrm{d}\mathbf{r}_1^*\mathrm{d}\mathbf{r}_2^*\exp(i(\mathbf{K}-\mathbf{Q})\cdot\mathbf{X})$$

$$\times\overline{\psi}_0(\mathbf{r}_1^*)\psi_0(\mathbf{r}_2^*)\psi_p(\mathbf{r}_1^*)\overline{\psi}_p(\mathbf{r}_2^*)\Big[2\Big|\Big(\frac{2\beta|E_H|m}{M}\Big)^{1/2}\mathbf{X}+\frac{m_e}{M}\mathbf{r}_1^*+\frac{m_p}{M}\mathbf{r}_2^*\Big|$$

$$-\Big|\Big(\frac{2\beta|E_H|m}{M}\Big)^{1/2}\mathbf{X}-\frac{m_p}{M}\mathbf{r}_1^*+\frac{m_p}{M}\mathbf{r}_2^*\Big|$$

$$-\Big|\Big(\frac{2\beta|E_H|m}{M}\Big)^{1/2}\mathbf{X}+\frac{m_e}{M}\mathbf{r}_1^*-\frac{m_e}{M}\mathbf{r}_2^*\Big|\Big]\Big\}. \tag{A.16}$$

In (A.16), all integration variables are dimensionless, in particular $\mathbf{r}_i^*$ is expressed in units of a_B. Moreover, the sum over diffusive states must be understood as an integral over k from 0 to ∞ and a discrete sum over l and m. When $\beta\to\infty$, $S_3(1,1)$ behaves as

$$S_3(1,1)\sim\frac{c_{at}}{8\pi^{3/2}(\beta|E_H|)^{1/2}}\exp(-\beta E_H) \tag{A.17}$$

with pure numerical constant

$$c_{at}=\sum_{p\neq 0}\frac{|E_H|}{E_H^{(p)}-E_H}\int \mathrm{d}\mathbf{Y}\mathrm{d}\mathbf{r}_1^*\mathrm{d}\mathbf{r}_2^*\frac{\exp(-|\mathbf{Y}|)}{|\mathbf{Y}|}\overline{\psi}_0(\mathbf{r}_1^*)\psi_0(\mathbf{r}_2^*)\psi_p(\mathbf{r}_1^*)\overline{\psi}_p(\mathbf{r}_2^*)$$

$$\times\Big[2\Big|\Big(\frac{m|E_H|}{M(E_H^{(p)}-E_H)}\Big)^{1/2}\mathbf{Y}+\frac{m_e}{M}\mathbf{r}_1^*+\frac{m_p}{M}\mathbf{r}_2^*$$

$$-\Big|\Big(\frac{m|E_H|}{M(E_H^{(p)}-E_H)}\Big)^{1/2}\mathbf{Y}-\frac{m_p}{M}\mathbf{r}_1^*+\frac{m_p}{M}\mathbf{r}_2^*\Big|$$

$$-\Big|\Big(\frac{m|E_H|}{M(E_H^{(p)}-E_H)}\Big)^{1/2}\mathbf{Y}+\frac{m_e}{M}\mathbf{r}_1^*-\frac{m_e}{M}\mathbf{r}_2^*\Big|\Big]. \tag{A.18}$$

Notice that only the second term ($\sum_{p\neq 0}\cdots$) in (A.16) contributes to asymptotic behavior (A.17) (the first term provide contributions smaller by a factor $\ln(\beta|E_H|)/(\beta|E_H|)$ as a consequence of the spherical symmetry of groundstate wavefunction $\psi_0(\mathbf{r}^*)=\psi_0(r^*)$). An accurate simplified expression for c_{at} can be derived by setting $m/M=m_e/M=0$ and $m_p/M=1$ in agreement with numerical value of ratio $m_e/m_p\simeq 1/1850$, i.e.

$$c_{at}\simeq -4\pi\sum_{p\neq 0}\frac{|E_H|}{E_H^{(p)}-E_H}\int \mathrm{d}\mathbf{r}_1^*\mathrm{d}\mathbf{r}_2^*\overline{\psi}_0(\mathbf{r}_1^*)\psi_0(\mathbf{r}_2^*)\psi_p(\mathbf{r}_1^*)\overline{\psi}_p(\mathbf{r}_2^*)|\mathbf{r}_1^*-\mathbf{r}_2^*| \tag{A.19}$$

which provides $c_{at}\simeq 10.1$.

Appendix B: Low-Temperature Behavior of Few-Body Partition Functions

B.1 Behavior of $Z(1,1)$

Two-body proton-electron partition function $Z(1,1)$ reads

$$Z(1,1) = 4\int \mathrm{d}\mathbf{x}\langle\mathbf{x}|[\exp(-\beta H_{pe})]^T_{\mathrm{Mayer}}|\mathbf{x}\rangle, \tag{B.1}$$

where reduced Hamiltonian H_{pe} describes a single particle with mass m submitted to attractive Coulomb potential $V_{pe}(\mathbf{x}) = -e^2/|\mathbf{x}|$. Here, for the sake of notational convenience, we set $\mathbf{x} = \mathbf{r}^*$, while z will denote a complex number. The integral over $\mathbf{x}$ can be splitted into two parts, $|\mathbf{x}| < \beta e^2$ and $\mathbf{x} > \beta e^2$, the contributions of which are determined as follows.

For $|\mathbf{x}| < \beta e^2$, truncated Mayer operator $[\exp(-\beta H_{pe})]^T_{\mathrm{Mayer}}$ is replaced by its definition (3.14) in (B.1). The contribution of second term in (3.14), as well as those of next terms involving imaginary-time evolutions of V_{pe} with kinetic Hamiltonian K_{pe}, are readily computed in terms of elementary functions by exploiting the Gaussian nature of matrix elements of $\exp(-\beta K_{pe})$. Such contributions are bounded by a power of β. The contribution of first term in (3.14) is analyzed by introducing the Green function $\widehat{G}(\mathbf{x},\mathbf{y};z)$ defined as the matrix elements of resolvent $(z + H_{pe})^{-1}$. That function is the solution of partial differential equation

$$\left(-\frac{\hbar^2}{2m}\Delta_{\mathbf{x}} - \frac{e^2}{|\mathbf{x}|} + z\right)\widehat{G}(\mathbf{x},\mathbf{y};z) = \delta(\mathbf{x}-\mathbf{y}), \tag{B.2}$$

with suitable boundary conditions [36]. Its exact expression reads [36]

$$\begin{aligned}\widehat{G}(\mathbf{x},\mathbf{y};z) = \frac{m\Gamma(1-i\nu)}{2\pi\hbar^2|\mathbf{x}-\mathbf{y}|}[&W_{i\nu,1/2}(-ikd_+)\dot{M}_{i\nu,1/2}(-ikd_-)\\ &- \dot{W}_{i\nu,1/2}(-ikd_+)M_{i\nu,1/2}(-ikd_-)],\end{aligned} \tag{B.3}$$

with $k = (-2mz/\hbar^2)^{1/2}$ $(\Im(k) > 0)$, $\nu = 1/(ka_B)$, $d_+ = |\mathbf{x}| + |\mathbf{y}| + |\mathbf{x}-\mathbf{y}|$ and $d_- = |\mathbf{x}| + |\mathbf{y}| - |\mathbf{x}-\mathbf{y}|$, while $\Gamma(u)$ is the familiar gamma-function and $W_{i\nu,1/2}(u)$, $M_{i\nu,1/2}(u)$ are Whittaker functions [31] ($\dot{W}_{i\nu,1/2}(u) = \partial W_{i\nu,1/2}(u)/\partial u$, $\dot{M}_{i\nu,1/2}(u) = \partial M_{i\nu,1/2}(u)/\partial u$). Green function $\widehat{G}(\mathbf{x},\mathbf{y};z)$ is analytical in z in the whole complex plane, except on the negative real axis ($\Re(z) \le 0$, $\Im(z) = 0$) which is a cut line, and also at $z = z_n = -E_H/n^2$ $(n \ge 1)$ which are simple poles (of course, such singularities are controlled by the spectrum of H_{pe}). When $\mathbf{x} \to \mathbf{y}$, $\widehat{G}(\mathbf{x},\mathbf{y};z)$ diverges as $m/(2\pi\hbar^2|\mathbf{x}-\mathbf{y}|)$, as shown by expanding Whittaker functions for arguments close to $-2ik|\mathbf{x}|$. That $1/|\mathbf{x}-\mathbf{y}|$-behavior, is also displayed by free Green function $\widehat{G}_0(\mathbf{x},\mathbf{y};z) = m\exp(ik|\mathbf{x}-\mathbf{y}|)/(2\pi\hbar^2|\mathbf{x}-\mathbf{y}|)$, and it can be interpreted by quoting that (B.2) reduces to Poisson equation for $|\mathbf{x}-\mathbf{y}|$ small. It is convenient to define

$$\begin{aligned}\widehat{H}(\mathbf{x},\mathbf{y};z) &= \widehat{G}(\mathbf{x},\mathbf{y};z) - \widehat{G}_0(\mathbf{x},\mathbf{y};z) + \int \mathrm{d}\mathbf{r}\widehat{G}_0(\mathbf{x},\mathbf{r};z)V_{pe}(|\mathbf{r}|)\widehat{G}_0(\mathbf{r},\mathbf{y};z)\\ &= \int \mathrm{d}\mathbf{r}_1\mathrm{d}\mathbf{r}_2\widehat{G}_0(\mathbf{x},\mathbf{r}_1;z)V_{pe}(|\mathbf{r}_1|)\widehat{G}_0(\mathbf{r}_1,\mathbf{r}_2;z)V_{pe}(|\mathbf{r}_2|)\widehat{G}(\mathbf{r}_2,\mathbf{y};z)\end{aligned} \tag{B.4}$$

where the second equality follows from a standard identity for interacting and free Green functions. That function $\widehat{H}(\mathbf{x},\mathbf{y};z)$ has the same analytical properties as $\widehat{G}(\mathbf{x},\mathbf{y};z)$. Using

above expansions of Whittaker functions, we find that $\widehat{H}(\mathbf{x},\mathbf{x};z)$ reads

$$\widehat{H}(\mathbf{x},\mathbf{x};z)=\frac{-imk\Gamma(1-i\nu)}{2\pi\hbar^2}\Big[2\dot{W}_{i\nu,1/2}\dot{M}_{i\nu,1/2}-\ddot{W}_{i\nu,1/2}M_{i\nu,1/2}-W_{i\nu,1/2}\ddot{M}_{i\nu,1/2}\Big](-2ik|\mathbf{x}|)-\frac{imk}{2\pi\hbar^2}-\frac{m^2e^2}{4\pi^2\hbar^4}\int d\mathbf{r}\frac{\exp(2ik|\mathbf{x}-\mathbf{r}|)}{r|\mathbf{x}-\mathbf{r}|^2}. \tag{B.5}$$

Notice that, contrarily to $\widehat{G}-\widehat{G}_0$ which diverges as $-2m^2e^2\ln(|k||\mathbf{x}|)/(\pi\hbar^4)$ when $\mathbf{x}\to\mathbf{0}$, $\widehat{H}(\mathbf{x},\mathbf{x};z)$ remains finite at $\mathbf{x}=\mathbf{0}$ thanks to the addition of the integral of $\widehat{G}_0V_{pe}\widehat{G}_0$ in (B.4).

Since $\widehat{G}(\mathbf{x},\mathbf{y};z)$ is nothing but the Laplace transform with respect to β of density matrix $\langle\mathbf{x}|\exp(-\beta H_{pe})|\mathbf{y}\rangle$, the standard inversion formula provides

$$\langle\mathbf{x}|\exp(-\beta H_{pe})|\mathbf{y}\rangle=\frac{1}{2i\pi}\int_{D_\sigma}dz\exp(\beta z)\widehat{G}(\mathbf{x},\mathbf{y};z) \tag{B.6}$$

where D_σ is any straight line parallel to imaginary axis and which cuts real axis at $\sigma>-E_H$. Inserting decomposition of $\widehat{G}$ in terms of $\widehat{G}_0$, V_{pe} and $\widehat{H}$ into (B.6), we find that the contribution of terms involving $\widehat{G}_0$ give raise to free density matrix $\langle\mathbf{x}|\exp(-\beta K_{pe})|\mathbf{y}\rangle=\exp(-|\mathbf{x}-\mathbf{y}|^2/(2\lambda_{pe}^2))/(2\pi\lambda_{pe}^2)^{3/2}$. The resulting expression of $\langle\mathbf{x}|\exp(-\beta H_{pe})|\mathbf{y}\rangle$ can be specified to diagonal elements $\mathbf{x}=\mathbf{y}$ because $\widehat{H}(\mathbf{x},\mathbf{x};z)$ is finite. The integral of $\widehat{H}(\mathbf{x},\mathbf{x};z)\exp(\beta z)$ along D_σ is then transformed by applying Cauchy's theorem with contour $C_{\sigma,\delta}$ shown in Fig. 13 ($-E_H/4<\delta<-E_H$). Function $\widehat{H}(\mathbf{x},\mathbf{x};z)\exp(\beta z)$ is analytical inside $C_{\sigma,\delta}$ except at $z=z_1=-E_H$ which is a simple pole with residue $|\psi_0(\mathbf{x})|^2\exp(-\beta E_H)$. Moreover, it satisfies Jordan's lemma on the circular parts of $C_{\sigma,\delta}$ which connect D_δ to D_σ, so the corresponding parts of the contour integral vanish when the radius is sent to infinity. This provides

$$\begin{aligned}&\langle\mathbf{x}|\exp(-\beta H_{pe})|\mathbf{x}\rangle\\&=|\psi_0(\mathbf{x})|^2\exp(-\beta E_H)-\frac{1}{2i\pi}\int_{D_\delta}dz\exp(\beta z)\widehat{H}(\mathbf{x},\mathbf{x};z)\\&\quad+\frac{1}{(2\pi\lambda_{pe}^2)^{3/2}}\Big[1+\frac{\beta e^2}{|\mathbf{x}|}\int_0^1 ds\,\Phi(|\mathbf{x}|/(\sqrt{2}s(1-s)\lambda_{pe}))\Big]\end{aligned} \tag{B.7}$$

where Φ is the familiar Error function [31]. Last term in (B.7) is bounded by a power of β. Along D_δ, index $i\nu$ of Whittaker functions follows a closed curve in complex plane which cuts real axis at non-strictly positive integers. At the same time, their argument $u=-2ik|\mathbf{x}|$ remains inside sector $-3\pi/8<\arg(u)<3\pi/8$. Consequently, $|\widehat{H}(\mathbf{x},\mathbf{x};z)|$ remains bounded by a constant when z runs along D_δ. The modulus of the corresponding integral in (B.7) is then bounded by a power of β times $\exp(\beta\delta)$. Taking into account above power-law bounds for the contributions of truncated terms in $[\exp(-\beta H_{pe})]^T_{\text{Mayer}}$, and noting that $\psi_0(\mathbf{x})$ decays exponentially fast for $|\mathbf{x}|>\beta e^2$, we eventually obtain

$$\int_{|\mathbf{x}|<\beta e^2}d\mathbf{x}\langle\mathbf{x}|[\exp(-\beta H_{pe})]^T_{\text{Mayer}}|\mathbf{x}\rangle=\exp(-\beta E_H), \tag{B.8}$$

Fig. 13 Path in complex plane

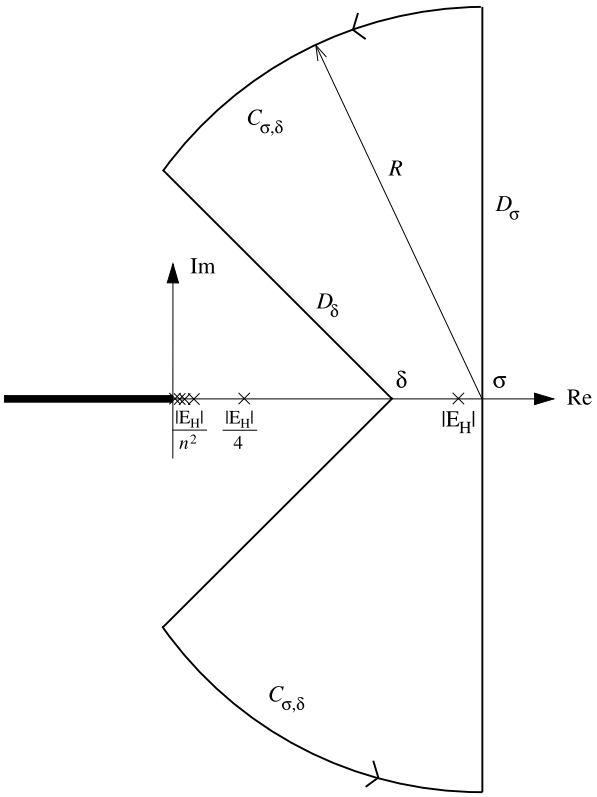

discarding additional terms which are exponentially smaller than $\exp(-\beta E_H)$ when $\beta \to \infty$.

For $|\mathbf{x}| > \beta e^2$, it is convenient to use Feynman-Kac expression of $\langle \mathbf{x}|[\exp(-\beta \times H_{pe})]^T_{\text{Mayer}}|\mathbf{x}\rangle$. Within the variable change $\mathbf{x} = \beta e^2 \mathbf{v}$, the corresponding integral is rewritten as

$$\begin{aligned}
&\int_{|\mathbf{x}|>\beta e^2} \mathrm{d}\mathbf{x} \langle \mathbf{x}|[\exp(-\beta H_{pe})]^T_{\text{Mayer}}|\mathbf{x}\rangle \\
&\quad = \frac{1}{(2\pi)^{3/2}} \left(\frac{\beta e^2}{\lambda_{pe}}\right)^3 \int_{|\mathbf{v}|>1} \mathrm{d}\mathbf{v} \int \mathcal{D}(\boldsymbol{\xi}) \\
&\qquad \times \left[\exp\left(\int_0^1 \mathrm{d}s \left| \mathbf{v} + \frac{\lambda_{pe}}{\beta e^2} \boldsymbol{\xi}(s) \right|^{-1} \right) - 1 - \int_0^1 \mathrm{d}s \left| \mathbf{v} + \frac{\lambda_{pe}}{\beta e^2} \boldsymbol{\xi}(s) \right|^{-1} \right. \\
&\qquad \left. - \frac{1}{2} \left(\int_0^1 \mathrm{d}s \left| \mathbf{v} + \frac{\lambda_{pe}}{\beta e^2} \boldsymbol{\xi}(s) \right|^{-1} \right)^2 - \frac{1}{6} \left(\int_0^1 \mathrm{d}s \left| \mathbf{v} + \frac{\lambda_{pe}}{\beta e^2} \boldsymbol{\xi}(s) \right|^{-1} \right)^3 \right]. \qquad \text{(B.9)}
\end{aligned}$$

When $\beta \to \infty$, ratio $\lambda_{pe}/\beta e^2$ vanishes. Then, potential $|\mathbf{v} + \frac{\lambda_{pe}}{\beta e^2} \boldsymbol{\xi}(s)|^{-1}$ can be merely replaced by $|\mathbf{v}|$ because the mean extension of $\boldsymbol{\xi}(s)$ is of order 1. The corresponding functional integral over $\boldsymbol{\xi}(s)$ reduces to 1 by normalization of Wiener measure $\mathcal{D}(\boldsymbol{\xi})$, and the remaining

integral over $\mathbf{v}$ is a pure number. Thus, the integral in the l.h.s. of (B.9) behaves as a power of β, and it becomes exponentially smaller than (B.8) when $\beta \to \infty$. This implies

$$Z(1,1) = 4\exp(-\beta E_H) \tag{B.10}$$

discarding terms which are exponentially smaller when $\beta \to \infty$. Next corrections to that leading behavior arising from excited atomic states, can be readily obtained within a similar approach by adjusting the position δ between two successive poles, i.e. $z_{n+1} < \delta < z_n$ with $n > 1$.

B.2 Behavior of $Z(1,2)$

The low-temperature behavior of $Z(1,2)$, which involves one proton and two electrons, is determined by a straightforward extension of previous methods applied to $Z(1,1)$. If an exact expression of three-body Green function is not available, its main properties of interest can be guessed, under rather weak assumptions, by exploiting relations and analogies with its free counterpart, as well as known results on the spectrum of $H_{1,2}$. Such properties appear to be quite natural extensions of the exact behaviors observed in the two-body case.

Let $\mathbf{R} = (m_p\mathbf{R}_a + m_e\mathbf{r}_1 + m_e\mathbf{r}_2)/M_{H^-}$ be the position of center of mass ($M_{H^-} = m_p + 2m_e$), while $\mathbf{x}_1 = (\mathbf{r}_1 - \mathbf{r}_2)/\sqrt{2}$ and $\mathbf{x}_2 = (m_p/M_{H^-})^{1/2}(\mathbf{r}_1 + \mathbf{r}_2 - 2\mathbf{R}_a)/\sqrt{2}$ are the reduced variables. After expressing $H_{1,2}$ in terms of those variables, we find that three-body partition function $Z(1,2)$ can be rewritten as

$$\begin{aligned} Z(1,2) = 2\int \mathrm{d}\mathbf{x}_1\mathrm{d}\mathbf{x}_2\{&2\langle \mathbf{x}_1\mathbf{x}_2|\exp(-\beta H^*_{1,2})|\mathbf{x}_1\mathbf{x}_2\rangle \\ &- \langle -\mathbf{x}_1\mathbf{x}_2|\exp(-\beta H^*_{1,2})|\mathbf{x}_1\mathbf{x}_2\rangle + \cdots\} \end{aligned} \tag{B.11}$$

with reduced Hamiltonian

$$\begin{aligned} H^*_{1,2} = &-\frac{\hbar^2}{2m_e}\Delta_{\mathbf{x}_1} - \frac{\hbar^2}{2m_e}\Delta_{\mathbf{x}_2} + \frac{e^2}{\sqrt{2}|\mathbf{x}_1|} - \frac{\sqrt{2}e^2}{|\mathbf{x}_1 + (M_{H^-}/m_p)^{1/2}\mathbf{x}_2|} \\ &- \frac{\sqrt{2}e^2}{|\mathbf{x}_1 - (M_{H^-}/m_p)^{1/2}\mathbf{x}_2|}. \end{aligned} \tag{B.12}$$

Off-diagonal matrix elements in the r.h.s. of (B.11) are associated with the exchange of the electrons. First potential term in (B.12) describes Coulomb repulsion between those electrons, while the second and third ones account for Coulomb attractions between the proton and each electron. In the double integral involved in (B.11), we make a partition of space integration into three domains $\Omega^{(i)}$ ($i = 0, 1, 2$), such that i, and only i, sides of triangle $(\mathbf{0}, \mathbf{x}_1, \mathbf{x}_2)$ are smaller than βe^2 in $\Omega^{(i)}$.

For $\mathbf{x}_1, \mathbf{x}_2$ inside $\Omega^{(2)}$, we express matrix elements of $\exp(-\beta H^*_{1,2})$ as inverse Laplace transforms of Green function $\widehat{G}(\mathbf{x}_1, \mathbf{x}_2; \mathbf{y}_1, \mathbf{y}_2; z)$ solution of

$$(H^*_{1,2} + z)\widehat{G}(\mathbf{x}_1, \mathbf{x}_2; \mathbf{y}_1, \mathbf{y}_2; z) = \delta(\mathbf{x}_1 - \mathbf{y}_1)\delta(\mathbf{x}_2 - \mathbf{y}_2) \tag{B.13}$$

with suitable boundary conditions. That Green function is analytical in z in the whole complex plane, except on a part of real axis with $\Re(z) < -E_{H^-}$, while $z_1 = -E_{H^-}$ is a simple (isolated) pole with residue $\psi_0(\mathbf{x}_1, \mathbf{x}_2)\overline{\psi}_0(\mathbf{y}_1, \mathbf{y}_2)$ (ψ_0 is the groundstate wavefunction of

$H^*_{1,2}$ with energy E_{H^-}). For a given z not close to its singularities, $\widehat{G}(\mathbf{x}_1, \mathbf{x}_2; \mathbf{y}_1, \mathbf{y}_2; z)$ displays a position-dependence analogous to that of free Green function $\widehat{G}_0(\mathbf{x}_1, \mathbf{x}_2; \mathbf{y}_1, \mathbf{y}_2; z)$ solution of Helmholtz equation in six dimensions. In particular, for $\mathbf{x}_i$ close to $\mathbf{y}_i$, potential terms in (B.13) can be omitted and $\widehat{G}(\mathbf{x}_1, \mathbf{x}_2; \mathbf{y}_1, \mathbf{y}_2; z)$ also diverges as $1/[(\mathbf{x}_1 - \mathbf{y}_1)^2 + (\mathbf{x}_2 - \mathbf{y}_2)^2]^2$, i.e. the Coulomb potential in six dimensions. In order to handle such divergences for diagonal matrix elements, we consider identity

$$\begin{aligned}
&\widehat{G}(\mathbf{x}_1, \mathbf{x}_2; \mathbf{y}_1, \mathbf{y}_2; z) \\
&\quad = \widehat{G}_0(\mathbf{x}_1, \mathbf{x}_2; \mathbf{y}_1, \mathbf{y}_2; z) \\
&\qquad - \int \mathrm{d}\mathbf{r}_1 \mathrm{d}\mathbf{r}_2 \widehat{G}_0(\mathbf{x}_1, \mathbf{x}_2; \mathbf{r}_1, \mathbf{r}_2; z) V^*_{1,2}(\mathbf{r}_1, \mathbf{r}_2) \widehat{G}(\mathbf{r}_1, \mathbf{r}_2; \mathbf{y}_1, \mathbf{y}_2; z)
\end{aligned} \tag{B.14}$$

where $V^*_{1,2}$ is the potential part of $H^*_{1,2}$. Successive iterations of formula (B.14) generate the perturbative expansion of $\widehat{G}(\mathbf{x}_1, \mathbf{x}_2; \mathbf{y}_1, \mathbf{y}_2; z)$ in powers of $V^*_{1,2}$. We define $\widehat{H}(\mathbf{x}_1, \mathbf{x}_2; \mathbf{y}_1, \mathbf{y}_2; z)$ as $\widehat{G}(\mathbf{x}_1, \mathbf{x}_2; \mathbf{y}_1, \mathbf{y}_2; z)$ minus the first six terms (up to order $(V^*_{1,2})^5$ included) of that expansion. Similarly to (B.4), $\widehat{H}$ has the same analytical properties as $\widehat{G}$, while $\widehat{H}(\mathbf{x}_1, \mathbf{x}_2; \mathbf{x}_1, \mathbf{x}_2; z)$ is now finite. After inserting the expression of $\widehat{G}$ in terms of $\widehat{G}_0$, $V^*_{1,2}$ and $\widehat{H}$ into the inversion formula for diagonal matrix element of $\exp(-\beta H^*_{1,2})$, we find that terms built with $\widehat{G}_0$ and $V^*_{1,2}$ are bounded by powers of β. For dealing with the contribution of $\widehat{H}$, we introduce a closed contour $C_{\sigma,\delta}$ in complex plane similar to that shown in Fig. 13, with $z_2 < \delta < z_1$ and $-z_2$ the first singularity of $\widehat{H}$ below z_1. Along that contour, z stays at a finite distance at any singularity of $\widehat{H}$. Also, for $|z|$ large, in the expression of $\widehat{H}$ as a spatial integral of $\widehat{G}_0 V^*_{1,2} \widehat{G}_0 \cdots V^*_{1,2} \widehat{G}$ (similar to that involved in (B.4)), $\widehat{G}$ can be replaced by $\widehat{G}_0$. Therefore, $\widehat{H}$ goes to zero as a power of k, as shown by variable changes $\mathbf{r}_i \to |k|\mathbf{r}_i$ (integrals over the $\mathbf{r}_i$'s do converge thanks to exponentially decaying factors $\exp(ik|\mathbf{r}_i - \mathbf{r}_j|)$ arising from the $\widehat{G}_0$'s). Hence, we conclude that $|\widehat{H}(\mathbf{x}_1, \mathbf{x}_2; \mathbf{x}_1, \mathbf{x}_2; z)|$ remains bounded along D_δ, while Jordan's lemma applies to the integral of $\widehat{H}(\mathbf{x}_1, \mathbf{x}_2; \mathbf{x}_1, \mathbf{x}_2; z) \exp(\beta z)$ upon the circular parts of $C_{\sigma,\delta}$. This provides

$$2\langle \mathbf{x}_1 \mathbf{x}_2 | \exp(-\beta H^*_{1,2}) | \mathbf{x}_1 \mathbf{x}_2 \rangle = 2|\psi_0(\mathbf{x}_1, \mathbf{x}_2)|^2 \exp(-\beta E_{H^-}) \tag{B.15}$$

discarding terms which are exponentially smaller. Within similar methods, we can also estimate the off-diagonal matrix element $\langle -\mathbf{x}_1 \mathbf{x}_2 | \exp(-\beta H^*_{1,2}) | \mathbf{x}_1 \mathbf{x}_2 \rangle$. Contributions of terms involving $\widehat{G}_0$'s and $V^*_{1,2}$'s are readily bounded by powers of β by rescaling positions in units of λ_e. Contribution of $\widehat{H}$ is treated as above since $\widehat{H}(-\mathbf{x}_1, \mathbf{x}_2; \mathbf{x}_1, \mathbf{x}_2; z)$ is bounded along D_δ and decays sufficiently fast for $|z|$ large. After using $\psi_0(-\mathbf{x}_1, \mathbf{x}_2) = \psi_0(\mathbf{x}_1, \mathbf{x}_2)$ ($H^*_{1,2}$ is invariant under transformation $\mathbf{x}_1 \to -\mathbf{x}_1$ at fixed $\mathbf{x}_2$), we find

$$\langle -\mathbf{x}_1 \mathbf{x}_2 | \exp(-\beta H^*_{1,2}) | \mathbf{x}_1 \mathbf{x}_2 \rangle = |\psi_0(\mathbf{x}_1, \mathbf{x}_2)|^2 \exp(-\beta E_{H^-}), \tag{B.16}$$

discarding terms which are exponentially smaller. Next terms $\cdots$ in the r.h.s. of (B.11), which arise from truncation in $[\exp(-\beta H_{1,2})]^T_{\text{Mayer}}$, can be also estimated by similar techniques. For instance, term

$$\int_0^\beta \mathrm{d}\tau \exp[-(\beta - \tau)(H_{1,1} + H_{0,1})] V_{at,e} \exp[-\tau(H_{1,1} + H_{0,1})] \tag{B.17}$$

provides a contribution which can be rewritten as the inverse Laplace transform of

$$\int \mathrm{d}\mathbf{y}_1\mathrm{d}\mathbf{y}_2\langle\mathbf{x}_1\mathbf{x}_2|(z+H^*_{pe,e})^{-1}|\mathbf{y}_1\mathbf{y}_2\rangle V_{at,e}(\mathbf{y}_1,\mathbf{y}_2)\langle\mathbf{y}_1\mathbf{y}_2|(z+H^*_{pe,e})^{-1}|\mathbf{x}_1\mathbf{x}_2\rangle \tag{B.18}$$

with

$$H^*_{pe,e}=-\frac{\hbar^2}{2m_e}\Delta_{\mathbf{x}_1}-\frac{\hbar^2}{2m_e}\Delta_{\mathbf{x}_2}-\frac{\sqrt{2}e^2}{|\mathbf{x}_1+(M_{H^-}/m_p)^{1/2}\mathbf{x}_2|} \tag{B.19}$$

and

$$V_{at,e}(\mathbf{x}_1,\mathbf{x}_2)=\frac{e^2}{\sqrt{2}|\mathbf{x}_1|}-\frac{\sqrt{2}e^2}{|\mathbf{x}_1-(M_{H^-}/m_p)^{1/2}\mathbf{x}_2|}. \tag{B.20}$$

Green function defined as matrix elements of $(z+H^*_{pe,e})^{-1}$, is analytical with respect to z in the whole complex plane, except on part $\Re(z)\le -E_H$ of the real axis. In the Laplace inversion formula, we introduce a contour analogous to that of Fig. 13 with $\delta > -E_H$. We also define a regular part of $\langle\mathbf{x}_1\mathbf{x}_2|(z+H^*_{pe,e})^{-1}|\mathbf{y}_1\mathbf{y}_2\rangle$ which remains finite at $\mathbf{x}_i=\mathbf{y}_i$. When z follows D_δ, $\Im(k)$ remains larger than a given positive constant, so previous regular part is bounded by an exponentially decaying function of $[(\mathbf{x}_1-\mathbf{y}_1)^2+(\mathbf{x}_2-\mathbf{y}_2)^2]^{1/2}$ (for large separations of the arguments, Coulomb potential terms vanish so Green functions behave as their free counterparts which decay exponentially on a scale $(\Im(k))^{-1}$). This implies that (B.18) remains bounded by a constant along D_δ. Contribution of (B.17) is then found to be bounded by a power of β times $\exp(\beta\delta)$, with δ arbitrarily close to $-E_H$. Since $-E_H < -E_{H^-}$, that contribution is exponentially smaller than (B.15) and (B.16). Contributions of all the other truncated terms in $[\exp(-\beta H_{1,2})]^T_{\mathrm{Mayer}}$ behave similarly because groundstate energies of Hamiltonians $(H_{1,0}+H_{0,2})$ and $(H_{1,0}+H_{0,1}+H_{0,1})$ (which both vanish) are strictly larger than E_{H^-}. Since volume of $\Omega^{(2)}$ is bounded by a constant times $(\beta e^2)^6$ on one hand, while $\psi_0(\mathbf{x}_1,\mathbf{x}_2)$ decays exponentially fast for $|\mathbf{x}_i|$ large on another hand, we eventually obtain

$$\begin{aligned}&\int_{\Omega^{(2)}}\mathrm{d}\mathbf{x}_1\mathrm{d}\mathbf{x}_2\{2\langle\mathbf{x}_1\mathbf{x}_2|\exp(-\beta H^*_{1,2})|\mathbf{x}_1\mathbf{x}_2\rangle-\langle-\mathbf{x}_1\mathbf{x}_2|\exp(-\beta H^*_{1,2})|\mathbf{x}_1\mathbf{x}_2\rangle+\cdots\}\\&\quad=\exp(-\beta E_{H^-})\end{aligned} \tag{B.21}$$

discarding terms which are exponentially smaller.

For $\mathbf{x}_1,\mathbf{x}_2$ inside $\Omega^{(1)}$, two of three distances $|\mathbf{x}_1|$, $|\mathbf{x}_1-\mathbf{x}_2|$, $|\mathbf{x}_2|$ are larger than βe^2. For instance, we may have both $|\mathbf{x}_1|$ and $|\mathbf{x}_1-\mathbf{x}_2|$ larger than βe^2, while $|\mathbf{x}_2|$ is smaller than βe^2. For such configurations, both distances $|\mathbf{x}_1|$ and $|\mathbf{x}_1-(M_{H^-}/m_p)^{1/2}\mathbf{x}_2|$ are larger than βe^2. In the Feynman-Kac formula for $\langle\mathbf{x}_1\mathbf{x}_2|\exp(-\beta H^*_{1,2})|\mathbf{x}_1\mathbf{x}_2\rangle$, potentials $\int_0^1\mathrm{d}s e^2/\sqrt{2}|\mathbf{x}_1+\lambda_e\boldsymbol{\xi}_1(s)|$ and $-\int_0^1\mathrm{d}s\sqrt{2}e^2/|\mathbf{x}_1+\lambda_e\boldsymbol{\xi}_1(s)-(M_{H^-}/m_p)^{1/2}(\mathbf{x}_2+\lambda_e\boldsymbol{\xi}_2(s))|$ can then be replaced by their classical counterparts $e^2/\sqrt{2}|\mathbf{x}_1|$ and $-\sqrt{2}e^2/|\mathbf{x}_1-(M_{H^-}/m_p)^{1/2}\mathbf{x}_2|$ respectively, because $\lambda_e/\beta e^2$ goes to zero when β diverges. Thus, $\langle\mathbf{x}_1\mathbf{x}_2|\exp(-\beta H^*_{1,2})|\mathbf{x}_1\mathbf{x}_2\rangle$ behaves as

$$\langle\mathbf{x}_1\mathbf{x}_2|\exp(-\beta H^*_{pe,e})|\mathbf{x}_1\mathbf{x}_2\rangle\exp(-\beta V_{at,e}(\mathbf{x}_1,\mathbf{x}_2)) \tag{B.22}$$

at leading order, where $H^*_{pe,e}$ and $V_{at,e}(\mathbf{x}_1,\mathbf{x}_2)$ are given by (B.19) and (B.20) respectively. A similar estimation holds for truncated terms in $[\exp(-\beta H_{1,2})]^T_{\mathrm{Mayer}}$ built with powers of

$V_{at,e}$, so the corresponding full contribution integrated upon considered configurations behaves as

$$2\int_{|\mathbf{x}_1|,|\mathbf{x}_1-\mathbf{x}_2|>\beta e^2,|\mathbf{x}_2|<\beta e^2} d\mathbf{x}_1 d\mathbf{x}_2 \langle \mathbf{x}_1\mathbf{x}_2|\exp(-\beta H^*_{pe,e})|\mathbf{x}_1\mathbf{x}_2\rangle \times \left[\exp(-\beta V_{at,e}(\mathbf{x}_1,\mathbf{x}_2)) + \beta V_{at,e}(\mathbf{x}_1,\mathbf{x}_2) - \frac{1}{2}(\beta V_{at,e}(\mathbf{x}_1,\mathbf{x}_2))^2 + \frac{1}{6}(\beta V_{at,e}(\mathbf{x}_1,\mathbf{x}_2))^3\right]. \tag{B.23}$$

According to above properties of Green functions, $\langle \mathbf{x}_1\mathbf{x}_2|\exp(-\beta H^*_{pe,e})|\mathbf{x}_1\mathbf{x}_2\rangle$ is bounded by some power of β times $\exp(\beta\delta)$ with $-E_H < \delta < -E_{H^-}$. Therefore, integral (B.23) is also bounded by a power of β times $\exp(\beta\delta)$, because purely classical integral

$$\int_{|\mathbf{x}_1|,|\mathbf{x}_1-\mathbf{x}_2|>\beta e^2,|\mathbf{x}_2|<\beta e^2} d\mathbf{x}_1 d\mathbf{x}_2 \left[\exp(-\beta V_{at,e}(\mathbf{x}_1,\mathbf{x}_2)) + \beta V_{at,e}(\mathbf{x}_1,\mathbf{x}_2) - \frac{1}{2}(\beta V_{at,e}(\mathbf{x}_1,\mathbf{x}_2))^2 + \frac{1}{6}(\beta V_{at,e}(\mathbf{x}_1,\mathbf{x}_2))^3\right] \tag{B.24}$$

is proportional to $(\beta e^2)^6$ as shown by rescaling $\mathbf{x}_i$ in units of βe^2. A similar analysis applies to the contributions of the other terms in $[\exp(-\beta H_{1,2})]^T_{\text{Mayer}}$. When off-diagonal matrix elements are involved, we use bounds inferred from properties of Green functions, which decay exponentially fast with respect to relative distances between different arguments. For instance, $|\langle -\mathbf{x}_1\mathbf{x}_2|\exp(-\beta H^*_{1,2})|\mathbf{x}_1\mathbf{x}_2\rangle|$ is bounded by a constant times $\exp(-\beta E_{H^-})\exp(-c|\mathbf{x}_1|/a_B)$ with $c > 0$, so

$$-\int_{|\mathbf{x}_1|,|\mathbf{x}_1-\mathbf{x}_2|>\beta e^2,|\mathbf{x}_2|<\beta e^2} d\mathbf{x}_1 d\mathbf{x}_2 \langle -\mathbf{x}_1\mathbf{x}_2|\exp(-\beta H^*_{1,2})|\mathbf{x}_1\mathbf{x}_2\rangle \tag{B.25}$$

decays exponentially faster than $\exp(-\beta E_{H^-})$. Previous analysis can be also repeated for the other configurations belonging to $\Omega^{(1)}$, i.e. $\{|\mathbf{x}_2|, |\mathbf{x}_1-\mathbf{x}_2| > \beta e^2, |\mathbf{x}_1| < \beta e^2\}$ and $\{|\mathbf{x}_1|, |\mathbf{x}_2| > \beta e^2, |\mathbf{x}_1-\mathbf{x}_2| < \beta e^2\}$. We eventually find that

$$\int_{\Omega^{(1)}} d\mathbf{x}_1 d\mathbf{x}_2 \{2\langle \mathbf{x}_1\mathbf{x}_2|\exp(-\beta H^*_{1,2})|\mathbf{x}_1\mathbf{x}_2\rangle - \langle -\mathbf{x}_1\mathbf{x}_2|\exp(-\beta H^*_{1,2})|\mathbf{x}_1\mathbf{x}_2\rangle + \cdots\} \tag{B.26}$$

decays exponentially faster than $\exp(-\beta E_{H^-})$.

For $\mathbf{x}_1, \mathbf{x}_2$ inside $\Omega^{(0)}$, all distances $|\mathbf{x}_1|$, $|\mathbf{x}_1-\mathbf{x}_2|$, and $|\mathbf{x}_2|$ are larger than βe^2. For diagonal matrix elements, potential parts can be treated classically at leading order, as immediately seen from Feynman-Kac formula by noting that $\lambda_e/\beta e^2$ vanishes. Such matrix elements then behave as their free counterparts times classical Boltzmann factors. The corresponding full contribution integrated upon $\Omega^{(0)}$ is shown to be proportional to $(\beta e^2/\lambda_e)^6$, as shown by variable changes $\mathbf{x}_i = \beta e^2 \mathbf{v}_i$. The contribution of remaining terms with off-diagonal matrix elements decays exponentially faster than $\exp(-\beta E_{H^-})$, thanks to the existence of bounds which are proportional to $\exp(-\beta E_{H^-})$ and decay exponentially fast for large separations (over a finite length scale proportional to a_B). Thus, and like (B.26), contribution of $\Omega^{(0)}$ to $Z(1,2)$ also decays exponentially faster than $\exp(-\beta E_{H^-})$, so we even-

tually obtain

$$Z(1,2) = 2\exp(-\beta E_{H^-}) \tag{B.27}$$

discarding terms which are exponentially smaller when $\beta \to \infty$.

B.3 Behaviors of $Z(2,1)$, $Z(2,2), \ldots$

The low-temperature behaviors of $Z(2,1)$ and $Z(2,2)$ can be also determined by previous methods introduced for studying $Z(1,1)$ and $Z(1,2)$. Again, analytic properties of Green functions associated with resolvents $(z + H^*_{2,1})^{-1}$ and $(z + H^*_{2,2})^{-1}$ play a crucial role in the derivations. Such functions are analytical in the whole complex plane, except on a part of real axis with $\Re(z) < -E_{H_2^+}$ or $\Re(z) < -E_{H_2}$, while $z_1 = -E_{H^-}$ or $z_1 = -E_{H_2}$ is a simple (isolated) pole. Along integration contours analogous to that described in Fig. 13, they can be bounded as above, within quite plausible arguments based on the properties of their free counterparts, solutions of Helmholtz equation in six or nine dimensions. Integration space upon reduced positions is splitted into several parts according to the values of relative distances compared to βe^2. The parts inside which all relative distances are smaller than βe^2, provide the leading contributions, i.e.

$$Z(2,1) = 2\exp(-\beta E_{H_2^+}) \tag{B.28}$$

and

$$Z(2,2) = \exp(-\beta E_{H_2}) \tag{B.29}$$

discarding terms which are exponentially smaller when $\beta \to \infty$.

The analysis can be applied to any partition function $Z(N_p, N_e)$. However, when the infimum of reduced Hamiltonian $H^*_{N_p,N_e}$ is not separated from the rest of the spectrum (i.e. in the corresponding groundstate, the N_p protons and the N_e electrons are not binded together), the first singularity (with the largest real part) $z_1 = -E^{(0)}_{N_p,N_e}$ of Green function associated with $(z + H^*_{N_p,N_e})^{-1}$, is a branching point which is not isolated from other singularities. Then, contour $C_{\sigma,\delta}$ cuts real axis at $\delta > z_1$, so the previous methods show that $|Z(N_p, N_e)|$ is bounded by a power of β times $\exp(\beta\delta)$. A more detailed analysis of the behavior of Green function for z close to z_1 is then required for determining the precise leading behavior of $Z(N_p, N_e)$. Nevertheless, since previous bound is valid for δ arbitrarily close to z_1, it is quite reasonable to assume that $Z(N_p, N_e)$ then behaves as a power of β times $\exp(-\beta E^{(0)}_{N_p,N_e})$ (such a behavior is indeed observed for $Z(2,0)$ with $E^{(0)}_{2,0} = 0$).

Appendix C: Leading Contributions of Interactions between Atoms and Ionized Charges

C.1 Expression of $W(1,1|1,1)$

The low-temperature behavior of bare contributions of Figs. 8b and 8c, is determined along similar lines as that of polarization contribution (A.13). The integrals of interest are again expressed in terms of the atom mass centers and of the reduced variables. Matrix elements are also evaluated *via* insertions of the closure relation for a suitable basis. Each eigenstate in that basis, is the product of plane waves describing mass center motions, times atomic

internal wavefunctions. The resulting integrals over times τ_i are readily performed for each set of involved eigenstates. According to the scaling prescriptions defined in Sect. 3, full bare contribution of Figs. 8b and 8c is then rewritten as (3.41) plus terms which decay exponentially faster than $\rho^* \exp(\beta E_H)$. Like $Z(1,1)$ or $S_3(1,1)$, function $W(1,1|1,1)$ is determined by atomic groundstate contributions, and further contributions of excited states might be bounded by methods similar to that exposed in Appendix B:. Similarly to expression (A.16) for $S_3(1,1)$, $W(1,1|1,1)$ reduces to the product $\exp(-2\beta E_H)$ of atomic groundstate Boltzmann factors, times a function of $\beta|E_H|$ which remains bounded by a power law at low temperatures. Its asymptotic form when $\beta \to \infty$ is given by (3.42), where $c_{at,at}$ is the pure numerical coefficient

$$
\begin{aligned}
c_{at,at} = \frac{2}{\pi}\Bigg\{ & \frac{M}{m}\int \mathrm{d}\mathbf{K}\frac{|D^{(at,at)}_{00,00}(\mathbf{K})|^2}{K^6} \\
& + \sum_{(p_1,p_2)\neq(0,0)}\int \mathrm{d}\mathbf{K}\frac{2|E_H|}{(E_H^{(p_1)}+E_H^{(p_2)}-2E_H+\hbar^2K^2/(Ma_B^2))}\frac{|D^{(at,at)}_{0p_1,0p_2}(\mathbf{K})|^2}{K^4}\Bigg\} \\
& \times \frac{-1}{\pi^3}\Bigg\{\left(\frac{M}{m}\right)^2\int \mathrm{d}\mathbf{K}\mathrm{d}\mathbf{Q}\frac{D^{(at,at)}_{00,00}(\mathbf{K})D^{(at,at)}_{00,00}(\mathbf{Q}-\mathbf{K})D^{(at,at)}_{00,00}(-\mathbf{Q})}{K^4Q^4|\mathbf{K}-\mathbf{Q}|^2} \\
& + \sum_{(p_1,p_2,p_3,p_4)\neq(0,0,0,0)}\int \mathrm{d}\mathbf{K}\mathrm{d}\mathbf{Q}\frac{2|E_H|}{(E_H^{(p_1)}+E_H^{(p_2)}-2E_H+\hbar^2K^2/(Ma_B^2))} \\
& \times \frac{2|E_H|}{(E_H^{(p_3)}+E_H^{(p_4)}-2E_H+\hbar^2Q^2/(Ma_B^2))} \\
& \times \frac{D^{(at,at)}_{0p_1,0p_2}(\mathbf{K})D^{(at,at)}_{p_1p_3,p_2p_4}(\mathbf{Q}-\mathbf{K})D^{(at,at)}_{p_30,p_40}(-\mathbf{Q})}{K^2Q^2|\mathbf{K}-\mathbf{Q}|^2}\Bigg\}.
\end{aligned}
\tag{C.1}
$$

In (C.1), $\mathbf{K}$ and $\mathbf{Q}$ are dimensionless (units a_B^{-1}) wavenumbers, while function $D^{(at,at)}_{0p_1,0p_2}(\mathbf{K})$ reduces to

$$
\begin{aligned}
D^{(at,at)}_{0p_1,0p_2}(\mathbf{K}) = {} & \langle\psi_0|\exp\left(-i\frac{m}{m_e}\mathbf{K}\cdot\mathbf{r}^*\right)|\psi_{p_1}\rangle\langle\psi_0|\exp\left(i\frac{m}{m_e}\mathbf{K}\cdot\mathbf{r}^*\right)|\psi_{p_2}\rangle \\
& + \langle\psi_0|\exp\left(i\frac{m}{m_p}\mathbf{K}\cdot\mathbf{r}^*\right)|\psi_{p_1}\rangle\langle\psi_0|\exp\left(-i\frac{m}{m_p}\mathbf{K}\cdot\mathbf{r}^*\right)|\psi_{p_2}\rangle \\
& - \langle\psi_0|\exp\left(-i\frac{m}{m_e}\mathbf{K}\cdot\mathbf{r}^*\right)|\psi_{p_1}\rangle\langle\psi_0|\exp\left(-i\frac{m}{m_p}\mathbf{K}\cdot\mathbf{r}^*\right)|\psi_{p_2}\rangle \\
& - \langle\psi_0|\exp\left(i\frac{m}{m_p}\mathbf{K}\cdot\mathbf{r}^*\right)|\psi_{p_1}\rangle\langle\psi_0|\exp\left(i\frac{m}{m_e}\mathbf{K}\cdot\mathbf{r}^*\right)|\psi_{p_2}\rangle.
\end{aligned}
\tag{C.2}
$$

C.2 Expressions of $W(1,1|1,0)$ and $W(1,1|0,1)$

A straightforward extension of previous methods provides the low-temperature behaviors of bare contributions of Figs. 9a–f. Using again the scaling prescriptions defined in Sect. 3, the corresponding full bare contribution is then rewritten as (3.45) plus terms which decay exponentially faster than $\rho^* \exp(\beta E_H)$. Functions $W(1,1|1,0)$ and $W(1,1|0,1)$ are also determined by atomic groundstate contributions. They behave as $\exp(-\beta E_H)$ times functions

of $\beta|E_H|$ which remain bounded by power laws. Their asymptotic forms when $\beta \to \infty$ are given by 3.46, where pure numerical constants reduce to

$$
\begin{aligned}
c_{at,\alpha}^{(2)} = \frac{2}{\pi}\Bigg\{ & \frac{2m_\alpha M}{m(m_\alpha+M)} \int \mathrm{d}\mathbf{K} \frac{|D_{00}^{(at,\alpha)}(\mathbf{K})|^2}{K^6} \\
& + \sum_{p_1 \neq 0} \int \mathrm{d}\mathbf{K} \frac{2|E_H|}{(E_H^{(p_1)} - E_H + \hbar^2K^2/(2Ma_B^2) + \hbar^2K^2/(2m_\alpha a_B^2))} \frac{|D_{0p_1}^{(at,\alpha)}(\mathbf{K})|^2}{K^4} \Bigg\} \\
& \times \frac{-1}{\pi^3} \Bigg\{ \left(\frac{2m_\alpha M}{m(m_\alpha+M)} \right)^2 \int \mathrm{d}\mathbf{K}\mathrm{d}\mathbf{Q} \frac{D_{00}^{(at,\alpha)}(\mathbf{K}) D_{00}^{(at,\alpha)}(\mathbf{Q}-\mathbf{K}) D_{00}^{(at,\alpha)}(-\mathbf{Q})}{K^4 Q^4 |\mathbf{K}-\mathbf{Q}|^2} \\
& + \sum_{(p_1,p_2)\neq(0,0)} \mathrm{d}\mathbf{K}\mathrm{d}\mathbf{Q} \frac{2|E_H|}{(E_H^{(p_1)} - E_H + \hbar^2K^2/(2Ma_B^2) + \hbar^2K^2/(2m_\alpha a_B^2))} \\
& \times \frac{2|E_H|}{(E_H^{(p_2)} - E_H + \hbar^2Q^2/(2Ma_B^2) + \hbar^2Q^2/(2m_\alpha a_B^2))} \\
& \times \frac{D_{0p_1}^{(at,\alpha)}(\mathbf{K}) D_{p_1p_2}^{(at,\alpha)}(\mathbf{Q}-\mathbf{K}) D_{p_20}^{(at,\alpha)}(-\mathbf{Q})}{K^2 Q^2 |\mathbf{K}-\mathbf{Q}|^2} \Bigg\},
\end{aligned}
\tag{C.3}
$$

with

$$
\begin{aligned}
D_{0p_1}^{(at,p)}(\mathbf{K}) &= -D_{0p_1}^{(at,e)}(\mathbf{K}) \\
&= \langle \psi_0 | \exp\left(-i \frac{m}{m_e} \mathbf{K}\cdot\mathbf{r}^* \right) | \psi_{p_1} \rangle - \langle \psi_0 | \exp\left(i \frac{m}{m_p} \mathbf{K}\cdot\mathbf{r}^* \right) | \psi_{p_1} \rangle .
\end{aligned}
\tag{C.4}
$$

References

1. Alastuey, A., Ballenegger, V., Cornu, F.: Low temperature isotherms of the hydrogen plasma: comparisons between analytical and Monte Carlo results. ENS Lyon preprint
2. Alastuey, A., Martin, Ph.A.: Absence of exponential clustering for static quantum correlations and time-displaced correlations in charged fluids. Eur. Phys. Lett. **6**, 385–390 (1988)
3. Alastuey, A., Martin, Ph.A.: Absence of exponential clustering in quantum Coulomb fluids. Phys. Rev. A **40**, 6485–6520 (1989)
4. Alastuey, A., Perez, A.: Virial expansion of the equation of state of a quantum plasma. Europhys. Lett. **20**, 19–24 (1992)
5. Alastuey, A., Perez, A.: Virial expansion for quantum plasmas: Fermi–Bose statistics. Phys. Rev. E **53**, 5714–5728 (1996)
6. Alastuey, A., Cornu, F., Perez, A.: Virial expansion for quantum plasmas: diagrammatic resummations. Phys. Rev. E **49**, 1077–1093 (1994)
7. Alastuey, A., Cornu, F., Perez, A.: Virial expansion for quantum plasmas: Maxwell–Boltzmann statistics. Phys. Rev. E **51**, 1725–1744 (1995)
8. Alastuey, A., Ballenegger, V., Cornu, F., Martin, Ph.A.: Screened cluster expansions for partially ionized gases. J. Stat. Phys. **113**, 455–503 (2003)
9. Alastuey, A., Cornu, F., Martin, Ph.A.: Van der Waals forces in presence of free charges: an exact derivation from equilibrium quantum correlations. J. Chem. Phys. **127**, 054506 (2007)
10. Ballenegger, V.: Étude des phénomènes d'écran et de polarisation dans un plasma quantique par la méthode des graphes de Mayer. PhD thesis, École Polytechnique et Fédérale de Lausanne (2002)
11. Ballenegger, V., Martin, Ph.A.: Quantum Coulomb systems: some exact results in the atomic limit. Physica A **306**, 59–67 (2002)
12. Ballenegger, V., Martin, Ph.A.: Dielectric versus conductive behavior in quantum gases: Exact results for the Hydrogen plasma. Physica A **328**, 97–144 (2003)

13. Ballenegger, V., Martin, Ph.A., Alastuey, A.: Quantum Mayer graphs for Coulomb systems and the analog of the Debye potential. J. Stat. Phys. **108**, 169–211 (2002)
14. Brydges, D.C., Martin, Ph.A.: Coulomb systems at low density: a review. J. Stat. Phys. **96**, 1163–1330 (1999)
15. Ceperley, D.M.: Fermion nodes. J. Stat. Phys. **63**, 1237–1267 (1991)
16. Ceperley, D.M.: Path integrals in the theory of condensed helium. Rev. Mod. Phys. **67**, 279–355 (1995)
17. Ceperley, D.M.: In: Binder, E.K., Ciccotti, G. (eds.) Monte Carlo and Molecular Dynamics of Condensed Matter Systems. Editrice Compositori, Bologna (1996)
18. Conlon, J.G., Lieb, E.H., Yau, H.T.: The Coulomb gas at low temperature and low density. Commun. Math. Phys. **125**, 153–180 (1989)
19. Cornu, F.: Correlations in quantum plasmas, I: resummations in Mayer-like diagrammatics. Phys. Rev. E **53**, 4562 (1996)
20. DeWitt, H.E., Schlanges, M., Sakakura, A.Y., Kraeft, W.D.: Low density expansion of the equation of state for a quantum electron gas. Phys. Lett. A **197**, 326–329 (1995)
21. Dyson, F., Lenard, A.: Stability of matter I. J. Math. Phys. **8**, 423–434 (1967)
22. Dyson, F., Lenard, A.: Stability of matter II. J. Math. Phys. **9**, 698–711 (1968)
23. Ebeling, W.: Ann. Phys. Leipz. **19**, 104 (1967)
24. Ebeling, W.: Coulomb interaction and ionization equilibrium in partially ionized plasmas. Physica **63**, 293 (1969)
25. Ebeling, W.: Statistical derivation of the mass-action law for interacting gases and plasmas. Physica **73**, 573–584 (1974)
26. Ebeling, W., Kraeft, W.D., Kremp, D.: Theory of Bound States and Ionization Equilibrium in Plasmas and Solids. Akademie, Berlin (1976)
27. Fefferman, C.: The atomic and molecular nature of matter. Rev. Math. Iberoam. **1**, 1–44 (1985)
28. Fefferman, C.: The n-body problem in quantum mechanics. Commun. Pure Appl. Math. **39**(S1), 67–109 (1986)
29. Gell-Mann, M., Brueckner, K.A.: Correlation energy of an electron gas at high density. Phys. Rev. **106**, 364–368 (1957)
30. Ginibre, J.: Some applications of functional integration in statistical mechanics. In: DeWitt, C., Stora, R. (eds.) Statistical Mechanics and Quantum Field Theory. Gordon and Breach, les Houches (1971)
31. Gradsteyn, I.S., Ryzhik, I.M.: In: Jeffrey, A. (ed.) Tables of Integrals, Series and Products. Academic Press, London (1994)
32. Gruter, P., Laloe, F.: Ursell operators in statistical physics I. J. Phys. I. (France) **5**, 1255 (1995)
33. Gruter, P., Laloe, F.: Ursell operators in statistical physics II. J. Phys. I. (France) **5**, 181 (1995)
34. Gruter, P., Laloe, F.: Ursell operators in statistical physics III. J. Phys. I. (France) **7**, 485 (1997)
35. Hill, L.T.: Statistical Mechanics. McGraw-Hill, New York (1956)
36. Hostler, L.: Coulomb's Green functions and the Furry's approximation. J. Math. Phys. **5**, 591 (1964)
37. Kahlbaum, T.: The quantum-diffraction term in the free energy for Coulomb plasma and the effective-potential approach. J. Phys. IV **10**(P5), 455 (2000)
38. Kleinert, H.: Path Integrals in Quantum Mechanics, Statistics, Polymer Physics and Financial Markets. World Scientific, Singapore (2004)
39. Kraeft, W.D., Kremp, D., Ebeling, W., Ropke, G.: Quantum Statistics of Charged Particle Systems. Plenum, New York (1986)
40. Krauth, W.: Statistical Mechanics: Algorithms and Computations. Oxford University Press, Oxford (2006)
41. Kremp, D., Kraeft, W.D., Lambert, A.J.M.D.: Equation of state and ionization equilibrium for non-ideal plasmas. Physica A **127**, 72–86 (1984)
42. Landau, L.D., Lifchitz, E.M.: Quantum Mechanics, 3rd edn. Course of Theoretical Physics, vol. 3. Pergamon, Oxford (1977)
43. Lebowitz, J., Pena, R.: Low density form of the free energy of real matter. J. Chem. Phys. **59**, 1362–1364 (1973)
44. Lieb, E.H., Lebowitz, J.: The constitution of matter: existence of thermodynamics for systems composed of electrons and nuclei. Adv. Math. **9**, 316–398 (1972)
45. Macris, N., Martin, Ph.A.: Ionization equilibrium in the proton-electron gas. J. Stat. Phys. **60**, 619–637 (1990)
46. Martin, Ph.A.: Quantum Mayer graphs: applications to Bose and Coulomb gases. Acta Phys. Pol. B **34**, 3629 (2003)
47. Militzer, B., Ceperley, D.M.: Path integral Monte Carlo calculation of the deuterium hugoniot. Phys. Rev. Lett. **85**, 1890–1893 (2000)
48. Militzer, B., Ceperley, D.M.: Path integral Monte Carlo simulation of the low-density hydrogen plasma. Phys. Rev. E **63**, 066404 (2001)

49. Militzer, B., Pollock, E.L.: Variational density matrix method for warm, condensed matter: application to dense hydrogen. Phys. Rev. E **61**, 3470–3482 (2000)
50. Montroll, E.W., Ward, J.C.: Quantum statistics of interacting particles: General theory and some remarks on properties of an electron gas. Phys. Fluid **1**, 55 (1958)
51. Morita, T.: Equation of state of high temperature plasma. Prog. Theor. Phys. **22**, 757 (1959)
52. All spectroscopic calculations were performed by V. Robert, who used a coupled cluster (CCSD(T)) approach including an extended basis set for hydrogen atoms ($4s3p2d1f$)
53. Roepstorff, G.: Path Integral Approach to Quantum Physics. Springer, Berlin (1994)
54. Rogers, F.J.: Statistical mechanics of Coulomb gases of arbitrary charge. Phys. Rev. A **10**, 2441 (1974)
55. Rogers, F.J.: Equation of state of dense, partially degenerate, reacting plasmas. Phys. Rev. A **24**, 1531 (1981)
56. Rogers, F.J.: Occupation numbers for reacting plasmas—the role of the Planck–Larkin function. Astrophys. J. **310**, 723 (1986)
57. Rogers, F.J.: A distribution function approach for effective occupation numbers and the equation of state of hydrogen plasmas. Astrophys. J. **352**, 689 (1990)
58. Rogers, F.J.: In: Chabrier, G., Schatzman, E. (eds.) The Equation of State in Astrophysics. Cambridge University Press, New York (1994)
59. Rogers, F.J., Young, D.A.: Validation of the activity expansion method with ultrahigh pressure shock equations of state. Phys. Rev. E **56**, 5876 (1997)
60. Saha, M.: Philos. Mag. **40**, 472 (1920)
61. Schulman, L.S.: Techniques and Applications of Path Integrals. Wiley, New York (1981)
62. Simon, B.: Functional Integration and Quantum Physics. Academic, New York (1979)